Foredune morphodynamics and seasonal sediment budget patterns: Humboldt Bay National Wildlife Refuge, Northern California, USA.

By

Alana Marie Rader
B.Sc., University of Victoria, 2014

A Thesis Submitted in Partial Fulfillment
of the Requirements for the Degree of

MASTER OF SCIENCE

In the Department of Geography

Supervisory Committee

Foredune morphodynamics and seasonal sediment budget patterns:
Humboldt Bay National Wildlife Refuge, Northern California, USA.

By

Alana Marie Rader
B.Sc., University of Victoria, 2017

Supervisory Committee

Dr. Ian J. Walker
Department of Geography, University of Victoria
School of Geographic Science and Urban Planning and School of Earth and Space Exploration, Arizona State University
Supervisor

Dr. Bernard O. Bauer
Department of Geography, University of Victoria
Department of Earth, Environmental, and Geographic Sciences, University of British Columbia Okanagan
Departmental Member

Andrea J. Pickart
Humboldt Bay National Wildlife Refuge, United States Fish and Wildlife Service
Outside Member

Abstract

Delivery of sediment to beach-dune complexes along the northern California coast, as elsewhere, is controlled by littoral and aeolian processes governed largely by oceanic and meteorological conditions such as wind speed and direction, wave characteristics and water level fluctuations. Furthermore, patterns of sediment deposition on foredunes are controlled by the zonation, density and physical structure of dominant vegetation assemblages. This study explores the link between varying oceanic, meteorological and ecological patterns and coastal foredune morphodynamics at a site within the Humboldt Bay National Wildlife Refuge (HBNWR) near Arcata, CA, to provide coastal managers a local context of foredune erosion and accretion. At a site within the HBNWR a 75-year north to south alongshore gradient in foredune response was observed during the study period. Foredunes in the north experience seaward progradation (up to +0.51 m a^{-1}) and greater sediment volumes then southern foredunes, characterized by foredune retreat (up to -0.49 m a^{-1}) and larger erosive feature areas. Seasonal signatures of a previously observed bi-directional littoral drift partially inform the interpretation of an alongshore gradient in foredune position. In the summer, wind and wave directions were out of the NNW, combined with north to south littoral drift and significant sediment input into the northern beaches. During the winter, the dominant drift direction was from the south to the north, accompanied by large waves, high water levels and beach erosion. Following a comprehensive morpho-ecological model of foredune evolution (Hesp, 1988; 2002), greater foredune volumes, dense vegetation and seaward progradation are indicative of stage 1 foredunes. Transitioning to the south, lower vegetation densities and seaward retreat support a classification of stage 3

developed foredunes, characterized by shorter, more hummocky morphologies. Meteorological patterns and disturbance to vegetation concurrently influence foredune response and recovery to erosive wind, wave and water level events. As such, seasonal to interannual patterns of foredune morphodynamics may be altered following periods of both environmental and human induced vegetation disturbance (i.e., seasonal phenology, dynamic restoration).

At a section of foredune in the northern HBNWR, a dynamic restoration project was implemented with the first stages of vegetation removal occurring in August, 2015. In a year following vegetation disturbance through preliminary stages of restoration an annual sediment budget examination indicates net accretion on the foredune (+0.54 m^3 m^{-2}) while net erosion occurred on the beach (-0.38 m^3 m^{-2}). At smaller seasonal scales site-wide erosion occurred in the winter due to high-water and wave run-up recorded during intense storms. Summer monitoring reveals site-wide accretion due to beach rebuilding, heightened aeolian activity and an increase in vegetation cover. As such, seasonal sediment budgets that influence longer-term patterns of foredune development may be primarily controlled by the amount of sediment available on the beach for aeolian transport and secondarily by localized presence/absence of vegetation. Results of this study provide insight into the impact of continued coastal disturbance on foredune morphodynamics, around which a framework for future vegetation management projects may be implemented.

Table of Contents

List of Tables

List of Figures

Acknowledgements

I would like to thank my supervisor Dr. Ian J. Walker for his continued support during both my undergraduate and graduate career at UVic. Dr. Walker's Coastal Erosion and Dune Dynamics Lab has introduced me to the importance of coastal research and provided me the opportunity to travel to breathtaking field locations. Thank you to my committee members, Andrea J. Pickart and Dr. Bernard O. Bauer for pushing me to read critically between the lines. Special thanks to Jeremy Bubiak and Diane Braithwaite for helping me organize countless FedEX dramas.

A special thank you to Dr. Patrick Hesp of Flinders University, whose expertise and influence on my research goes unmatched.

Thank you to my colleagues in the CEDD Lab, Alex Lausanne, Michael Grilliot, Derek Heathfield, Felipe Gomez and Jordan Eamer for your friendship and good vibes- it has been fun holding down the fort with you all while Ian has been away! Special shout out to Michael and Derek for their assistance in the field and technical support, I truly couldn't have done it without either of you.

To my family and partner: Thank you for your unconditional support in the moments when I truly needed it.

1. Introduction

1.1 Research context

This study was undertaken to explore foredune morphodynamics at decadal, interannual and seasonal scales in order to improve our understanding of beach-foredune sediment budgets at the Humboldt Bay National Wildlife Refuge (HBNWR), northern California. The HBNWR Lanphere and Ma-le'l sand dune units have experienced both environmental (storm energy, climate forcing) and human based (vegetation introduction and restoration) disturbances to the foredune, potentially altering natural foredune morphodynamics. Therefore, this research contributes information regarding the impact of continued coastal disturbance on cycles of sediment erosion and accretion and resultant foredune development.

1.1.1 Foredune morphology and sediment budget dynamics

Coastal foredunes are shore-parallel ridges formed by aeolian processes on the landward margin of a backshore within beach-dune complexes. There are two main types of foredunes; incipient and established foredunes. Incipient foredunes are landforms that develop along the upper beach within stabilizing matrices such as sea wrack, large woody debris and pioneer plant communities (Hesp, 2002; 2012; Hesp and Walker, 2013). Incipient foredunes often occur seasonally during the annual vegetation growth period, unless establishment of perennial vegetation species occurs (Hesp, 2002). Under certain circumstances, primarily dependent on vegetation characteristics, wind velocity and sediment availability, incipient foredunes can grow in size and morphological complexity to create established foredunes. As such, foredune morphology and development are

intricately coupled with sediment transport onto the beach and related transport pathways between the beach and foredune (Short and Hesp, 1982; Psuty, 1988; Sherman and Bauer, 1993).

Seasonal variation in oceanic (wave height, water level), meteorological (precipitation, wind speed, direction) and ecological (phenology, composition, disturbance) conditions drive a complex feedback loop between beach and foredune sediment budgets (Shepard, 1950). Multiple studies have modeled the relationship by drawing comparisons between beach morphology (Short and Hesp, 1982), sediment supply (Psuty, 1988) and seasonal wind and wave dynamics (Shepard, 1950). For example, in a study of beach-dune profiles in southern California, transportation of nearshore sediment supplies onto the beach by summer swell waves and increase aeolian transport potential during periods of low precipitation led to sediment deposition along the backshore and resultant development of the foredune (Shepard, 1950). Following, erosive winter storm waves can cause extensive erosion of sediment deposits within the incipient foredune and established foredune toe, returning sediment into the nearshore (Shepard, 1950). Subsequently, sediment in the nearshore zone is made available for transportation onto the beach through the littoral drift system (Shepard, 1950; Thom and Hall, 1992; Sherman and Bauer, 1993). Models relating morphodynamics beach state to dune system dynamics and resulting analysis of beach-dune sediment budgets are often time-dependent, and as such, variations in sediment budget patterns may occur over longer-temporal scales (Sherman and Bauer, 1993).

Previous studies (e.g., Hesp 1982; 1988b; Carter, 1988; Saunders and Davidson-Arnott, 1990; Law and Davidson-Arnott, 1990; Arens and Wiesma, 1990; 1994; Arens,

1996; Giles and McCan, 1997; Hesp, 1999) have classified foredunes according to stages of morphological development, largely based on patterns of sediment accretion on the beach and recovery (or lack thereof) of the foredune following erosive events. Hesp (1988; 2002) synthesizes previous classifications into a comprehensive morpho-ecological model of established foredune development. Hesp (1988; 2002) draws linkages between beach and foredune morphologies and vegetation characteristics (presence/absence, density) to define 5 dominant stages of foredune evolution. The 5 stages range from topographically simple, densely vegetated and stable to accretionary Stage 1 foredunes to topographically complex, less densely vegetated and erosional Stage 5 foredunes (Hesp 1988; 2002). Stage 1, 2 and 3 foredunes are characterized by seaward progradation, as high inputs of sediment onto the beach are transported to the stoss slope, where an increase in surface friction from dense vegetation coverage and resultant decrease in transport velocities leads to deposition and storage of transported beach sediment (Hesp, 1988; 2002; Kuriyama et al., 2005; Luna et al., 2011). Consistent with findings of Arens (1996), as vegetation cover decreases from Stage 2 to Stage 5 foredunes, aeolian sediment transport flow patterns reach higher elevations along the foredune stoss and into the lee-slope and backdune, leading to lower elevation and broader foredunes. Aeolian transport patterns on foredunes with low density vegetation coverage facilitate sediment deposition leeward of the foredune crest and potential landward migration of the foredune (Arens, 1996).

In addition to the presence or absence of vegetation, foredune morphology (i.e., height and breadth) controls the patterns of sediment deposited over the foredune and in landward backdune regions. Previous studies have found that tall, narrow foredunes

(often characteristic of Stage 1 and densely vegetated foredunes) reduces aeolian sand transport processes and cause sediment deposition along the stoss slope (Hesp 1988; 2002; Kuriyama et al., 2005; Zarnetske et al., 2012; Walker et al., 2013). As such, plant community diversity may be reduced within backdune ecosystems that depend on natural aeolian disturbance processes for sediment and nutrient cycling. Alternatively, over shorter, broader foredunes, aeolian processes may promote the transport of sediment over the foredune crest and into the backdune, contributing to the vegetation burial and regrowth process required by some coastal species (Seabloom and Wiedemann, 1994; Wiedemann and Pickart, 1996; Walker et al., 2013; Darke et al., 2016).

1.1.2 Geospatial technologies and morphological considerations

Coastal landforms evolve rapidly due to seasonal variations in wind and wave energy. Previous studies (e.g., McLean and Thom, 1975; Ollerhead et al., 2013; Darke et al., 2013; 2016; Eamer and Walker, 2013; Walker et al., 2013) have relied on cross-shore profiles, real-time kinematic (RTK) geographic positioning system (GPS) and total station surveying for topographic data collection and observation of sedimentation patterns through time. These methods can be time intensive, potentially making data collection before and after coastal storms difficult. Additionally, reliance on user defined measurement locations results in variations in observation density, leading to potential bias and increased measurement error. For example, due to the need for the observer to subjectively choose each data collection position, there may be a larger number of observations over certain parts of the landscape than others. This may cause measurement values from areas with a larger number of observations to be weighted more heavily when interpolating data values across the study area (Lee et al., 2013).

The rapid advance of geospatial technologies allows for acquisition of higher-resolution data at a variety of spatial and temporal scales (Lim et al., 2005; Smith et al., 2009; Lindbergh et al., 2011; Bishop et al., 2012). Technological advancements may benefit coastal research by allowing for faster data collection that may isolate particular disturbance events and resultant geomorphic change. Modern surveying technologies such as light detection and ranging (LiDAR) and digital Structure from Motion (SfM) photogrammetry allow for efficient collection of high-resolution topographic data. Higher frequency of monitoring using LiDAR and photogrammetry survey methods allows for accurate spatial-temporal analysis of coastal morphodynamics and feature evolution through the creation of bare earth digital elevation models (DEMs) and orthophotographs.

Throughout this study four main datasets were collected at a variety of spatial and temporal scales (Figure 1). Traditional data collection methods, including aerial photograph analysis and cross-shore profile monitoring were performed from 1939 – 2017. Additionally, high-resolution datasets were collected using advanced terrestrial laser scanning (TLS) and kite aerial photography (KAP) technologies. Resulting LiDAR and SfM datasets were collected in reference to the preliminary stages of a dynamic restoration project at the HBNWR, to draw linkages between the presence and absence of vegetation, seasonal sediment budgets and impacts on longer-term foredune development (Figure 1).

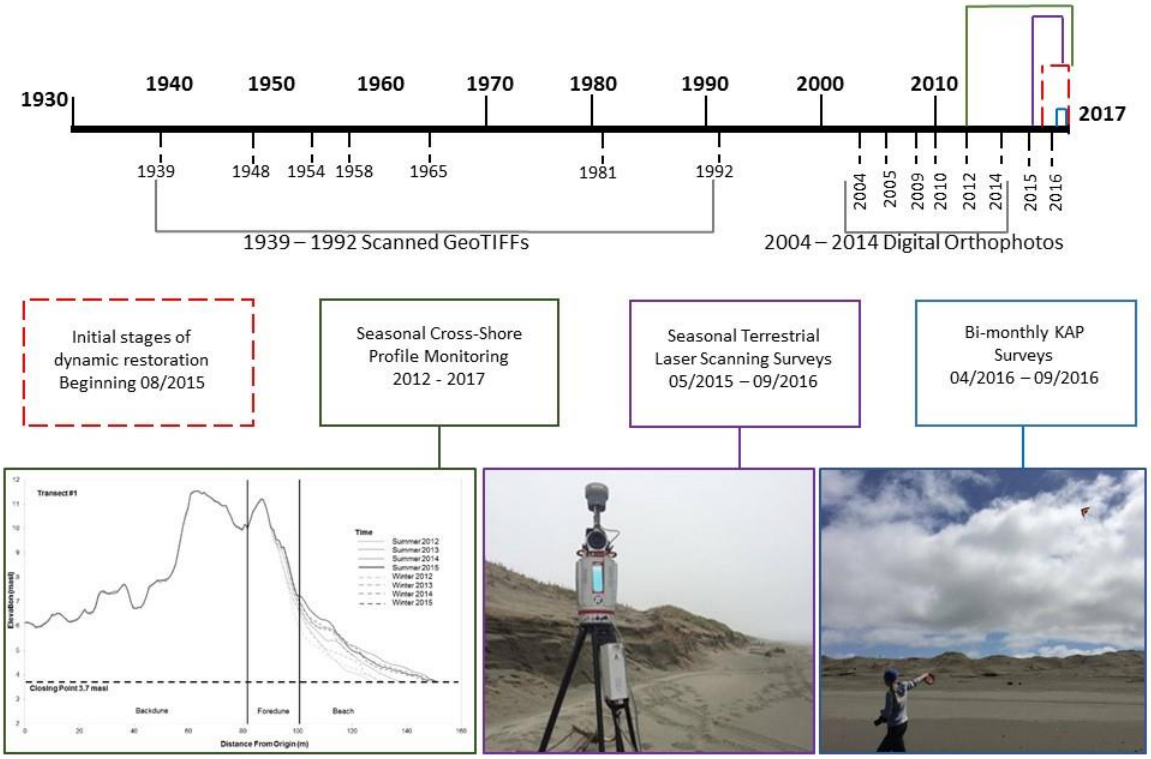

Figure 1. Timeline of collection of four main datasets used in this thesis. The initial stages of a dynamic restoration project, beginning in August , 2015 is indicated on the timeline in red.

1.1.3 Research gap

Sandy coastal ecosystems along the Pacific coast of North America are continually experiencing disturbance through human settlement, recreation, invasive vegetation and high energy storm events (Defeo et al., 2009; Nordstrom et al., 2011). However, only a handful of studies have focused on sandy coastal ecosystems in this region, with the majority of research focused on the coasts of British Columbia (Walker et al., 2013; Darke et al., 2013;2016; Eamer and Walker; 2013), Oregon (Seabloom and Wiedemann, 1994; Zarnetske et al., 2012), and central and southern California (Griggs, 1988; Moore et al., 1999; Storlazzi et al., 2000; Moore and Griggs, 2002). A regional

study of the California coast used aerial photography and cross shore transects to calculate the historical rate of shoreline change. The northern California facet of the regional study spanned only a 6 km stretch of shoreline in the Eureka Littoral cell, from Trinidad Head south to Cape Mendocino, with specific cross-shore profile locations outside of the bounds of the study region of this thesis in HBNWR (Hapke et al., 2006; 2009). This study focuses in much greater detail on a smaller reach of shoreline at the Lanphere and Ma-le'l dunes, in combination with higher resolution datasets, to provide insight into the relationship between the presence and absence of vegetation and local foredune morphodynamics and development following seasonal to interannual periods of disturbance from winter storm erosion, invasive vegetation establishment and the initial stages of a dynamic restoration project.

1.2 Thesis structure, purpose and objectives

The thesis is structured around two results sections (chapters 2 and 3) that focus on: i) historic to interannual rates of foredune position and feature change at HBNWR and ii) seasonal patterns of beach-foredune sedimentation and recovery following multiple disturbance events at HBNWR. These chapters are bookended with an introduction (chapter 1) that sets the research context and a summary and conclusions section (chapter 4) that reviews key findings and contributions of the research.

The general purpose of this research is to gain insight on how short-term foredune morphodynamics and sediment budget patterns are nested within from long-term (~75 year) historical cycles of foredune erosion and accretion, following both human and environmental disturbances. This research was funded in partnership with the US Fish and Wildlife Service to provide coastal managers at the HBNWR insights into the

geomorphic response and recovery processes of the Lanphere and Ma-le'l sand dune units to seasonal disturbance intervals, including disturbance from managed removal of invasive vegetation as part of an ongoing ecological restoration program. The purpose of chapter 2 is to examine and quantify historic changes in morphology and position of the established foredune using traditional aerial photograph analysis and cross shore profile monitoring. The specific objectives of this section are to: 1) analyze and interpret interannual to decadal scale changes in foredune position and geomorphic feature evolution from aerial photography (1939 – 2014) and 2) to determine sediment budget implications of recent seasonal (January 2012 – July 2015) erosion and accretion patterns and resulting foredune morphological development.

The purpose of chapter 3 is to quantify the initial sediment budget response of a foredune to disturbance from dynamic restoration activity and vegetation re-establishment using high resolution bare earth DEMs from terrestrial laser scanner (TLS) surveys and orthophotographs from structure from motion (SfM) surveys. The specific objectives of this section are: 1) examine deviations in seasonal foredune morphology from longer term 5 year trends (January 2012 – February 2017) in the year following vegetation removal, 2) analyze beach-foredune sediment budget responses to vegetation presence/absence and high energy wind and wave events in the year following initial vegetation removal (May 2015 – September 2016), 3) assess the impact of seasonal sediment budgets and vegetation presence/absence on foredune recovery following winter storm erosion.

2. Foredune morphodynamics and sediment budgets at seasonal to decadal scales: Humboldt Bay National Wildlife Refuge, California, USA.

2.1 Abstract

Coastal foredunes are diverse and dynamic shore-parallel ridges along the backshore, which are spatially and seasonally linked to natural sedimentation cycles. Aeolian and littoral sediment transport to the beach-dune complexes of California are largely controlled by dynamic meteorological patterns, climate forcing events (i.e., ENSO) and presence/absence of vegetation. Previous studies on shoreline change in Northern California report only broad rates of erosion and accretion related to regional meteorological regimes and as such may not be applicable at smaller spatial scales. A 5 year monitoring history of the sand dunes in the Humboldt Bay National Wildlife Refuge (HBNWR) provided opportunity to assess decadal to seasonal beach-dune morphodynamics at a 2.5 km stretch of foredune. Aerial photograph analysis examined historical (1939 -2014) foredune position, using the Digital Shoreline Analysis Software (DSAS) and assessed interannual morphodynamic changes through the digitization of geomorphic features. Seasonal volumetrics were analyzed from cross-shore transect data, providing information on sedimentation patterns in the foredune and beach. These findings set the historical context of foredune morphodynamics and allow exploration of the implications of seasonal meteorological variation on long-term (75-year) foredune evolution and development at the HBNWR.

DSAS describes maximum foredune progradation in the north (up to +0.51 m a^{-1}) and maximum foredune retreat in the south (up to -0.49 m a^{-1}). Analysis of aerial photography from 2004 – 2014 shows statistically significant larger erosive features in

the south zone than in the north and central zones. Seasonal volume calculations from cross-shore profiles indicate statistically significant differences in alongshore transect elevation and foredune volume, with larger elevations and volumes in the north and central zones than in the south. Combined with evidence of seasonal bidirectional littoral drift, these data support a north to south gradient in sediment availability, foredune position and resulting stages of established foredune development. Seasonal storm energies and climate forcing events introduce variability in erosive patterns, but support the persistence of alongshore developmental stages. Future research should explore foredune morphodynamics on a smaller spatial scale and changes related to presence/absence of multiple vegetation assemblages.

2.2 Introduction

Coastal foredunes evolve as a consequence of aeolian sediment transport across the beach and subsequent deposition on the backshore in the presence of roughness elements such as vegetation, wrack, and wood debris (Godfrey, 1977; Goldsmith, 1989; Hesp, 1989; Hemming and Nieuwenhuize, 1990; Arens, 1996; Hesp, 2002; Eamer and Walker, 2010 Luna et al., 2011). Incipient foredunes often develop as shore-parallel ridges that evolve via sedimentation within pioneer plant communities and backshore debris (Hesp, 1984; 2002; Arens and Wiersma, 1994; Eamer and Walker, 2010; Luna et al., 2011; Nordstrom et al., 2011a; 2011b). Under stable coastline conditions and with sustained sand delivery to the backshore, incipient dunes may grow and become established foredunes, characterized by morphological complexity and late-stage successional plant communities (Hesp, 1988; 2002; Pickart and Sawyer, 1998; Heathfield and Walker, 2011). Deposition patterns on foredunes are thus widely dependent on the

spatial zonation, density, distribution, and physical characteristics of dune plant species (Hesp, 1988; Arens, 1996; Ruggiero et al., 2011). Open sand surface areas and increased exposure to aeolian action are greatest during winter months on some coasts and in latitudes north of 40 degrees, whereas increased vegetation cover, surface sheltering, and aeolian deposition within the plant canopy prevail during the summer growth season. Such phenological controls are most pronounced in areas where vegetation dies back to a point where it is unable to recover to its previous extent. The absence of vegetation may lead to an increase in wave erosion in the winter coupled with pronounced aeolian transport of drier sediments across foredunes during the summer (Goldsmith, 1989; Arens, 1996; Hesp, 2002; Kuriyama et al., 2005; Walker et al., in press).

Foredune morphodynamics are also affected by the littoral sediment budget that fronts the beach-foredune system. (Short and Hesp, 1982; Hesp, 1988; 2002; Sherman and Bauer, 1993; Scott et al., 2010; Ollerhead et al., 2013; Houser and Ellis, 2013). Sediment transport and delivery within and between major morphological components (i.e., the beach, foredune and backdune) is controlled by beach-surf zone type and variations in wind speed, direction, and available beach fetch (e.g., Bauer and Davidson-Arnott, 2002; Miot da Silva and Hesp, 2010; Delgado-Fernandez and Davidson-Arnott, 2009; 2011; Houser and Ellis, 2013; Hesp and Smyth, 2016). Dynamic wind, wave and water levels related to seasonal storms or climatic variability may alter littoral and aeolian sediment transport exchanges between morphological components. For example, previous research in the Pacific Northwest has linked occurrences of El Niño Southern Oscillation (ENSO) phases to increased mean water level, increased significant wave height, and shifts in dominant wave direction (Ruggiero et al., 2001; Subbotina et al.,

2001; Allan and Komar, 2002; Barnard et al. 2015). Changes in these conditions with ENSO phases can, in turn, alter the local sediment budget response of shorelines as has been observed across the Pacific Ocean basin (Storlazzi et al., 2000; Allan and Komar, 2002; Heathfield et al., 2013; Barnard et al., 2015). As a consequence, a sediment budget (volumetric change) approach can be used to provide insight into the link between key morphological components of the beach-dune ecosystem and the resultant evolution of the foredune.

Previous studies have shown that beach-foredune sediment budgets can be easily quantified at the meso-scale (with a spatial extent of 10s of meters to kilometers and an annual to decadal temporal scale) (Davidson-Arnott and Law, 1996; Darke et al., 2016). Despite this, there are relatively few meso-scale studies of beach-dune sediment transport repeated frequently enough to capture seasonal controls on foredune morphodynamics (e.g., McLean and Thom, 1975; Anthony et al., 2006; Delgado-Fernandez and Davidson-Arnott, 2009; Arens et al., 2013; Hesp, 2013; Ollerhead et al., 2013; Walker et al., in press). Repeat morphological monitoring using cross-shore transects (e.g., McLean and Thom, 1975; Ollerhead et al., 2013) or detailed land surveys (e.g., Darke et al., 2013; Eamer and Walker, 2013) allow for observation of erosion and deposition and related volumetric changes. In turn, these observations can be quantified to estimate seasonal volume change and/or foredune development in coastal dune ecosystems.

The purpose of this chapter is to examine and quantify historical changes in foredune morphology and position in relation to beach-foredune sediment budgets at the Humboldt Bay National Wildlife Refuge (HBNWR) in Northern California. Dunes at this site have been the focus of several coastal management projects, and there exists an extensive

dataset of morphological changes, predominantly from aerial photographs and cross-shore topographic survey transects. The monitoring history at this site provides a unique opportunity to quantify meso-scale sediment budget patterns and foredune morphodynamics. The specific research objectives of this study are to analyze and interpret interannual to decadal scale changes in coastal foredune position and other geomorphic changes from aerial photography between 1939 and 2014. In addition, the study examines recent seasonal variability in erosion and accretion patterns in the beach-dune system and addresses the implications for the long-term evolution of the foredune complex.

2.3 Study site

This study was conducted in the Lanphere and Ma-le'l sand dune systems within HBNWR located near Arcata in Northern California. The study area consisted of a 2.5 km stretch of established foredunes to the north of Humboldt Bay and the Eel River and south of the Little and Mad Rivers (Figure 2). The site was divided into north, central and south zones according to dominant long-term (1939 – 2014) trends in foredune position (Figure 2).

The established foredunes at the study site are continuous alongshore and often fronted by incipient foredunes that vary in size and persistence over time, depending on wind and wave run-up patterns, storm frequency, beach widths, and the presence or absence of pioneer plant communities. The foredunes are backed by active parabolic and transgressive dune fields oriented toward the SE, in alignment with formative onshore winds from the NNW during late spring through summer (April – September). The resultant drift direction is 128.7° for aeolian sediment transport based on estimation of

regional transport using the model of Fryberger and Dean (1979) (Figure 3). Dominant offshore winds from the SE also occur in the fall and winter months (October – March). A sediment transport threshold of 6.76 m s^{-1} was calculated using the Bagnold (1941) model and the average grain size (D_{50} = 0.23 mm).

Dominant wave direction varies seasonally, coming from the NNW from April to September and predominantly from the WNW from October to March (Figure 4). Furthermore, wave height and period is higher in the fall-winter (October to March) than in the spring-summer (April to September) (Figure 4). Seasonal shifts in wind and wave regimes lead to bi-directional longshore drift for the Eureka Littoral Cell (Dingler and Clifton, 1994; Hapke et al., 2006; 2009). For example, wind and wave directions from the NW combine with sediment supply from the Little and Mad Rivers to drive a net southerly longshore drift direction during the summer months (Figure 2 and 3). During the winter season, from October to March, dominant offshore wind directions from the SE and wave directions out of the WNW align with a seasonal southward and offshore shift in the Hawaiian High Pressure system. These meteorological conditions contribute to a net (but variable) littoral drift direction from the south to the north (relative to the orientation of the shoreline, which is oriented slightly NE-SW) (Hapke et al., 2006; 2009). An increase in storm-generated North Pacific Swell reaching the coast, normally having the capacity to bring sediment onshore, may instead cause localized erosion if offshore sediment supply is limited. Erosion at the southern portion of the study site from winter storm waves may occur as net northerly waves deposit transported offshore sediment from the Eel River when contacting the Humboldt Bay Jetty system. North

Pacific Swell waves may result in net erosion at the southern end of the study site and subsequent variability in deposition of eroded sediment onto the beach moving north.

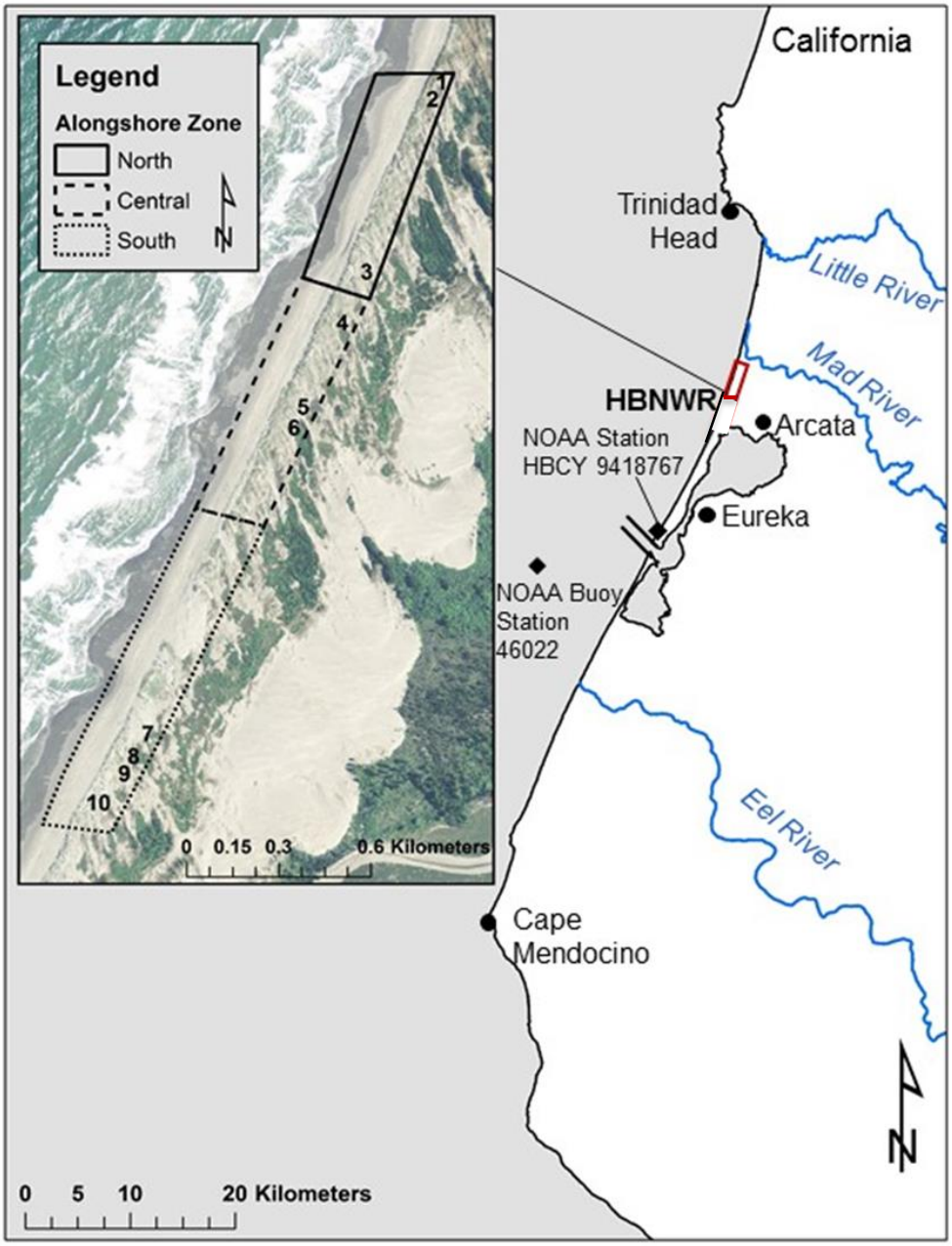

Figure 2. Regional map of (HBNWR) near Arcata and Eureka in Northern California, USA. Inset photo shows north, central and south alongshore zones. Coincident topographic survey locations are also indicated.

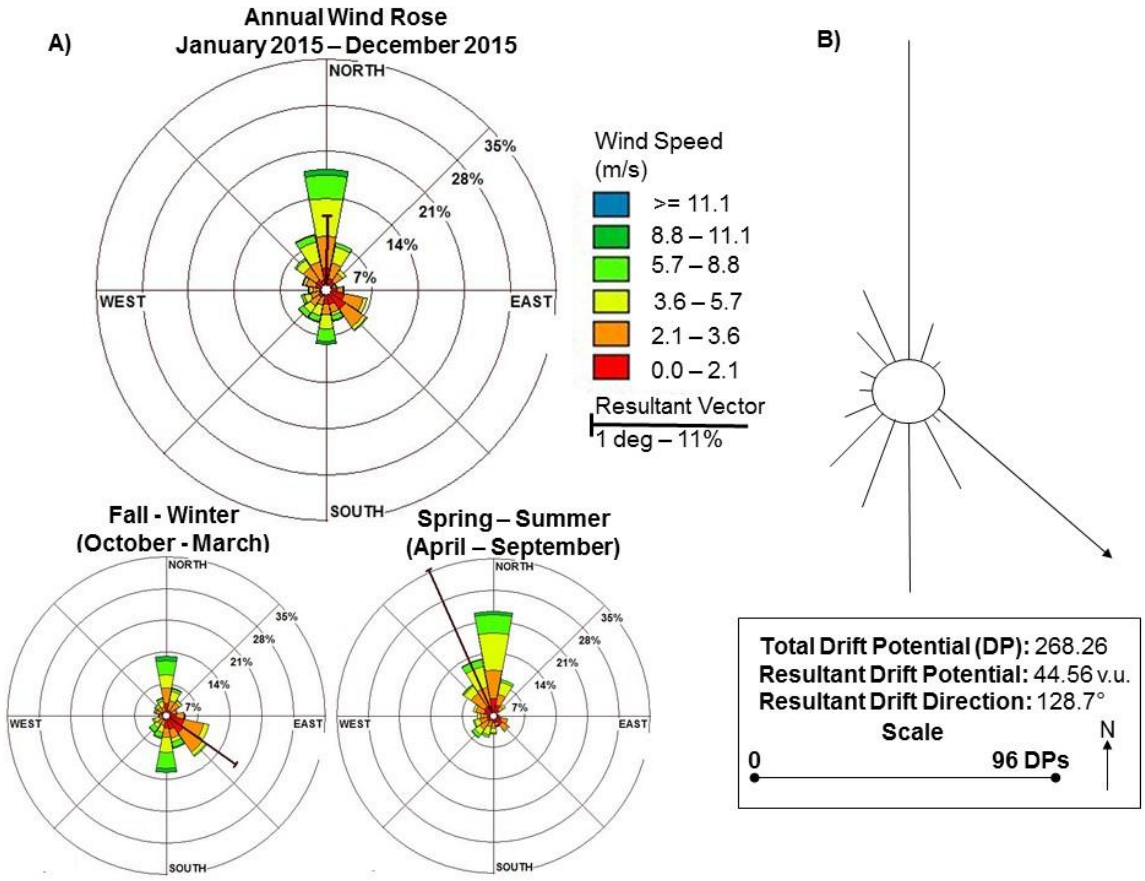

Figure 3. Annual wind rose (A) and aeolian sediment drift potential rose (B) generated from 24-hour observations for 2015 for North Spit, CA. Resultant wind vectors (black) show average wind direction. The sediment drift potential rose shows drift potential (DP) from almost all compass directions and the resultant drift direction vector (RDD, black arrow length in vector units) toward the SSE. Wind rose was generated using Lakes Environmental's WR Plot (https://www.weblakes.com/products/wrplot) while sediment drift rose was produced using the Fryberger and Dean (1979) method with m s^{-1} wind data per Miot da Silva and Hesp (2010). (Data source: Station HBYC1, 94187667 at North Spit, CA).

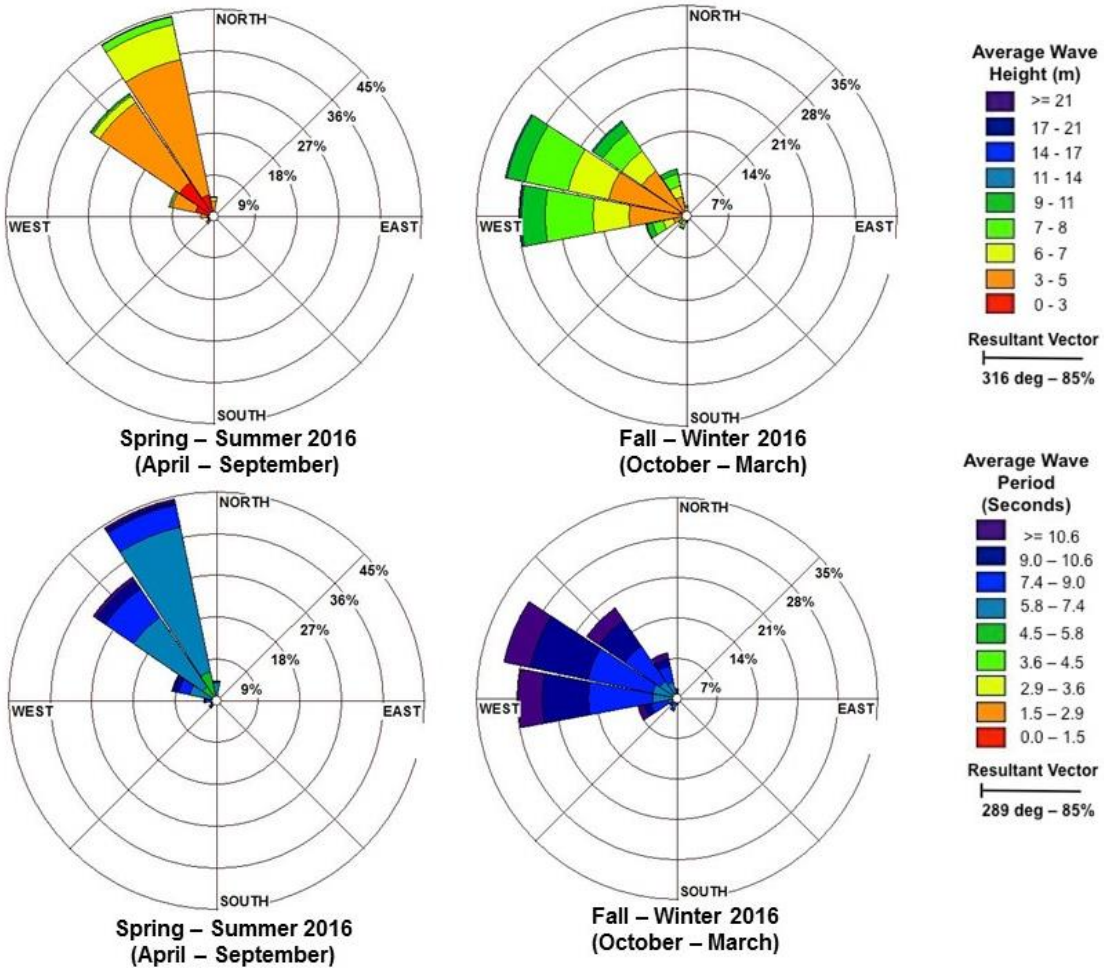

Figure 4. Annual wave roses generated from 24-hour observations of significant wave height (m), average wave period (seconds) and wave direction (degrees) in 2016 at the NOAA Buoy Station 46022 at Eel River, CA. Wave roses were generated using Lakes Environmental's WR Plot (https://www.weblakes.com/products/wrplot).

Table 1.Annual significant wave height (m), average wave period (s) and long term monthly water level (m) for the period 1980 to 2014. Annual maxima and minima are listed in brackets. Wave data recorded at NOAA Buoy Station 46022 at Eel River, CA (Data acquired: March 14, 2017 from http://www.ndbc.noaa.gov/station_history.php?station=46022). Long term (1980 – 2014) average monthly water level data recorded from NOAA Tidal Station 9418767 (Date acquired: March 28, 2017. Data source: https://tidesandcurrents.noaa.gov/datums.html?units=1&epoch=0&id=9418767&name=North+Spit&state=CA)

	Annual	Fall - Winter (November – March)	Spring - Summer (April – October)
Hourly Average Significant Wave Height (m)	2.53 (10.79, 0.01)	2.96	2.01
Hourly Average Wave Period (seconds)	7.32 (16.81, 2.55)	8.09	6.77
Monthly Mean Water Level (m)	5.57 (7.45, 3.55)	5.62	5.53

2.4 Methods

2.4.1 Meteorological data and analysis

Wind speed and direction data for 2015 were collected from 24-hour observations for North Spit, CA. These data were used to produce annual and seasonal wind roses and frequency tables for the 16 cardinal directions using Lakes Environmental WRPlot View software. Mean grain size of surface sediment samples was calculated using GRADISTAST version 8 (Blott and Pye, 2011) and used to calculate a sediment transport threshold using the Bagnold (1941) model. Finally, a sediment drift rose was produced using the Fryberg and Dean (1979) model and m s^{-1} transport threshold per methods outlined in Miot da Silva and Hesp (2010).

Seasonal storm events typically generate elevated storm surges, wave heights and wave run-up causing potential erosion and landward shoreline retreat when water surge exceeds a mean high high water level (MHHWL) (Allan and Komar, 2002; Allan et al.,

2003). For this study, the seaward toe of the established foredune was identified from a light detection and ranging (LiDAR) derived bare earth model from May 2015. The line delineating the foredune toe represents a threshold above which the established foredune can be eroded by wave action. The foredune toe line was digitized in QT Modeler software version 8. Elevation values from the digitized foredune toe were averaged across the study site and used as a proxy for a foredune erosional threshold in reference.

Variability in sea level and wave dynamics occur during phases of climate forcing phenomena. Recent research has shown a link between positive phases of monthly to interannual ENSO phases (El Niño) and multi-year to decadal Pacific Decadal Oscillation (PDO) events to increased frequency of extreme storms on the west coast of North America (Abeysirigunawardena and Walker, 2008; Abeysirigunawardena et al., 2009). For example, El Niño and (PDO) are both characterized by warmer sea surface temperatures in the coastal northeastern Pacific and localized variability in precipitation and wind regimes (Wolter and Timlin, 1993; Storlazzi and Wingfield, 2005; Barnard, 2015). Average monthly values of three main climate indices commonly used to quantify phases of climate variability and ocean-atmosphere anomalies were collected from NOAA Earth System Research Laboratory for the period 1982 – 2012. Positive values of the Multivariate ENSO Index (MEI) and the Pacific Decadal Oscillation (PDO) are associated with conditions characteristic of warm ENSO (El Niño) and PDO phases respectively, such as warmer sea surface temperatures and increased water levels along the west coast of North America. Negative values of the MEI and PDO indices are associated with conditions characteristic of cold ENSO phases (La Niña), in which lower sea surface temperatures and increased upwelling in the eastern Pacific have been

observed. The Northern Oscillation Index (NOI) is a regionally defined index that describes positive and negative ENSO phases according to variations in sea level pressure in the Northeast Pacific and Darwin, Australia (Schwing, et al., 2002). NOI values, in contrast to the MEI and PDO indices, associates positive NOI values with La Niña and negative NOI values with El Niño. Climate variability index values were plotted against corresponding water level and wave height data to isolate periods of increased localized energy that may be associated with climate forcing phenomena.

2.4.2 Aerial photograph analysis

Aerial photographs from 1939 to 2014 with sufficient coverage of the study site (i.e., seaward extent of vegetation visible, all transect locations visible) and relatively large scales (i.e., 1: 25,000 or greater) were analyzed to detect changes in foredune morphology and position (Table 2). All photographs were resampled within ArcGIS software to represent equal pixel resolutions of 1 m. A bilinear interpolation method was chosen to resample aerial photographs because the original continuous pixel values can be retained in the new resampled image. Resampled aerial photographs from 1939 through 1992 were georeferenced to the rectified USDA-NAIP 2014 photograph using 10 identical ground control points (GCP) identified from the corner of physical structures (i.e., houses, airports) and road intersections. The photos were orthorectified in QGIS using the UTM Zone 10 coordinate system and the 1983 North American Datum (NAD83). A nearest neighbor resampling method and Polynomial 1 transformation type were used to transform the georeferenced aerial photographs to the coordinates of the 2014 NAIP imagery (Thieler and Danforth, 1994). The resulting orthorectified geotiffs,

along with the USDA-NAIP digital aerial photograph series, were used as a reference for the digitization of the seaward extent of vegetation and other relevant geomorphic units.

Georeferencing error was accounted for using the root-mean-square error (RMSE) method per Wang et al. (2012) when assessing accuracy of the polynomial least squares geometric correction. RMSE values were calculated for each georeferenced (1939 -1992) air photograph using the residual x and y positional uncertainty values for the 10 GCPs in each photograph (Table 3). Industry standard accuracy values of 0.15 m were assigned for each photograph within the UDSA NAIP digital aerial photograph series (2004 - 2014) (Table 3).

Table 2. Date, source, original format and resampling information of 75-year aerial photograph record for geomorphic mapping and shoreline change analyses.

Aerial Photographs

Resampling Parameters:		
1 m resolution		Bilinear Interpolation
Original format: Scanned GeoTIFFs		**Used for:** - Long-term Foredune Position Change - Decadal-Scale Foredune Position Change
Date	**Original Resolution (m)**	**Source**
1939	0.29	Humboldt County Public Works
1948	0.70	Historic Atlas of Humboldt Bay and Eel River Delta
1954	0.75	as above
1958	0.50	as above
1965	0.70	as above
1981	1.00	as above
1992	1.00	as above
Original Format: Digital Orthophotographs		**Used for:** - Geomorphic Mapping - Long-term Foredune Position Change - Decadal-Scale Foredune Position Change
Date	**Original Resolution (m)**	**Source**
2004	1.00	USDA National Agriculture Imagery Program (NAIP)
2005	1.00	as above
2007	1.00	as above
2009	1.00	as above
2010	1.00	as above
2012	1.00	as above

Table 3. Georeferencing error (Wang et al., 2012) and digitization error (Thieler and Danforth, 1994) calculated for aerial photographs from 1939 – 2014. DSAS derived end point rate (EPR) error is calculated for each study interval using methods outlined by Thieler and Danforth (1994).

Georeferencing Error (m) **Method used:** Root mean square error (RMSE) of ground control point location residuals			**Digitization Error (m)** **Method used:** Average DSAS shoreline change envelope (SCE) statistic		
Date	**RMSE (m)**	**SCE (m)**	**Total Error (m)**	**EPR Intervals**	**Average of Total Errors (m)**	**DSAS EPR Error (m a^{-1})**
1939	10.15	7.07	17.23	**1939 - 1948**	18.10	2.01
1948	6.50	12.47	18.97	**1948 - 1954**	16.07	2.68
1954	5.02	8.15	13.18	**1954 - 1958**	14.23	3.56
1958	7.12	8.16	15.28	**1958 - 1965**	13.32	1.90
1965	6.05	5.32	11.37	**1965 - 1981**	13.26	0.83
1981	5.01	10.14	15.16	**1981 - 1992**	9.69	0.88
1992	2.23	2.00	4.23	**1992 - 2004**	4.04	0.34
2004	0.15	3.71	3.86	**2004 - 2005**	3.19	3.19
2005	0.15	2.36	2.51	**2005 - 2009**	3.27	0.82
2009	0.15	4.18	4.33	**2009 - 2010**	3.73	3.73
2010	0.15	3.28	3.43	**2010 - 2012**	3.16	1.58
2012	0.15	3.04	3.19	**2012 - 2014**	3.62	1.81
2014	0.15	4.20	4.35	**1939 - 2014**	9.01	0.12

2.4.3 Shoreline change analysis

Shoreline change values were estimated using the Digital Shoreline Analysis System (DSAS) developed by the United States Geological Survey (Thieler et al., 2009), which operates as a plugin for ArcGIS version 10. DSAS statistics are generated from the measurement of multiple digitized historical ‘shorelines’ in reference to a static user-defined baseline. For this study, a fixed baseline was established at the landward origin of ten topographic sampling transects. ‘Shoreline’ shapefiles were digitized using the seaward-most line of established foredune vegetation, excluding the incipient foredune. The incipient foredune was excluded due to inconsistencies in the ability to delineate

sparse pioneer plant communities within the backshore. The resulting line shapefile is considered a proxy for the seaward toe of the foredune (Figure 5). Cross shore transects were generated by DSAS at 5 m intervals alongshore to calculate shoreline positions and changes. DSAS-derived end point rate (EPR), or rate of annual shoreline position change, were calculated by dividing the total distance of shoreline movement by the number of years between the oldest and youngest shorelines as captured in the photos. EPR statistics were used to explore both the long-term average positional change of the foredune (1939 – 2014) and decadal-scale patterns of foredune change (i.e., 1939 – 1948, 1948 – 1954, 1954 – 1958, etc.) (Table 3).

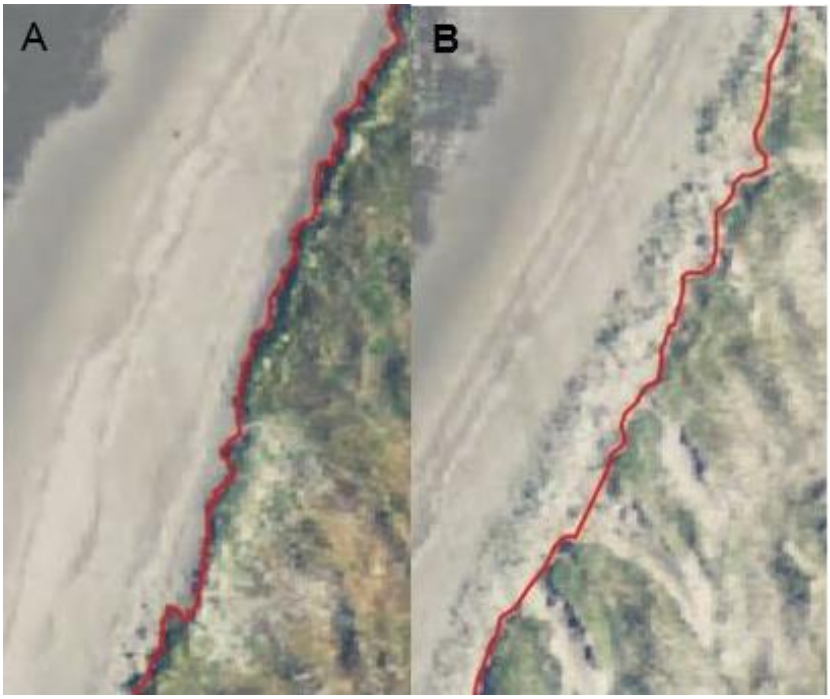

Figure 5. The identification of the visible vegetation line and the resultant digitization of this visible vegetation line to create a DSAS 'shoreline' from the 2012 USDA-NAIP aerial photograph. A) digitized shoreline shapefile (in red) in a simple delineation of the visible vegetation line with no incipient foredune zone B) shows complex delineation of the visible vegetation line where incipient foredune zones and blowouts are observed.

DSAS error thresholds comprise positional uncertainty (i.e., georeferencing RMSE) and measurement (digitization) uncertainty (Thieler and Danforth, 1994). The DSAS shoreline change envelope (SCE) was used to calculate digitization error for each photo year as suggested by Thieler and Danforth (1994) (Table 3). SCE represents the distance between shoreline shapefiles measured farthest from and closest to a defined baseline for each DSAS generated transect. Three shoreline shapefiles for each photo year were digitized from the visible seaward-most vegetation line by the same operator (Figure 6). The resulting duplicate shapefiles were input into DSAS to produce SCE statistics for their respective photo years. The total error was calculated for each photo by adding corresponding georeferencing and digitization error values (Table 3). Finally, per Thieler and Danforth (1994), EPR errors were calculated for each DSAS interval by dividing the average of the total error values of all aerial photographs included in each study interval by the number of years between the first and last photograph in each series (Table 3). The resulting error represents a detection threshold value for annual shoreline change (in m a^{-1}), below which shoreline change is considered undetectable, or within the margins of error.

2.4.4 Geomorphic mapping

Aerial photographs from 2004 to 2014 were used to identify and digitize changes in topography using ArcGIS. The high resolution and colorized format of this photo series allowed for accurate identification of erosional and depositional units, partly through the visual presence/absence of vegetation. Polygons delineating unvegetated deflation basins that occur on the established foredune (erosional unit) and visible pioneer plant communities seaward of the toe of established foredunes (depositional unit) were

digitized (Figure 6). Geomorphic units were grouped into north, central and south units, as defined by alongshore zones distinguished by different rates of change in foredune position (Figure 2). The total surface area of erosional and depositional units was calculated in ArcGIS and normalized by dividing the total erosional unit and incipient foredune areas in the north, central and south zone by the total area of each respective zone. The difference in mean normalized area and mean normalized annual areal change between north, central and south geomorphic units was examined in R using one-way analysis of variance (ANOVA) (Fischer, 1935). Tukey's honest significant difference (HSD) post-hoc statistical test was performed to identify pairs of zones for which statistically significant differences in area and areal change occurred. Investigation of normalized area and annual normalized areal change of erosive units and incipient foredunes from 2004 – 2014 provided information on spatial and temporal variability in geomorphic unit evolution.

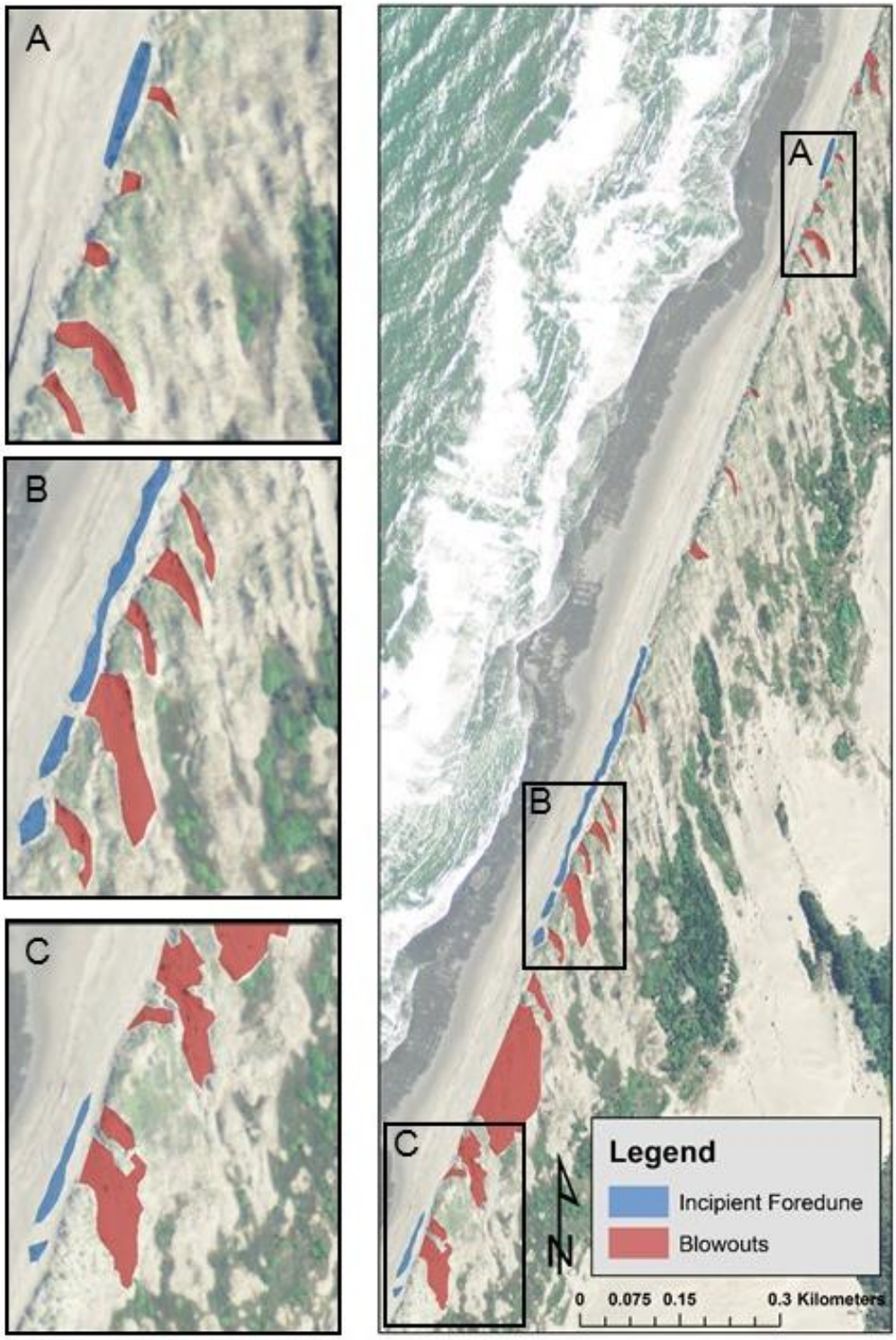

Figure 6. Examples of mapped erosional units in the established foredune (red) and of the incipient foredunes (in blue) in front of the established foredune.

2.4.5 Topographic survey transects

Ten topographic transects were established in January 2012 by the US Fish and Wildlife Service (USFWS) across the study site, as outlined in Pickart (2014). Profiles vary in length from 156 to 276 m from the survey benchmarks to the water line. Surveys were conducted bi-annually in winter and summer seasons, from establishment to July 2015. The locations of these transects were originally chosen to represent the three foredune vegetation assemblages or 'alliances' dominant in the study area (Sawyer et al., 2009): i) *Ammophila arenaria* herbaceous alliance (transects 1, 2), ii) *Elymus mollis* herbaceous alliance (5, 6, 8, 9) and, iii) Dune mat herbaceous alliance (3, 4, 7, 10).

Three geomorphic zones (backdune, foredune, and beach) were identified for each transect (Figure 7). However, only the foredune and beach were used for interpreting morphological and sediment volumetric changes due to little to no volumetric change observed in the backdune during the study. The foredune zone extended cross-shore from the first point of inflection on the lee slope (which remained unchanged through time) to the seaward-most vegetation line during measurement, including the incipient foredune. The stoss toe of the foredune is typically tied to the seaward most-extent of seasonal vegetation (Hesp 2002; 2013). As such, this line defines the boundary separating the backshore from the foredune. Alternatively, to shoreline shapefiles created for shoreline change analysis, the incipient foredune was included in the foredune zone definition because the profiles provide more consistent delineation of the incipient foredune and beach boundary than aerial photographs. The second zone, or unvegetated active beach, was defined by the area between the seaward vegetation line and the contour line associated with an elevation of 3.7 m above mean sea level (masl in reference to

NAVD88), a common closing point for all topographic transects to allow for sediment volumes to be compared.

Elevation data were collected from each of the 10 topographic transects bi-annually from winter 2012 to summer 2015. Topographic measurements were taken at 1-meter intervals along each transect from the benchmark in the backdune to the waterline. A Trimble R10 real-time kinematic global positioning system (RTK-GPS) was used to collect elevation measurements in reference to the NAVD88. A vertical error threshold of +/- 0.01 m was determined for the elevation values based on the largest reported vertical error from multiple 5-hour benchmark GPS observations.

2.4.4.1 Transect volume calculation

Topographic profile data were plotted (Figure 7) and an R script was created to calculate the area underneath the entire profile, the foredune, and the beach units for each season. The volume underneath each profile surface was calculated by multiplying the vertical change in elevation measurements by 1 m^2 in area to yield a volume measurement (m^3). The volume calculations varied between seasons depending on the location of the seaward extent of vegetation that marked the boundary between the beach and foredune zone. As such, normalized volume measurements were calculated by dividing the seasonal volume of the foredune and beach zones by the respective transect lengths in each season, to facilitate comparison of volume changes through time.

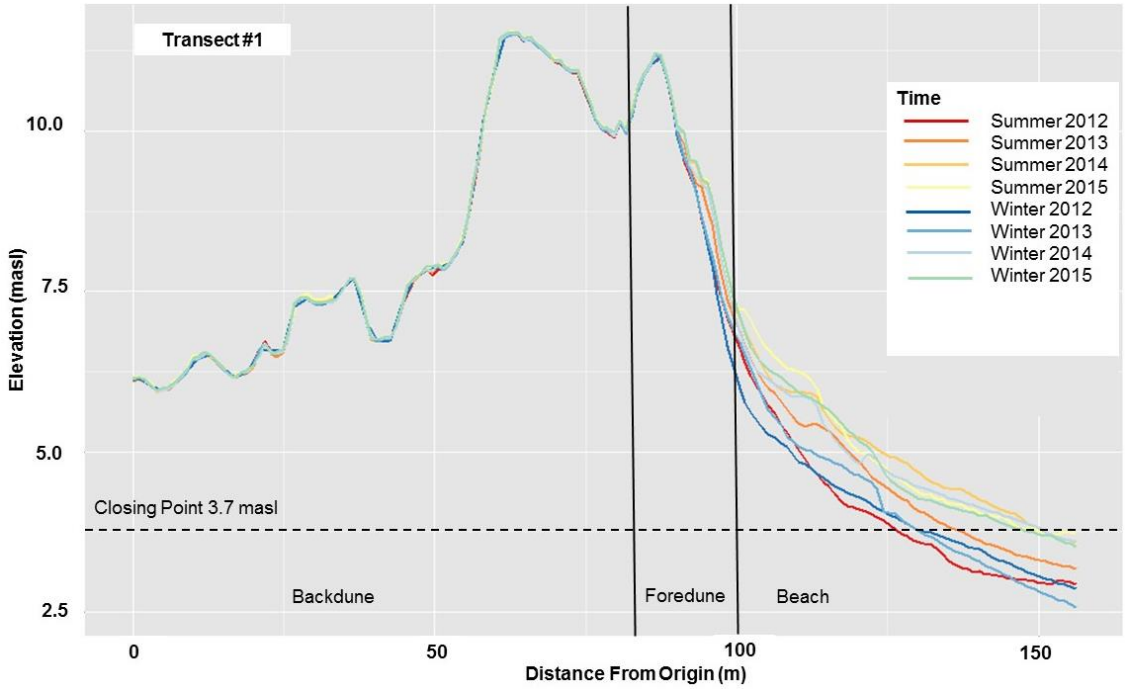

Figure 7. An example of topographic changes at transect 1 recorded from winter 2012 to summer 2015. The extent of three geomorphic zones delineated from winter 2012 topographic measurements indicate the backdune (which, in this case includes a stabilized secondary foredune ridge), foredune, and beach.

Statistically significant differences in the total (combined beach and foredune) transect elevations, beach width, normalized volume and normalized monthly volume change between transects in the north (1,2,3), central (4,5,6) and south (7,8,9,10) alongshore zones were analyzed using ANOVA and Tukey's HSD post-hoc test. Furthermore, Welch Two Sample t-tests were used to test a null hypothesis that normalized monthly volume change underneath transects is independent of spatial (i.e., beach vs. foredune) and temporal (i.e., summer vs. winter) variation. The first t-test examined the difference between normalized monthly volume change values of all 10 transects between the beach and foredune zones. The second t-test examined the

difference between normalized total (combined beach and foredune) monthly volume change of all 10 transects between the summer and winter monitoring periods.

Finally, a Spearman's rank-order correlation test was performed on four variables (normalized monthly volume change in the foredune zone, normalized monthly volume change in the beach zone, alongshore zone grouping from north to south and increasing time from winter 2012 to summer 2015) in order to examine relationships between independent (time, zone) and dependent (volume change) variables that could help explain temporal and spatial variation in volume across the study site. The Spearman correlation coefficient, *r*, was chosen as it can evaluate monotonic relationships between continuous and ordinal data. Time and alongshore zone were ranked ordinally for simplicity and consistency to be comparable within the correlation calculation. Time was ranked from 0, representing the baseline survey in winter 2012 up to 7, the last survey in summer 2015, while alongshore zone was ranked from 1 in the north to 3 in the south.

2.5 Results

2.5.1 Shoreline positional change analysis

The long-term (75-year, 1939 - 2014) spatially averaged annual change in foredune position, or end point rate (EPR) was -0.04 m a^{-1}. Figure 8 shows, however, that the northern portion of the foredune system migrated seaward at rates up to +0.51 m a^{-1}, while the southern portion retreated landward at rates up to -0.49 m a^{-1}. The central zone was characterized by areas of negligible foredune position change and slow rates of seaward foredune migration (from +0.13 to +0.27 m a^{-1}, +/- 0.12 m a^{-1}) and landward retreat (from -0.13 to -0.35 m a^{-1}, +/-0.12 m a^{-1}) (Figure 8). The spatial clustering of change rates derived from the long-term (1939 – 2014) foredune position trends were

used to define the north, central and south alongshore zones used in this and other parts of the analysis (Figure 2).

End point rate (EPR) values across the study site for 12 short-term aerial photograph intervals between 1939 and 2014 are displayed in Figure 9. Three photo intervals (1939 – 1948, 2005 – 2009, 2012 – 2014) exhibit similar EPR trends as the long-term 75-year study interval, with net seaward advance of the foredune in the north to landward retreat in the south. Intervals in between 1948 and 2005 are characterized by more spatially consistent rates of foredune position change across the entire study domain, with detectable trends largely dominated by net erosion (e.g., 1948 – 1954, 1992 – 2004) or net accretion (e.g., 1965 – 1981, 1981 – 1992) with minor variation in localized spots (Figure 9).

Figure 10 displays the variation (distance from the median) in EPR for 8 decadal photo intervals from 1939 – 2014. The largest average EPR values are from 1954 – 1958 (+4.19 m a^{-1}) and 2004 – 2014 (average EPR +2.25 m a^{-1}) (Table 4, Figure 10). Exactly half of the shorter time intervals exhibit negative average EPR values, indicative of landward retreat of the foredune (Table 4). An inset figure shows greater variation in EPR when examined at shorter more recent intervals from 2004 – 2014 (Figure 10). Average EPR for the north, central and south alongshore zones are compared in Figure 11. In all 12 aerial photograph intervals, the largest absolute EPR values are recorded in either the north or south zones, with smaller magnitude EPR values recorded in the central zone. The southern zone experienced larger magnitude EPR values then the northern zone in 7 of 12 intervals (Figure 11). Of these 7, the southern zone experienced negative average EPR rates, indicative of landward retreat, in 5 study intervals (Figure

11). Additionally, 3 of the 5 interannual aerial photograph intervals from 2004 – 2014 indicate positive EPR values in the north zone and negative EPR values in the south (Figure 11). During 3 time intervals from 1965 – 2004, EPR values in all zones remained relatively similar.

.

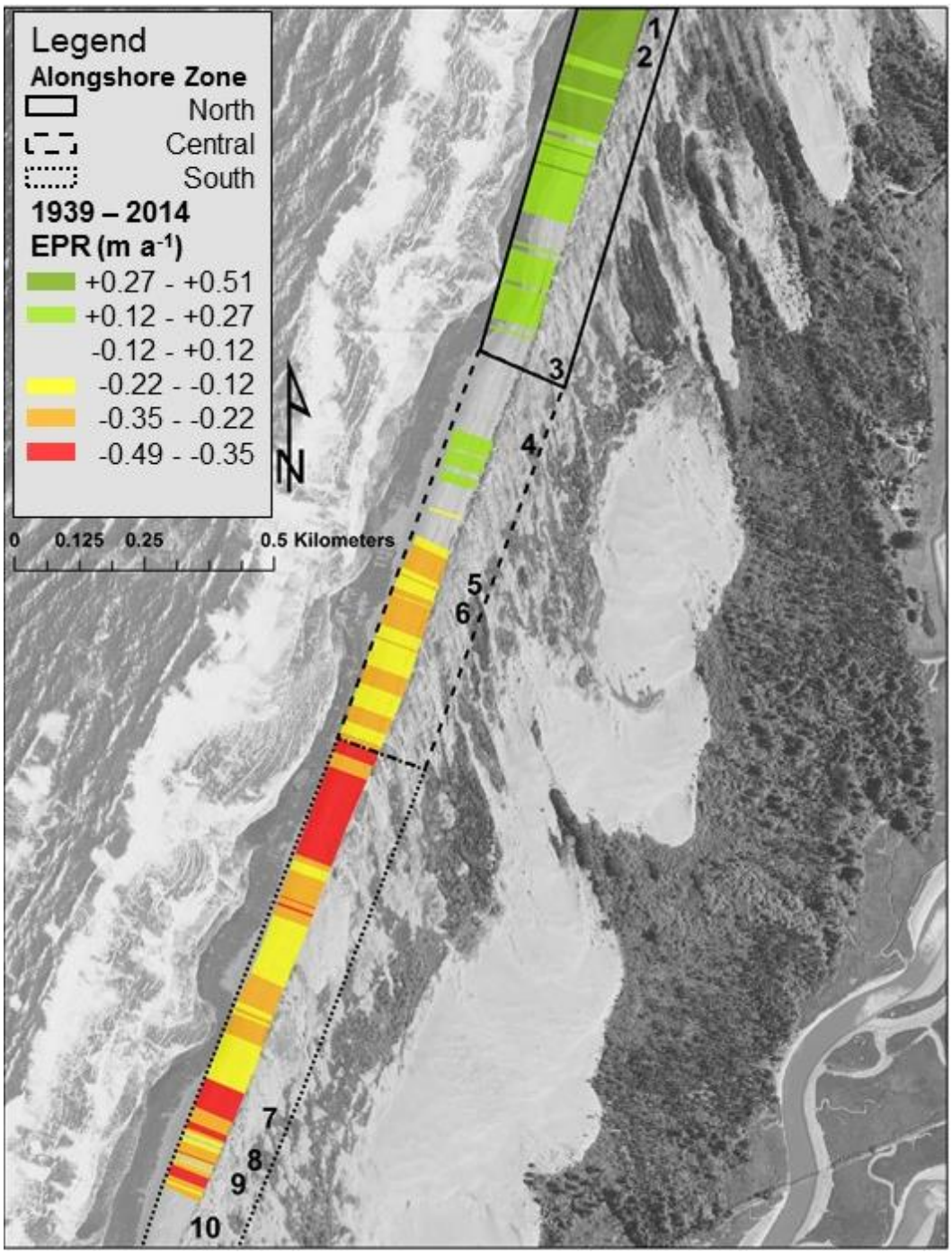

Figure 8. Annual rates of change (end point rate, EPR m a^{-1}) in seaward extent of the foredune across the Lanphere and Ma-le'l sand dune units from 1939 - 2014. Areas with no color, as indicated in the legend, represent insignificant change. These data were produced using the Digital Shoreline Analysis System (DSAS) (Thieler et al., 2009). The north, central and south alongshore zone boundaries and transect locations 1 – 10 are displayed for reference.

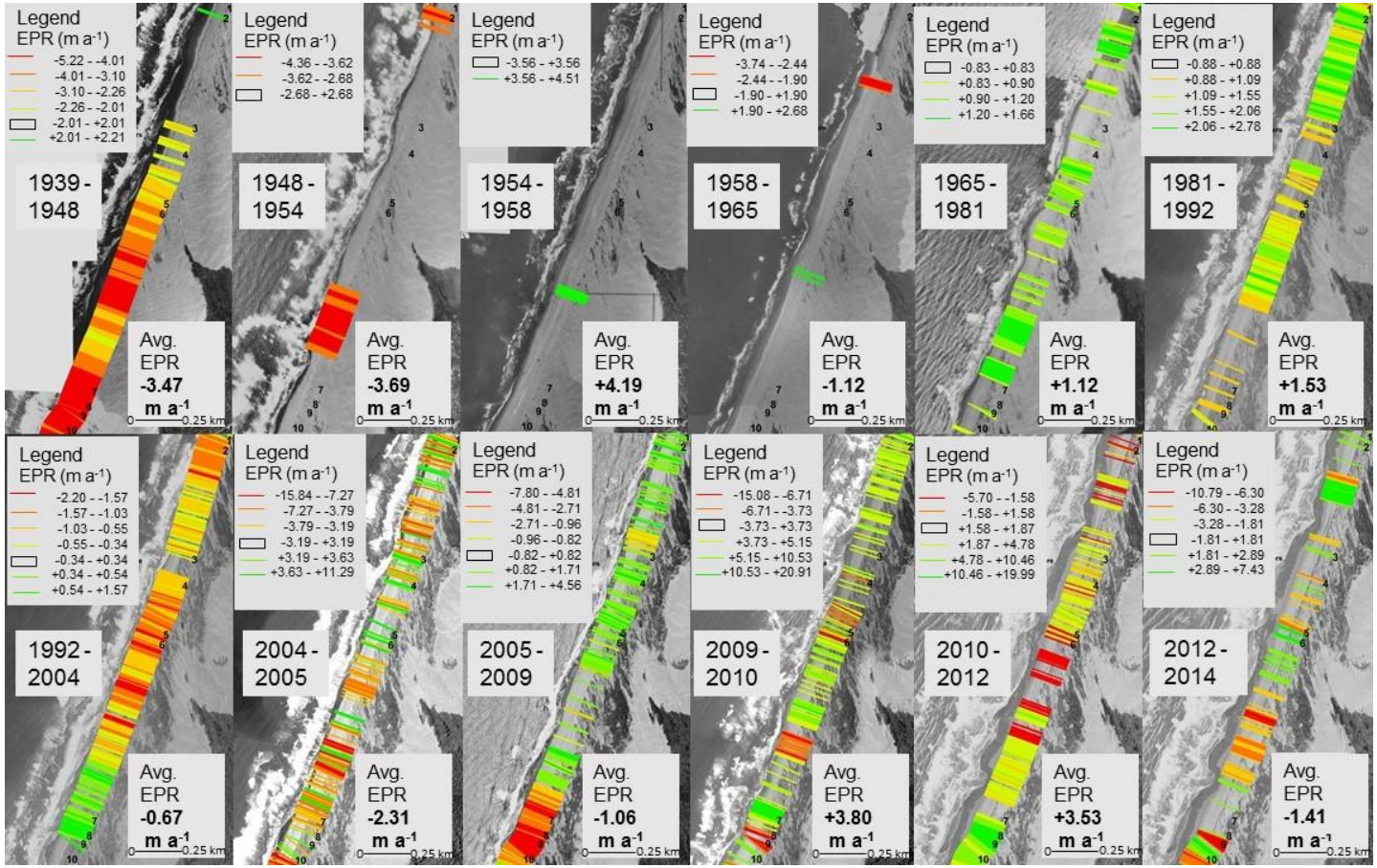

Figure 9. Annual rate of change (end point rate, EPR m a^{-1}) in seaward extent of the foredune for 12 aerial photo intervals from 1939 – 2014. EPR values are displayed over the last aerial photograph of each study interval. Areas with no color, as indicated in the legends, represent areas of insignificant change. Transect locations are displayed for reference. Note the large variability in EPR values between aerial photograph intervals. As such, EPR legends are not normalized across time intervals and similar colors do not represent similar rates of change between intervals.

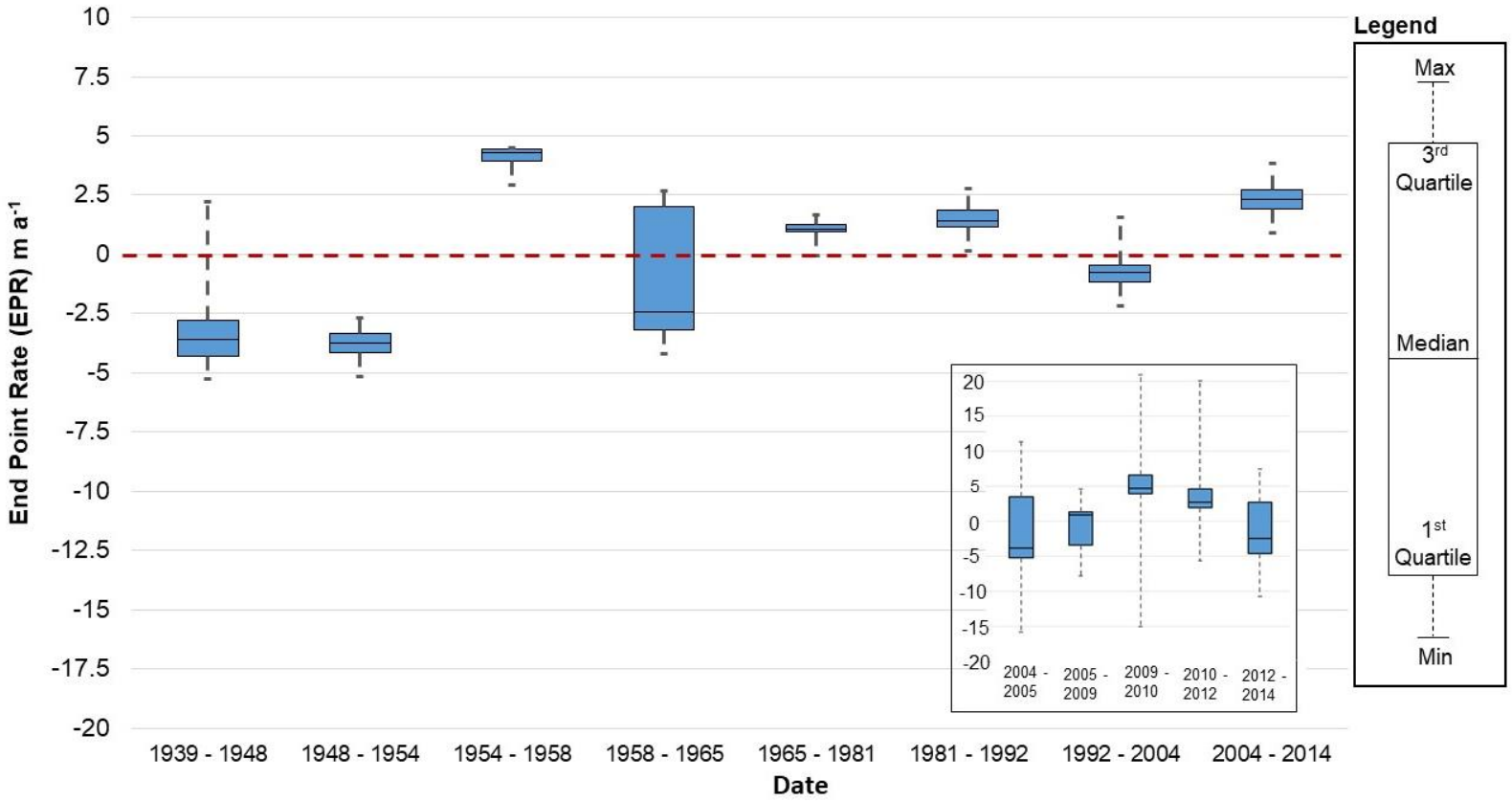

Figure 10. Distribution of annual EPRs around the median EPRs from 1939 – 2014 for 8 decadal time intervals. The lower and upper whisker indicates the minimum and maximum EPR value for each interval. The lower box boundary and upper box boundary represents the first quartile (25th percentile) and third quartile (75th percentile), respectively. The inset box and whisker plot shows the distribution of EPRs for shorter interannual intervals from 2004 – 2014.

Table 4. Minimum, median, maximum, 1st and 3rd quartile values used to create a boxplot of the distribution of annual EPR (m a^{-1}) for each photo interval from 1939 – 2014.

Date	**1939 - 1948**	**1948 - 1954**	**1954 - 1958**	**1958 1965**	**1965 – 1981**	**1981 - 1992**	**1992 - 2004**	**2004 - 2014**
Minimum (m a^{-1})	-5.22	-4.36	+3.57	-3.74	+0.84	+0.89	-2.2	-0.79
1st Quartile (m a^{-1})	-4.28	-4.15	+3.95	-3.21	+0.95	+1.15	-1.17	+1.91
Median (m a^{-1})	-3.57	-3.73	+4.28	-2.43	+1.08	+1.44	-0.78	+2.34
3rd Quartile (m a^{-1})	-2.77	-3.33	+4.45	+2.00	+1.28	+1.87	-0.45	+2.71
Maximum (m a^{-1})	+2.21	-2.69	+4.51	+2.68	+1.66	+2.78	+1.57	+3.82
Average EPR (m a^{-1})	**-3.47**	**-3.69**	**+4.19**	**-1.12**	**+1.12**	**+1.53**	**-0.67**	**+2.25**

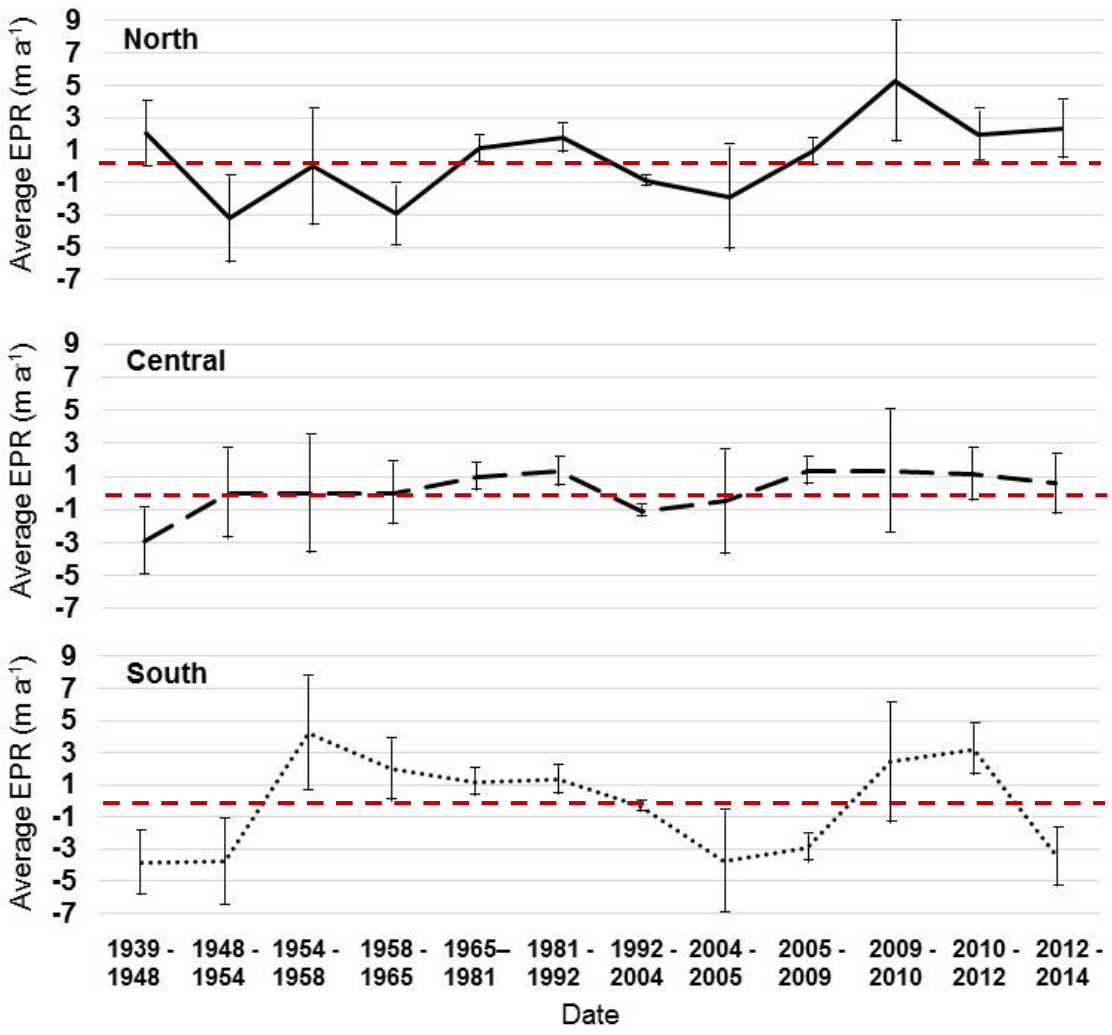

Figure 11. Average EPR values in the north, central and south alongshore zones for 12 aerial photograph intervals from 1939 – 2014.

2.5.2 Wind, wave and water level regimes

Monthly average significant wave height (Hs), wave period, mean water level and maximum water levels are plotted in Figure 12. A foredune erosional threshold value of 7.157 m in was calculated for the study site from a LiDAR point cloud and displayed in Figure 12 for reference. In general, the frequency of monthly average water level values

greater than the erosional threshold increases from 1982 – 2012. Monthly average Hs and wave period values were greatest from 2001 – 2008 (Figure 12). Figure 13 displays monthly average Hs and maximum water levels plotted against monthly average climate index values. Maximum Hs and water level values generally align with periods of El Niño, as indicated by large PDO index values (Figure 13). Additionally, large Hs values in February 1999 (4.18 m) and November 2007 (5.06 m) occur at the same time as positive NOI index values, indicative of La Niña phases (Figure 13).

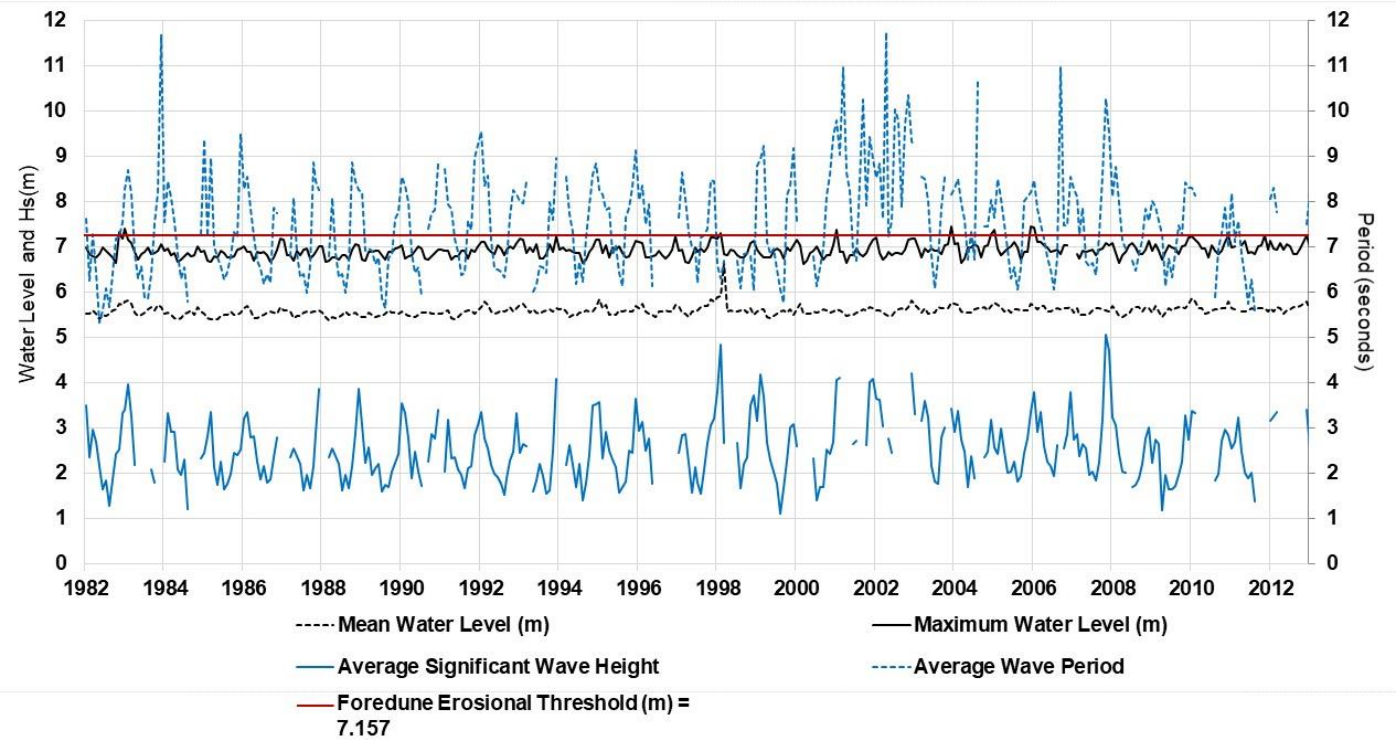

Figure 12. Plot displaying monthly average significant wave height (m), mean and maximum water level (m) and average monthly wave period (seconds). A recorded foredune erosional threshold is displayed in red for reference. Wave data was recorded at NOAA buoy station 46022 at Eel River, CA (Data acquired: March 14, 2017. Data source: http://www.ndbc.noaa.gov/station_history.php?station=46022). Average monthly water level data recorded from NOAA Tidal Station 9418767 (Date acquired: March 28, 2017. Data source: https://tidesandcurrents.noaa.gov/datums.html?units=1&epoch=0&id=9418767&name=North+Spit&state=CA)

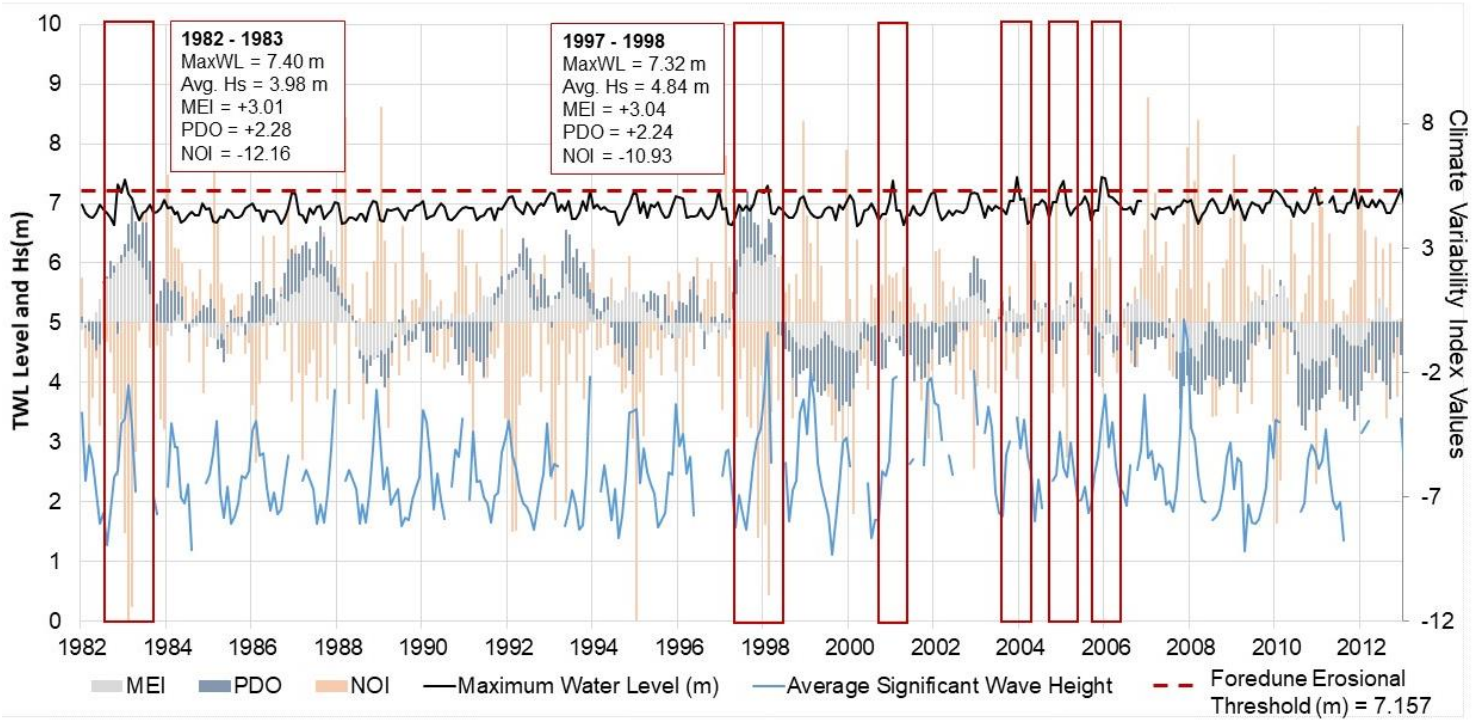

Figure 13. Time series displaying average monthly significant wave height (m) and maximum water level (m) plotted against a stacked bar graph of three climate variability index values MEI, PDO, NOI. Red boxes are drawn around time periods that exhibit maximum water level over an erosional threshold for foredunes at the study site. Maximum wave, water level and index values for 2 time periods regularly referenced for particularly extreme climate forcing events are indicated. Wave data was recorded at NOAA buoy station 46022 at Eel River, CA (Data acquired: March 14, 2017. Data source: http://www.ndbc.noaa.gov/station_history.php?station=46022). Average monthly water level data recorded from NOAA Tidal Station 9418767 (Date acquired: March 28, 2017. Data source: https://tidesandcurrents.noaa.gov/datums.html?units=1&epoch=0&id=9418767&name=North+Spit&state=CA). Climate Index data acquired from NOAA Earth System Research Laboratory (Data acquired: March 28, 2017. Data source: https://www.esrl.noaa.gov/psd/data/climateindices/list/).

2.5.3 Landform changes

Table 5 shows the total area and annual areal change of geomorphic units from 2004 – 2014 in the north, central and south zones. Erosive units in the north and central zones experienced alternating cycles of annual areal growth and reduction from 2004 – 2012, while southern erosive units increased steadily in area from 2004 – 2012. From 2012 – 2014, erosive units in the north, central and south zones experienced an annual areal decrease of -589, -776 and -2701 $m^2\ a^{-1}$ respectively. Annual areal change of incipient foredunes from 2004 – 2014 was predominantly positive across the study site.

Across the entire study site, erosive units generally increased in area from 2004 – 2010, particularly in the central and south zones, followed by an areal decrease from 2010 - 2014 (Figure 14). Annual areal change of incipient foredunes across the study site appeared relatively small in magnitude (< 1,000 m^2) from 2004 – 2012. From 2012 – 2014 the areal extent of incipient foredunes in the southern zone increased significantly (+2404 $m^2\ a^{-1}$). The largest areal changes in both erosive units (i.e., blowouts) and incipient foredunes occurred in the south, while the northern zone generally experienced the smallest annual areal changes in both geomorphic units (Table 5; Figure 14).

Although the north and central zones did not differ, ANOVA results (Table 6) show that erosional unit area in the south was significantly larger than both the north ($p = 2.5 \times 10^{-7}$) and central zones ($p = 1.4 \times 10^{-7}$). No statistically significant difference was found in mean incipient foredune area between the three zones ($p = 0.121$). Similarly, no difference in annual areal change of either erosive unit or incipient foredune area between zones was detected ($p= 0.92$ and 0.80, respectively).

Table 5. Total area (m^2) and annual areal change (m^2 a^{-1}) of geomorphic units (erosive units and incipient foredunes) in the north, central and south zones.

	Northern Erosive Units		Central Erosive Units		Southern Erosive Units	
Date	Total Area (m^2)	Change in Area (m^2 a^{-1})	Total Area (m^2)	Change in Area (m^2 a^{-1})	Total Area (m^2)	Change in Area (m^2 a^{-1})
2004	1592	-	1513	-	9546	-
2005	2449	+857	3241	+1728	11340	+1794
2009	1417	-258	1885	-339	18403	+1766
2010	2607	+1190	3407	+1522	22262	+3859
2012	1983	-312	+1903	-752	23112	+425
2014	805	-589	352	-776	17710	-2701
	Northern Incipient Foredune		**Central Incipient Foredunes**		**Southern Incipient Foredunes**	
Date	Total Area (m^2)	Change in Area (m^2 a^{-1})	Total Area (m^2)	Change in Area (m^2 a^{-1})	Total Area (m^2)	Change in Area (m^2 a^{-1})
2004	0	-	296	-	529	-
2005	0	0	1218	+922	402	-118
2009	303	+76	3541	+581	970	+142
2010	675	+372	3325	-216	313	-657
2012	477	-99	3061	-132	1496	+592
2014	2124	+824	3858	+399	6304	+2404

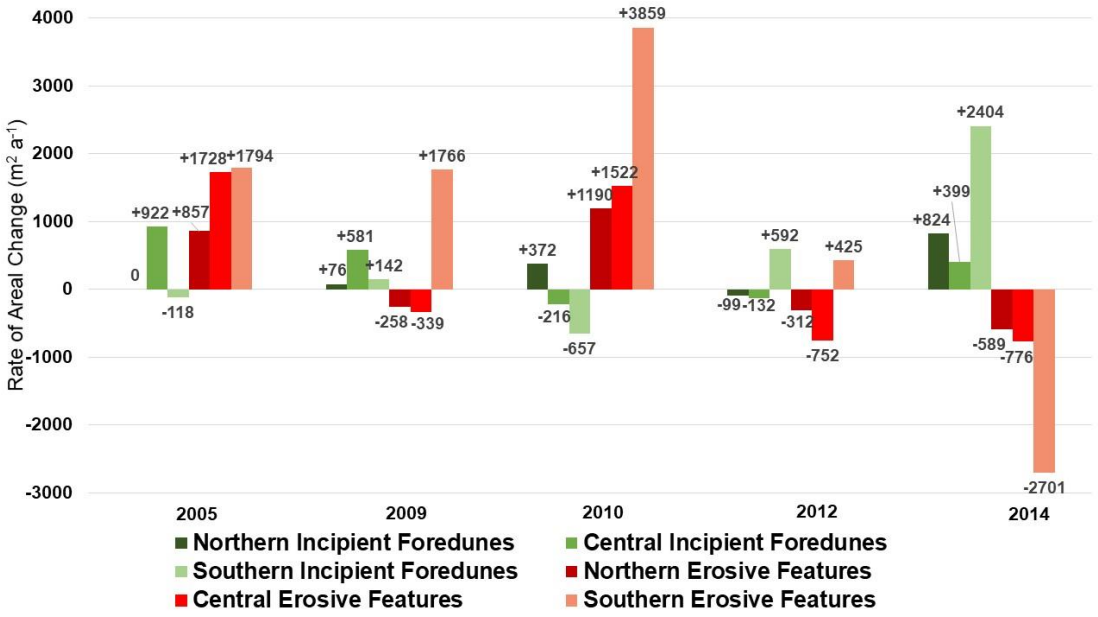

Figure 14. Changes in average annual areal coverage of geomorphic units across the entire study area as calculated from geomorphic mapping based on aerial photograph analysis.

Table 6. Summary of ANOVA and Tukey HSD test results for significant differences in area (m^2) and annual areal change ($m^2\ a^{-1}$) between geomorphic units in the north, central and south alongshore zones.

Analysis of Variance (ANOVA) Test

	Normalized erosive unit area (m^2)			Normalized incipient foredunes area (m^2)		
Location	North	Central	South	North	Central	South
Mean	0.09	0.15	1.30	0.03	0.18	0.13
ANOVA P Value	4.87×10^{-7}			0.121		
Statistically Different	✓			X		
Tukey HSD Comparison	North - Central	North - South	Central- South	North - Central	North - South	Central - South
P Value	0.93	2.5×10^{-7}	1.4×10^{-7}	-	-	-
Statistically Different	X	✓	✓	-	-	-
	Annual change in normalized area of erosive unit ($m^2\ a^{-1}$)			Annual change in normalized area of incipient foredune ($m^2\ a^{-1}$)		
Location	North	Central	South	North	Central	South
Mean	+0.01	+0.02	+0.02	+0.01	+0.02	+0.04
ANOVA P Value	0.92			0.80		
Statistically Different	X			X		

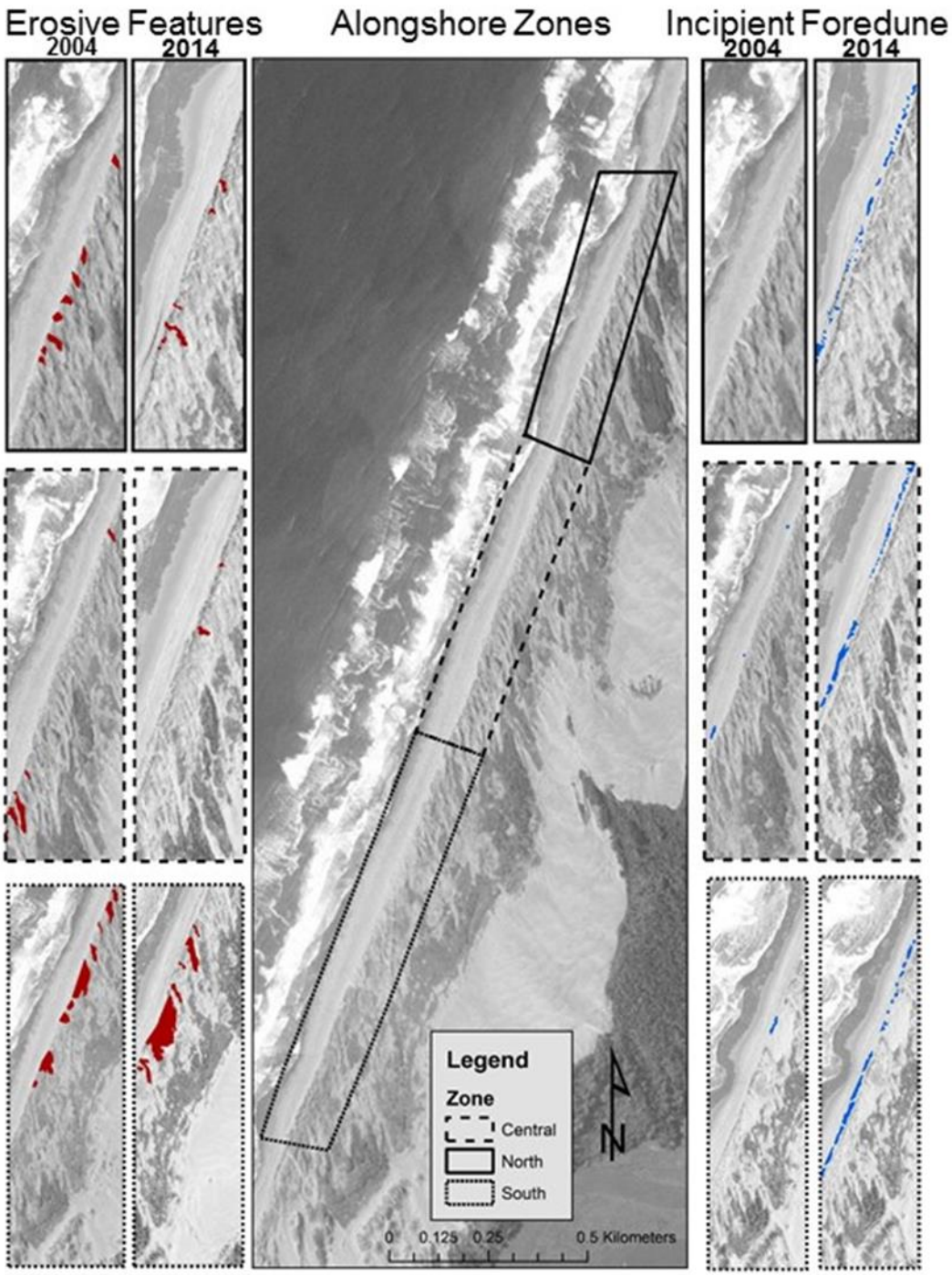

Figure 15. Evolution of erosive units (principally blowouts; red polygons) and incipient foredunes (blue polygons). Smaller panels display geomorphic units from the north, central and south zones from 2004 and 2014

2.5.4 Sediment volume change and statistical analysis

Minimum and maximum beach and foredune volumes for each transect are shown in Table 7. Figure 16 shows monthly residual values from the winter 2012 to summer 2015 site-wide average rate of foredune and beach volume change. Residual values of the average monthly rate of volume change that deviate the most from the site-wide average in the foredune (1.84 m^3 mo^{-1}) and the beach (2.23 m^3 mo^{-1}) are found in transect 9, while transect 2 and transect 10 display the smallest deviations in foredune and beach volume change, respectively. Fairly consistent rates of residual volume change in both the foredune and beach are seen in transects 2 – 4. Transects 5 and 6 are characterized by small scale monthly decreases in foredune and beach volume change (Figure 16). In the southern zone, transect 7 – 10 demonstrate variable rates of residual volume change (Figure 16).

ANOVA and Tukey HSD tests were performed to identify statistically significant differences in mean total (combined beach and foredune) transect elevation, mean beach width, mean normalized foredune and beach volumes and mean normalized foredune and beach monthly volume changes between northern, central and southern transects (Table 9). The mean total transect elevation and mean foredune volume are greater in the north and central zones than in the south (p values 2×10^{-16} and 5.95×10^{-9}, respectively). However, there is no significant difference in beach width, total volume, beach volume or normalized monthly volume changes in either beach or foredunes between alongshore zones.

A Welch Two Sample t-test demonstrated no statistically significant difference in average normalized monthly volume change between the beach and foredunes zones of

all 10 transects. A second t-test demonstrated a statistically significant (p-value < 0.05) difference between monthly normalized volume change in the summer (mean of -0.038 $m^3\ mo^{-1}$) and winter seasons (mean of +0.054 $m^3\ mo^{-1}$). Site-wide volume changes in both the beach and foredune zones are positively but weakly correlated with time, producing *r* values of 0.17 and 0.14, respectively (Figure 16). An *r* value of 0.38 indicates that the monthly site-wide foredune volume change is weakly positively correlated with monthly site-wide beach volume change (Figure 16).

Table 7. Minimum, maximum and average volume (m^3) in the foredune and beach zones of transects 1 – 10 across all monitoring periods (winter 2012 – summer 2015). The rate of volume change statistics (+/- 0.01 m^3 mo^{-1}) in the foredune and beach are listed in brackets for all transects.

Northern Transect Volumes (m^3)							
Foredune Transect	**Min. Volume**	**Max. Volume**	**Mean SE +/- 202.71 (m^3)**	**Beach Transect**	**Min. Volume**	**Max. Volume**	**Mean SE +/- 47.56 (m^3)**
1	150.30 (-15.70)	355.60 (+16.50)	241.38 (+2.65)	**1**	100.10 (-10.68)	167.80 (+10.28)	149.10 (+0.30)
2	209.30 (+0.30)	275.80 (+7.22)	257.81 (+1.58)	**2**	53.10 (-8.20)	293.50 (+21.55)	144.25 (+4.55)
3	756.00 (-9.50)	813.00 (+2.23)	781.64 (-0.34)	**3**	0.00 (-21.25)	326.30 (+20.55)	186.94 (+4.73)
Central Transect Volumes (m^3)							
4	591.60 (-8.92)	652.30 (+5.97)	614.96 (-0.14)	**4**	45.60 (-5.57)	253.80 (+22.43)	159.80 (+4.27)
5	847.30 (-11.82)	953.30 (+14.42)	912.36 (+0.62)	**5**	44.00 (-10.33)	182.80 (+21.05)	114.85 (+1.74)
6	533.00 (-4.82)	617.40 (+11.20)	571.26 (+1.45)	**6**	35.40 (-19.33)	198.50 (+16.87)	126.90 (+0.52)
Southern Transect Volumes (m^3)							
7	426.50 (-6.82)	607.00 (+20.88)	553.94 (+3.54)	**7**	46.70 (-114.30)	209.60 (+131.8)	128.29 (+5.76)
8	564.80 (-9.57)	632.90 (+9.83)	594.03 (+1.53)	**8**	65.90 (-11.80)	200.00 (+21.07)	133.54 (+0.50)
9	252.80 (-0.65)	502.70 (+36.42)	461.15 (+5.95)	**9**	79.50 (-33.40)	279.90 (+12.25)	156.93 (-2.18)
10	686.90 (-8.73)	800.50 (+8.87)	746.31 (+1.52)	**10**	88.90 (-8.52)	200.90 (+13.88)	145.41 (+2.08)

Table 8. Summary of ANOVA and Tukey HSD results testing for significant differences in total (beach and foredune) transect volume (m^3) and monthly total volume change (m3 mo^{-1}), normalized foredune volume (m^3) and volume change (m^3 mo^{-1}) and normalized beach volume (m^3) and volume change (m^3 mo^{-1}) between north, central and south alongshore zones.

	Total Transect Volume (m^3)			**Total Transect Volume Change (m^3 mo^{-1})**		
Location	North	Central	South	North	Central	South
Mean	587.04	833.38	674.56	4.49	2.82	3.72
ANOVA P Value	0.38			0.93		
Statistically Different	**X**			**X**		
	Normalized Foredune Transect Volume (m^3)			**Normalized Foredune Transect Volume Change (m^3 mo^{-1})**		
Location	North	Central	South	North	Central	South
Mean	9.23	9.00	8.01	-0.02	0.01	-0.07
ANOVA P Value	5.95×10^{-9}			0.96		
Statistically Different	✓			**X**		
Tukey HSD Comparison	North-Central	North-South	Central-South	North-Central	North-South	Central-South
P Value	0.5	0	4.1×10^{-6}	-	-	-
Statistically Different	**X**	✓	✓	-	-	-
	Normalized Beach Transect Volume (m^3)			**Normalized Beach Transect Volume Change (m^3 mo^{-1})**		
	North	Central	South	North	Central	South
Mean	4.31	4.31	4.40	+0.05	+0.07	+0.02
ANOVA P Value	0.79			0.97		
Statistically Different	**X**			**X**		

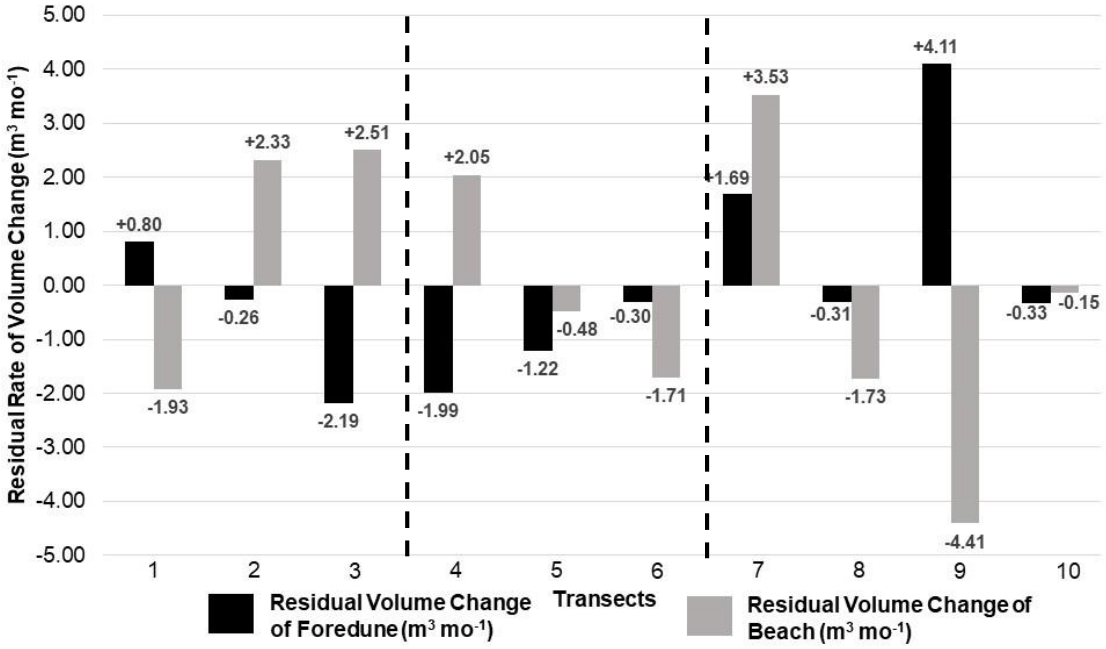

Figure 16. Residuals of monthly volume change ($m^3\ mo^{-1}$) for each transect from the long term (winter 2012 – summer 2015) average rate of monthly volume change across all transects. Dotted lines indicate the boundary lines for the north, central and south zones.

2.6 Discussion

2.6.1 Long-term changes in established foredune position

The rate of foredune position change, as defined by the average position of the visible foredune vegetation line over the 75-year study period, is characterized by an alongshore gradient (Figures 8 and 9) with maximum foredune progradation of +0.51 m a^{-1} in the north and foredune retreat (-0.49 m a^{-1}) in the south. Insignificant foredune position change in the northern half of the central zone transitions to small-scale landward retreat in the central-south zone boundary (Figure 8). Thus, the central zone represents a transitional regime in regard to the effect that aeolian transport, longshore littoral drift, and morphological sediment budget processes have on foredune position.

A regional scale study (Hapke et al., 2006) of short-term shoreline change for the Eureka region (extending from 6 km south of Trinidad Head to Cape Mendocino; Figure 2) reported a similar north to south gradient in regional shoreline position, although there was a large data gap in the vicinity of the North and South spits of Humboldt Bay. In their study Hapke et al., (2006; 2009) attribute long-term shoreline change patterns in the larger Eureka Littoral Cell to directional variations in waves and currents. At the study site, seasonal wave regimes are dominated by northwesterly wind waves (280° - 330°, 1 – 4 m, 3 – 10 s) during the summer and North Pacific swell (210° - 350°, 2 – 10 m, 10 – 25 s) in the winter (Table 1, Figure 4) (Storlazzi and Wingfield, 2005). Along most of the California coastline, seasonal summer northwest wind waves and winter Pacific swell waves combine with the California Current to drive net sediment transport to the south in most littoral cells (Storlazzi and Wingfield, 2005; Hapke et al., 2006; 2009). The Eureka Littoral Cell deviates from this trend with alongshore sediment transport to the north in association with the southward migration of the Hawaiian High Pressure system during the winter (Hapke et al., 2006; 2009). Rivers act as a primary source of coastal sediment with an average of 70 – 95% of beach sand in California being delivered from coastal streams (Runyon and Griggs, 2002; Hapke et al., 2006). Although the exact contribution of sediment to the littoral system remains unknown at this site, Wheatcroft and Sommerfield (2005) suggest that large suspended sediment fluxes from the Eel River, to the south of the study site, and the Mad River, to the north of the study site, are significant sources of sediment to the littoral system, and thence to the beaches and coastal dunes.

The presence of an extensive transgressive dune system on the North Spit of Humboldt Bay is consistent with significant sediment supply over the Holocene from the Mad River, which also offers a possible explanation for the north to south gradient in beach-dune response captured in the photo analysis in this study. The combined effect of sediment retention on the coastal shelf just north of the study site at the mouth of the Mad River (Figure 2) and dominant north to south littoral drift during the summer might result in a sediment supply gradient, decreasing toward the south. As a consequence, less sediment is available to be cycled on-and-offshore in the south, effecting foredune size, position, and morphology (de Vries et al., 2012).

2.6.2 Recent interannual changes in foredune position and morphodynamics

A distinct climatic shift is thought to have occurred in the late 1970s, resulting in more frequent and stronger storms linked to widespread erosion of sandy shorelines (Storlazzi et al., 2000; Allan and Komar, 2002; Storlazzi and Wingfield, 2005; Hapke et al., 2006; 2009). Following a shift to positive PDO values and with warm ENSO phase like conditions in 1977, subsequent El Niño and La Niña events have been relatively more extreme, with a general increase in maximum water level values and particularly high intensity events during the winter months of 1982/83 and 1997/98 (Figure 13) (Storlazzi et al., 2000; Sallenger et al., 2002; Allan and Komar, 2002). Often, El Niño is followed by a strong La Niña phase (positive NOI and negative MEI values), such as that in 1998/99 (Figure 13) (Allan and Komar, 2002). Typically, during El Niño and positive PDO events sea surface temperatures increase in the coastal northeastern Pacific Ocean and atmospheric circulation patterns weaken or reverse, yielding higher water levels along the coast of California that can cause beach erosion. However, the impact of both

El Niño and La Niña at the study site appear to be uncharacteristic of the California coast in general, with storm energies during the 1998/99 La Niña resulting in higher rates of shoreline erosion at the study site than previous El Niño periods, as seen in the 1992 – 2004 shoreline change interval (Figure 9). During this interval, site-wide foredune retreat was observed, with an average EPR of -0.67 m a^{-1}. Such localized variations in coastal response to climate forcing are not uncommon for the Pacific Ocean basin (Barnard et al., 2015).

Previous studies indicate that blowout contraction may occur through re-vegetation as incipient foredune growth and/or pioneer plant communities interrupt wind flow into the mouths of blowouts (Gares and Nordstrom, 1995; Hesp, 2002; Abhar et al., 2015). Stabilization of certain parts of blowouts may result in the extension and enlargement of blowouts in another direction or portion of the blowout, depending on local scale factors such as vegetation growth patterns, sediment availability and wind flow (Hesp, 2002; Abhar et al., 2015). Variation in erosive unit response to a site-wide incipient foredune increase in areal cover is observed at the study site from winter 2012 - 2014, with simultaneous stabilization of erosive units in the north and landward extension of erosive units in the south (Figure 14, Figure 15). A north to south gradient in sediment availability could explain some of the morphodynamic responses at the southern end of the study site, where the largest erosive units continue to extend landward into the transgressive dune field, as less sediment is stored in an incipient foredune zone (Figure 15). Additionally, a north to south gradient in erosive unit evolution might also reflect spatial variation in foredune stabilization and developmental stages (per Hesp 1988), with clear erosive unit expansion in the south and healing in the north.

2.6.3 Spatial variability in established foredune development

Hesp (1988; 2002) proposed five stages of foredune development that progress from stage 1 foredunes, characterized by simple topography (topographically continuous, gently undulating) and dense vegetation, to stage 5 foredunes, characterized by the presence of remnant knolls, blowouts, small sheets, and sparse vegetation cover. The stages of foredune development represent a measure of stability of the foredune, as determined by sediment supply, long-term sedimentation patterns and morphological characteristics (beach width, height, volume) (Hesp, 2002). At the study site, foredunes in the north exhibit statistically larger seasonal foredune elevations and volumes then those in the south zone (Table 9). Additionally, residual volume change values in the beach are predominantly positive in the north (i.e., transects 2 and 3) and highly variable with both maximum and minimum residual volume change values in the south (Figure 16).

In the context of this model, the northernmost foredunes are similar to stage 1 foredunes, based on dense vegetation cover (90 – 100% of both invasive *A. arenaria* and native dune grass species), and the observed pattern of sediment accumulation likely due to a net positive sediment input into the beach, resulting in long-term foredune progradation (up to +0.51 m a^{-1}) (Figure 8, Figure 17). Farther south, foredunes transition into more dynamic, lower and hummocky morphologies, or Hesp's stage 3, where maximum landward retreat of the foredune (up to -0.49 m a^{-1}), a statistically significant larger erosive unit area and visible erosive unit areal expansion is observed (Table 5, Figure 15). The central zone may be considered a transition zone between northern stage 1 foredunes and stage 3 foredunes in the south, exhibiting statistically similar height, volume and geomorphic unit evolution values as northern stage 1 foredunes (Table 5,

Table 9), and foredune position change values ranging from insignificant to small scale landward retreat (Figure 8). Hesp (1988; 2002) suggest that foredunes may evolve to different stages of development following erosive events (e.g., major wave scarping, blowout formation, and/or vegetation dieback), or accretional events (rebuilding through revegetation and sediment infill). With measures of elevation and volume characteristics being relatively equal between the north and central foredunes, central foredunes may be continually transitioning between stage 1 and stage 2 foredunes based on alongshore variation in littoral drift and sediment supply patterns following seasonal storm events (Hesp, 2002) (Figure 8).

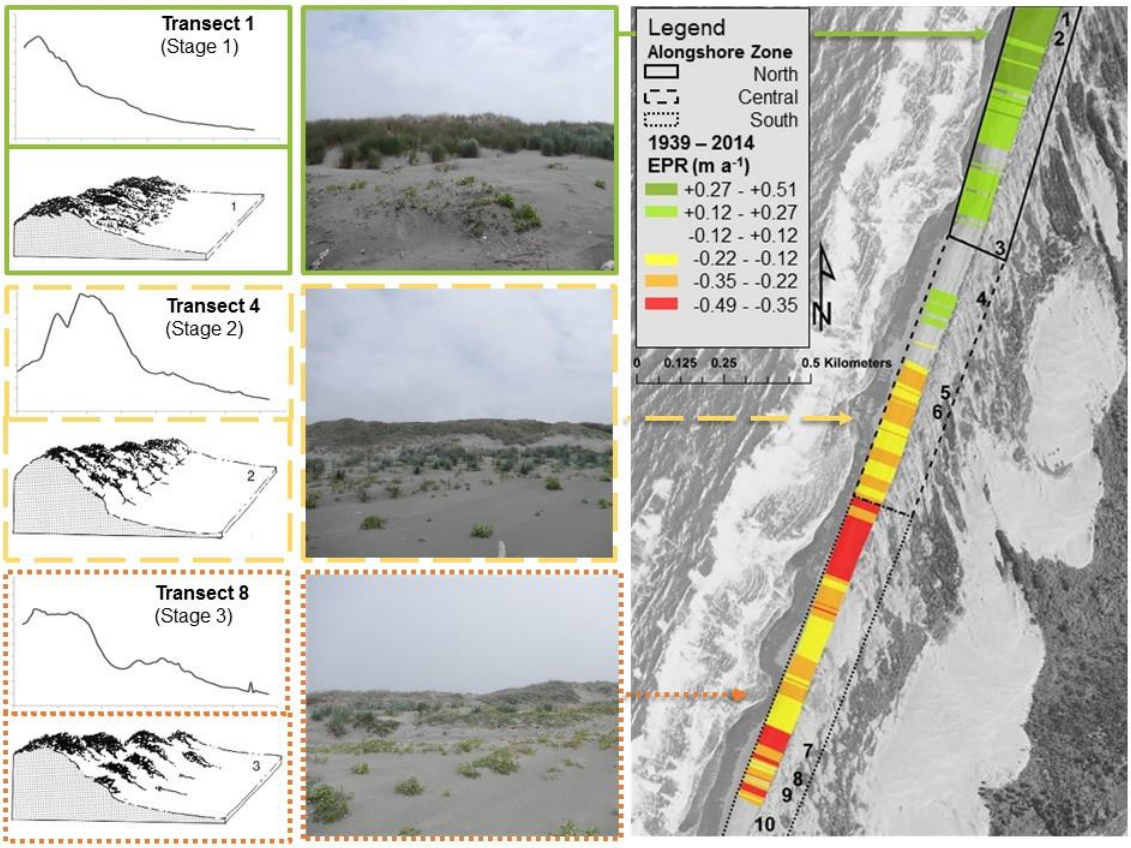

Figure 17. Cross-shore profiles from summer 2015 for transect 1, 4 and 8 located in the north, central and southern alongshore zones respectively. Photographs show the backshore and foredune morphologies of corresponding transects. Cross-shore profiles and photographs are set next to diagrams of foredune development stages 1 – 3, produced in Hesp (1988).

The observed gradient of generally stable foredunes in the north to more dynamic foredunes in the south and related foredune developmental stages might be dominantly related to interactions between sediment supply, surf zone type, and beach-dune dynamics (Short and Hesp, 1982; Hesp, 1988; Arens, 1996; Hesp, 2002). Previous studies (Cooper 1967; Psuty, 1988) suggest that foredune development may be a product of proximity to sediment source (e.g., river discharged sediment) and temporal variations in climate patterns that can alter sediment transport patterns. As such, the north to south gradient in foredune development (Figure 17) may result from alongshore variation in offshore sediment supply and transport following seasonal shifts in wave and aeolian transport energies. Across all transects examined in this study, seasonal volume changes were significantly greater in the beach zone than seasonal volume change in the established foredune, and greater in the winter season than in the summer season. Many studies show that the sediment volumes of beaches fluctuate greatly on a seasonal basis (Sherman and Bauer, 1993; Anthony et al., 2006; Ruggiero et al., 2010).

Summer northwest wind waves coupled with dominant littoral circulation to the south results in sediment being transported largely into the northern beach zone (Figure 4) (Harris et al., 2005; Storlazzi and Wingfield, 2005; Warrick, 2014). Higher sediment transport potential from the beach to the foredune, and through aeolian transport out of the NNW, supports the increase in dune ridge elevation and development of stage 1 foredunes in the north (Figure 3) (cf. Psuty, 1988). In contrast, lower sediment availability in the southern zone could result in smaller sediment inputs to the beach during the summer months, in turn resulting in topographic dune units with lower average elevations, such as the stage 3 foredunes (cf. Psuty, 1988). As such, erosive events fueled

by North Pacific swell coming out of the west and high water levels may result in seasonal destabilization of the foredune at the study site, particularly in the south, where foredunes are characterized by lower volumes and lower elevations (Figure 4, Table 9) (Storlazzi and Wingfield, 2005). With the return of summer littoral dynamics, foredunes in the north are replenished with higher offshore sediment supplies and transport potential into the beach, while limited sediment availability in the south lowers the opportunity for full foredune recovery, perpetuating the north to south trend in foredune development.

2.7 Conclusions

Historic patterns in foredune position and evolution of morphodynamic units, along with interannual sediment budget (volumetric) responses were analyzed at the Lanphere and Ma-le'l Dune units in HBNWR. The data allow an assessment of the various stages of morphological development of the foredunes and associated landform units across the study site. Key findings include:

1. Over a historic (decadal) observation period, the net alongshore foredune position has experienced an average annual advance of -0.04 m yr^{-1}. Rates of annual foredune advance and retreat vary across the study site, exhibiting a north to south erosional gradient with the highest rate of foredune advance (+0.51 m yr^{-1}) occurring in the northern foredunes and the highest rate of foredune retreat of -0.49 m yr^{-1} in the southern foredunes. The central zone was characterized by areas of negligible foredune position change and slow rates of seaward foredune migration (from +0.13 to +0.27 m a^{-1}, +/- 0.12 m a^{-1}) or landward retreat (from -0.13 to -0.35 m a^{-1}, +/-0.12 m a^{-1}). The long-term (75 year) trend in foredune position is fueled by seasonal variations in littoral drift processes characteristic of

the Eureka Littoral Cell, with dominant wind, wave and current dynamics driving littoral sediment transport from the north to the south in the summer and vice versa during winter storms and El Niño periods. Future studies should further focus on the role of vegetation in the controlling the rate of foredune position change.

2. Examination of foredune position at 12 shorter-term aerial photograph intervals between 1939 – 2014 revealed that 3 intervals (1939 – 1948, 2005 – 2009, 2012 – 2014) exhibited similar EPR trends to the long-term 75-year study interval. An examination at smaller time intervals exhibits high variability in foredune position change in more recent intervals (from 2004 to 2014). Higher variability in foredune position may be a geomorphic response to a recorded climatic shift in 1977, after which increased intensity and frequency of storm events was recorded. Storm energies are seen to alter dominant wind and wave directions, in turn interrupting the north to south littoral sediment drift direction and resulting gradient in foredune position.
3. An interannual study from 2004 – 2014 suggests that the development of erosional units may be a morphodynamic response to both sediment availability and areal increase of incipient foredunes. The greater sediment availability in the north allows for the seaward spread of pioneer vegetation and the greater development of incipient foredunes compared to the southern region. This, in turn, leads to closing of the mouths of blowouts in the north. In the south, lower sediment inputs mean that incipient foredunes do not develop as often or as well due to lower beach and backshore widths and sediment supply. Thus, aeolian

processes operate within the established foredune complex, causing landward extension of blowouts between stabilizing vegetation.

4. Foredune position change trends and geomorphic unit evolution indicate a north to south gradient in foredune evolution, with stage 1 foredunes in the north transitioning to stage 3 foredunes in the south. Developmental stages are fueled by variations in seasonal sediment inputs into the beach zone, contributing to volumetric increase of the beach and foredune following aeolian transport. Foredune volumes in the south are disproportionately affected by winter storm energies and experience longer recovery intervals due to lower availability of sediment. As such, foredunes in the south are unable to recover fully in summer months, limiting the opportunity for re-vegetation and development back towards a stage 2 morphology.

3. Foredune dynamics after vegetation disturbance and re-establishment: Humboldt Bay National Wildlife Refuge.

3.1 Abstract

Patterns of sediment deposition on foredunes are largely dependent on the zonation, density and physical characteristics of dominant plant species. As such, disturbance to vegetation alongside seasonal oceanic and meteorological patterns can alter local beach-dune sediment budgets and resulting foredune morphodynamics. Preliminary stages of dynamic restoration took place at a foredune system of the Humboldt Bay National Wildlife Refuge (HBNWR) beginning in August, 2015 with the complete removal of invasive species such as *Ammophila arenaria* along the foredune. Furthermore, high energy storm events in winter 2016 led to beach erosion and undercutting of the foredune toe. As such, a unique opportunity exists to explore the impact of multiple disturbances (i.e., invasive vegetation removal, winter storm events, vegetation re-establishment) on foredune morphodynamics, alongside the role of vegetation presence/absence on seasonal foredune recovery and development. Using a combination of cross-shore profile measurements, light detection and ranging (LiDAR) derived bare earth models and structure from motion (SfM) derived orthophotographs, changes in foredune morphodynamics and beach-dune sediment budgets following early stages of restoration were quantified.

In a year encompassing initial vegetation removal (May 2015 – September 2016), the foredune stoss slope was characterized by a net positive sediment budget (sediment accumulation up to +1.20 m a^{-1}) and net sediment erosion (up to -1.30 m a^{-1}) on the beach. When examining volumetric change at shorter seasonal scales, annual trends of

net beach erosion may be attributed to site-wide sediment loss on the beach and foredune from November 2015 – April 2016 following higher than average wave height and water level values in January 2016, indicative of a winter storm event. Site-wide sediment accumulation on the beach and foredune during spring-summer intervals indicates that sediment supply onto the beach and summer aeolian transport conditions result in the development of scarp fill ramps and beach-foredune recovery, despite the presence or absence of vegetation. Furthermore, in the summer of 2016, early stage development of seasonal incipient foredunes and an increase in vegetation density on the foredune stoss slope influenced localized areas of sediment transportation and deposition on the foredune. Together, sediment supply from the beach and the presence of vegetation effectively control the exchange of sediment between the beach, foredune stoss and lee slopes and the re-coupling of foredune-backdune sediment budgets following disturbance events.

3.2 Introduction

Coastal foredunes provide an important buffer for landward ecosystems and coastal settlements against storm surge, flooding, aeolian sediment transport, and sea level rise (Hesp, 1991; Davidson-Arnott et al., 2005; Hesp and Martinez, 2007; Houser et al., 2008; Eamer and Walker, 2010). Foredunes are formed by the deposition of aeolian sand within vegetation, woody debris, wrack and other roughness matrices contributing to a significant component of the coastal sediment budget (Short and Hesp, 1982, Hesp, 2002, Walker et al., 2013). Patterns of sediment deposition along the foredune are largely dependent on zonation, density, distribution and physical characteristics of dominant plant species (Hesp, 1988, Arens, 1996, Levin et al., 2008), while plant zonation is itself

responding to environmental gradients such as salinity, (via inundation and salt spray) and nitrogen deposition via wrack (Barbour and DeJong, 1977; Barbour, De Jong and Pavlik, 1985; Pickart and Barbour; 2007). The interaction between biotic and abiotic forcing factors results in a biophysical feedback loop (Zarnetske et al., 2012). In these complex setting both human and environmentally influenced vegetation disturbances (i.e., vegetation removal, over-stabilization and/or invasive species introduction, and seasonal phenology) alter natural foredune deposition patterns that support ecological and morphological processes (Seabloom and Wiedemann, 1994; Wiedemann and Pickart, 1996; Hesp, 1999; Pickart and Barbour, 2007; Zarnetske et al., 2012; Walker et al., 2013; Darke et al., 2016).

Non-native plant species such as *Ammophila arenaria* have been introduced to shorelines around the world to stabilize coastal areas from erosive processes. An increased height and density of vegetation reduces sediment transport and cycling within coastal foredunes, as sediment is trapped under dense vegetation canopies. Previous work suggests that the removal of invasive species and the planting of native vegetation on sand dunes will restore ecosystem dynamics with natural disturbance regimes (Pickart, 1988; Pickart and Sawyer, 1998; Pickart, 2013; Darke et al., 2013; 2016). Examination of the short-term morphodynamic effects of foredune reactivation through invasive vegetation removal, commonly known as ‘dynamic restoration’, has been a growing topic of interest in the Netherlands (e.g., Grootjans et al., 2002, Arens and Geelen, 2006, Van der Hagen et al., 2008, Riksen et al., 2008, Arens et al., 2013), Australia and New Zealand (e.g., Hilton, 2006; Hilton et al., 2006; 2009; Konlechner, 2008; Hesp and Hilton, 2013; Buckley et al., 2016) and the southern and east coasts of the United States

(e.g., Nordstrom et al., 2000; 2011). While dynamic foredune restoration efforts have been implemented along the coast of California on the west coast of North America for several decades, evaluation of their effects has been primarily through an ecological rather than geomorphic lens (Pickart and Sawyer 1998, Pickart 2013). West coast studies examining morphodynamic response have been limited to short-term regional studies in Oregon, Washington and British Columbia (Zarnetske et al., 2012; Walker et al., 2013; Eamer and Walker, 2013; Eamer et al., 2013; Darke et al., 2013; 2016). Topographic monitoring during multiple stages of the restoration process (invasive vegetation removal, vegetation re-establishment) can provide information on the impact of vegetation disturbance on local patterns of foredune erosion and deposition.

The rapid advance of geospatial technologies such as light detection and ranging (LiDAR) and digital photogrammetry techniques (Structure from Motion, SfM) from unmanned aerial systems (UAS) or kite aerial photogrammetry (KAP) surveys allow for the collection of high resolution topographic data at a range of spatial and temporal scales (Lim et al., 2005; Smith et al., 2009; Lindenbergh et al., 2011; Bishop et al., 2012). Increasing availability of high-resolution spatial-temporal topographic and land cover data allows for both quantitative and qualitative analysis of landscape morphodynamics (Pike, 2000; Bishop et al., 2012). Most sandy coastal ecosystem landforms evolve rapidly due to constantly changing wind and wave regimes. Information on coastal landform morphodynamics following specific disturbance periods (e.g., erosion events, dynamic restoration treatments) can be obtained using time efficient LiDAR and/or SfM survey methods.

The foredune system of the Humboldt Bay National Wildlife Refuge in Arcata, California has undergone several successful restoration efforts since the early 1990s (Pickart, 2013) to remove over stabilizing invasive plant species (primarily *Ammophila arenaria*) with the most recent project starting in August 2015. The restoration project provides a unique opportunity for examining initial foredune morphodynamics and sediment budget responses following the early stages of dynamic restoration. The purpose of this paper is to document and describe the initial responses of a foredune system following a disturbance phase resulting from dynamic restoration activity (invasive vegetation removal) and sediment budget implications of seasonal foredune disturbances (i.e., winter storm events and phenology) using detailed topographic surveys, sediment budget quantification, and morphodynamic mapping methods. Specific objectives include:

1. Examine and contrast short term seasonal changes in foredune morphology following vegetation removal with longer term trends using 5 years (January 2012 – February 2017) of cross-shore topographic profile data.
2. Analyze and distinguish the impacts of vegetation presence/absence and winter storm events on beach-foredune sediment budget responses in the year following vegetation removal using high resolution terrestrial laser scanning (TLS) and spatial change detection of resulting bare-earth digital elevation models (DEMs).
3. Assess the impact of seasonal sediment budgets and vegetation re-establishment on foredune recovery following erosion from winter storms using both data from TLS surveys (May 2015 – September 206) and alternating monthly kite aerial photogrammetry (KAP) surveys (April – September 2016).

3.3 Study site

3.3.1 Physical setting

The study site consists of a stretch of shoreline about 200 m in length located within Lanphere Dunes Unit of the Humboldt Bay National Wildlife Refuge (HBNWR) in Northern California (Figure 18). The foredune-blowout complex in this area is fronted by a high-energy, multiple-barred, dissipative beach system. Average long-term (1980 – 2016) winter significant wave height (Hs) (2.96 m) and mean water levels (5.62 m above NAVD88) are greater than summer values (2.01 m and 5.53 m above NAVD88, respectively) (data source: NOAA Buoy Station 46022 and NOAA Tidal Station 9418767 for wave and water level, respectively). Elevated storm surge and wave run-up also occur during winter months. Dominant wind and wave direction varies seasonally, coming from the NNW in April – September and from the WNW during October – March (Figure 19 and 20). Storlazzi and Winfield (2005) and Hapke et al. (2009) describe seasonal shifts in dominant wind, wave and resultant littoral drift direction as characteristic of the broader Eureka Littoral Cell, due to seasonal changes in the position of the Hawaiian (North Pacific) High Pressure system and multi-year El Niño Southern Oscillation (ENSO) events. A recent study of beach and foredune volumetric analyses indicate that this area experiences large-scale seasonal fluctuations in sediment volume between the beach and foredune zones (see Chapter 2). Despite erosive conditions during winter months resulting in steeper lower elevation beaches, the foredune complex of the Lanphere Dunes unit is migrating seaward at rates up to +0.51 m a^{-1} (see Chapter 2).

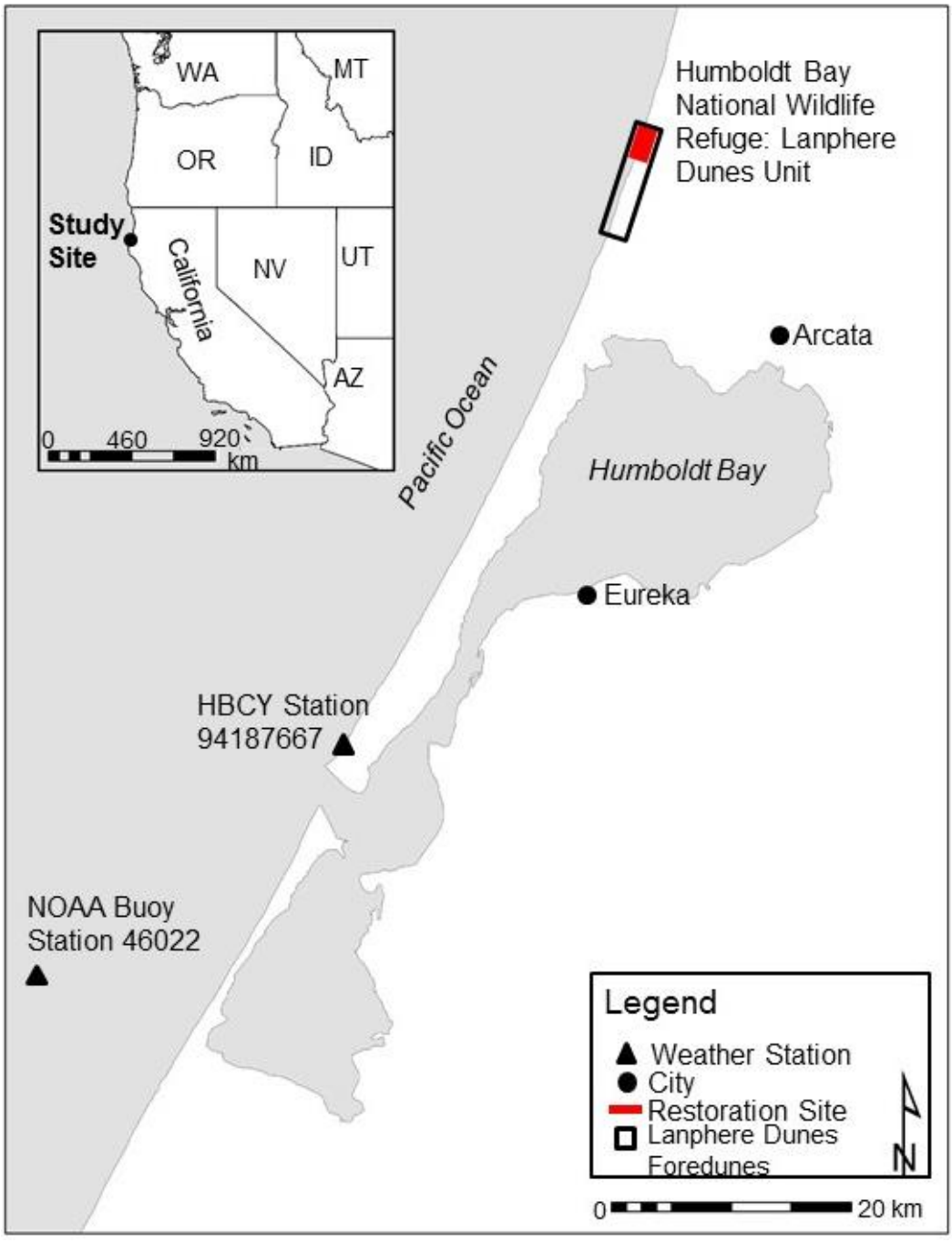

Figure 18. Location of the Lanphere Dunes foredune zone, Humboldt Bay National Wildlife Refuge and the specific study site (red rectangle) where vegetation removal occurred. Locations of NOAA buoy 46022 and meteorological station HBCY 94187667 used to calculate wind, wave and sediment transportation data are also identified.

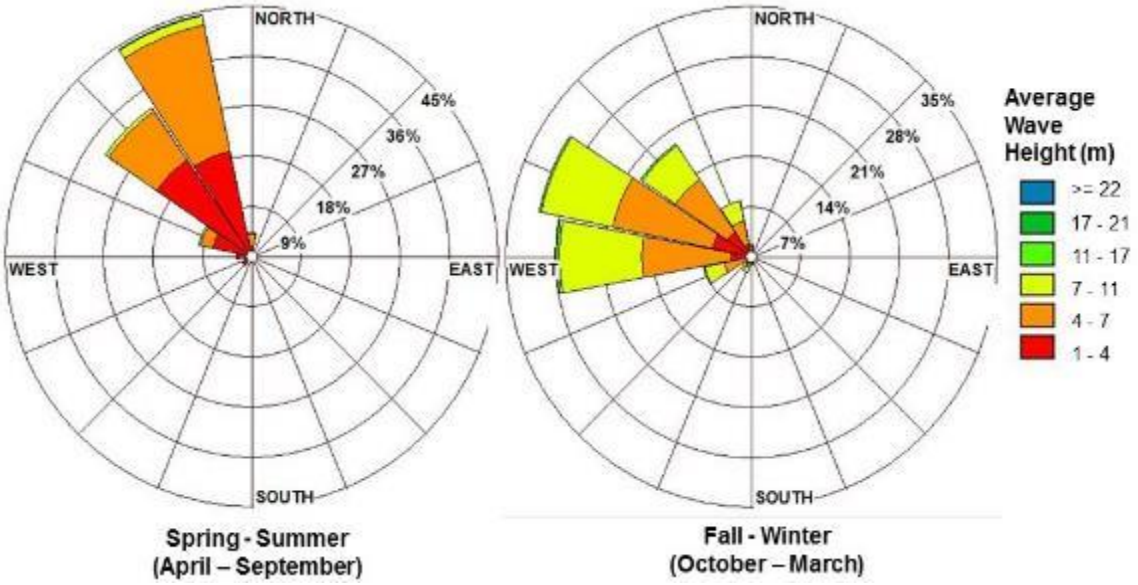

Figure 19. Annual wave roses generated from 24-hour observations of significant wave height, Hs (m) and wave direction (degrees) in 2016 at the NOAA Buoy Station 46022 located approximately 15 km offshore, to the SSW of the study site. Wave roses were generated using Lakes Environmental's WR Plot (https://www.weblakes.com/products/wrplot) (Data source: NOAA Buoy Station 46022 at Eel River, CA)

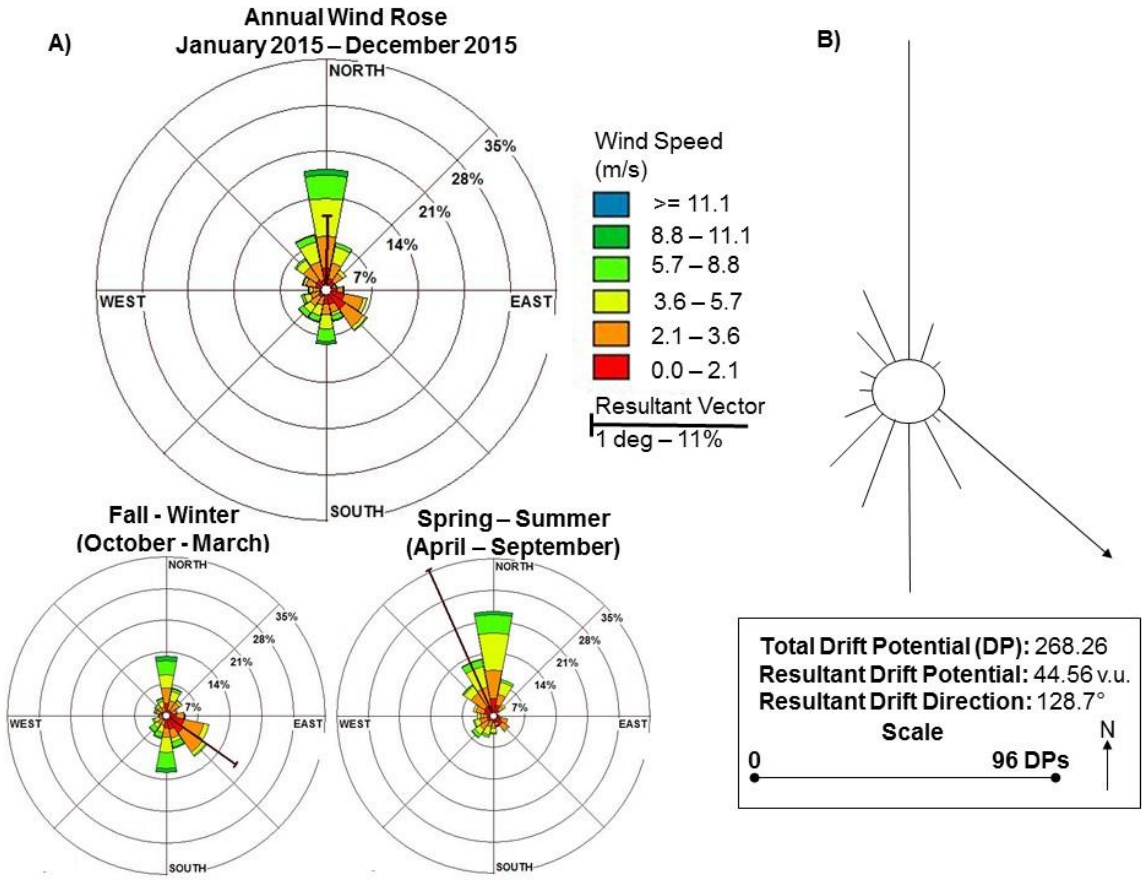

Figure 20. Annual wind rose (A) and sediment drift potential rose (D) generated from 24-hour observations from 2015 for NOAA Station HBCY1, 94187667 at North Spit, CA. Resultant wind vectors (black) show average wind direction and percent frequency, predominantly generated out of the N on an annual scale. Wind rose was generated using Lakes Environmental's WR Plot (https://www.weblakes.com/products/wrplot). The sediment drift potential rose was derived using m s^{-1} wind data and shows a resultant drift direction vector (RDD, black arrow) with dominant sediment transport toward the SE. DP values are in vector units (VU) per Miot da Silva and Hesp (2010). (Data source: NOAA Station HBYC1, 94187667 at North Spit, CA).

3.3.2 Vegetation management history

Invasive *Ammophila arenaria* first became established on what later became the Lanphere Dunes shortly before 1965. The species continued to spread, and the first, small-scale control efforts were launched in the 1980s, following recognition by

ecologists of its negative impacts on the beach-dune ecosystem (e.g., Esler, 1970; Pickart and Barbour, 2007). *Ammophila arenaria* was entirely removed within the boundaries of Lanphere Dunes during the 1990s following a major research project documenting its negative ecological impacts and testing effective restoration techniques (Pickart and Sawyer 1998, Pickart 2013). Measurement of restoration success at the time of these projects relied on biotic parameters such as species diversity, vegetation cover, and invertebrate and vertebrate responses (Pickart and Sawyer 1998). Subsequently, research elsewhere has examined dune restoration through a geomorphic, rather than ecological lens, quantitatively describing morphodynamic effects of invasive coastal vegetation establishment and removal (Hilton et al., 2005;2006; Hilton, 2006; Hesp and Hilton, 2013). When a new population of *Ammophila spp.* was incorporated through expansion of HBNWR in 2012, it presented an opportunity to test restoration methods explicitly designed to increase foredune resilience to sea level rise and extreme events through invasive vegetation removal and replanting native species of different morphologies and at different densities. This paper is limited to the initial vegetation removal phase of the experiment.

Restoration of the study site began in August 2015 with manual pulling and digging of *Ammophila arenaria* following well-established methods documented by Pickart and Sawyer (1998). This method relies on an initial removal of above ground vegetation, followed by periodic removal of resprouting rhizomes until stored carbohydrates are depleted and plants die. Initial labor was provided by the California Conservation Corps (CCC) (Figure 21). Throughout the following months, USFWS staff, CCC, and the California Department of Forestry and Fire Protection (CalFire) crews

continued follow-up stages of hand-pulling needed to achieve eradication. Because of delays in the removal schedule, there was insufficient dieback of *Ammophila arenaria* over the winter and replanting of native vegetation (*Elymus mollis*) was delayed until the following year. The remaining resprouts of *Ammophila arenaria* were sprayed with a combination of the herbicides glysophate and/or imazapyr in early March 2016 and left in situ through the summer months to reduce sand transport in the absence of native plantings (Figure 22). During the spring and summer of 2016, native vegetation began to colonize the study site alongside the presence of *Ammophila arenaria* stems. Multiple disturbances, such as vegetation removal and establishment, alter foredune morphodynamics, as sedimentation patterns are largely dependent on the zonation, density, and physical characteristics of plant species (e.g., Hesp 1988; Arens, 1996; Ruggiero et al., 2011). This study quantitatively documents the changes that occurred in the early stages of dune restoration associated with vegetation removal and re-establishment.

Figure 21. (A) Manual digging and pulling of invasive *Ammophila arenaria* at the study site in August 2015 by California Conservation Corps (CCC) employees. (B) Map showing 10 established cross-shore profiles in the region. Two transects located within the restoration site are outlined in yellow. (C) Oblique aerial photograph of the restoration site following vegetation removal (photo credit: Dave Kenworthy). The study site, location vegetation removal and two established cross shore transects are outlined in yellow. Large piles of removed *Ammophila arenaria,* removed manually, visible throughout the study site, were later burned.

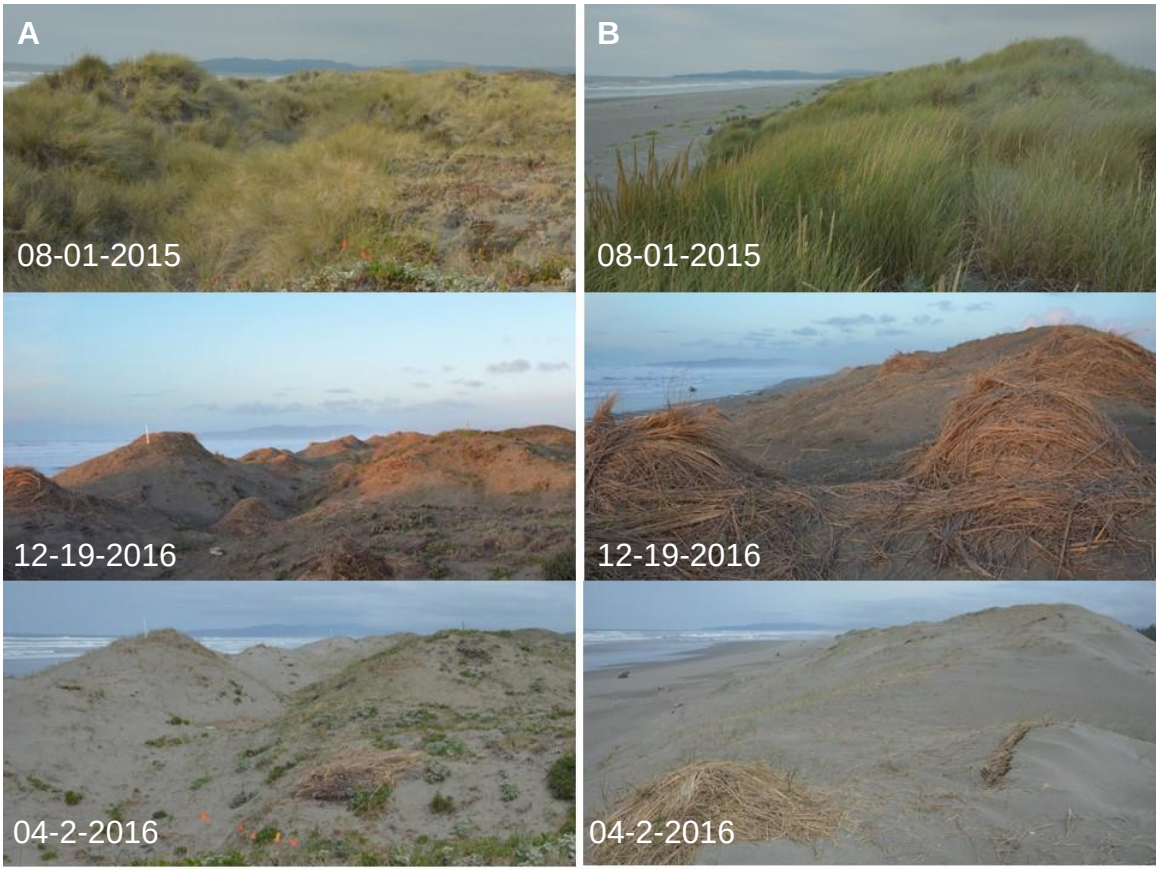

Figure 22. Photographs oriented to the north, taken immediately before and in the year following vegetation removal at the study site. A shows photographs taken behind the primary foredune south of transect 2. B shows an alongshore view of the foredune stoss slope south of transect 2. Transect 2 crosses the foredune north of the PVC markers seen in photographs.

3.4 Methods

3.4.1 Field data collection and analysis

3.4.1.1 Cross shore transect surveys

Two topographic transects were established within the study site in January 2012 as a part of a larger monitoring project by the US Fish and Wildlife Service (USFWS) (Pickart, 2014). Transects were oriented from NW to SE (azimuth 165°), in line with dominant summer wind and resultant annual aeolian sediment drift directions (Figure 19). The transects varied in length from origin in the backdune to the water line, depending on

width of the foredune complex and seasonal variation in tidal levels at the time of observation. Three geomorphic zones, the backdune, foredune and beach, were identified for each transect. The backdune was established in the area landward of the first topographic break at the base of the foredune lee slope. The foredune zone extended from the topographic break point on the lee slope (unchanging through the period of observation) to the seaward most vegetation point during the measurement period (which varied seasonally). The beach zone was defined by the area seaward of the vegetation line at the time of measurement to an elevation of 3.7 m above mean sea level (masl), a common closing point for both topographic transects to allow for accurate comparison of seasonal elevation values and change. Due to the presence of a relict secondary foredune ridge within the backdune zone of transects 1 and 2, the primary foredune crest was identified by the seaward most point of highest elevation.

Surveys were conducted bi-annually in winter and summer seasons from establishment in January 2012 to February 2017 (Table 9) (Figure 23). Topographic measurements were taken using a Trimble R-10 real time kinematic differential global positioning system (RTK-DGPS) at 1-meter intervals from January 2012 to July 2015. From February 2016 to February 2017, topographic measurements were taken every 2 meters on the foredune and at every 4 meters on the beach and backdune. Topographic profile data were plotted in R Statistical Program for comparison of elevation over time. The monthly rate of foredune crest migration was calculated from July 2015 to February 2017 by subtracting the cross shore distance of the point of highest elevation of the foredune zone along the transect in each time period and dividing the resulting difference by the number of months in between each survey.

3.4.1.2 Terrestrial laser scanning (TLS) surveys

Bi-annual Terrestrial Laser Scanning (TLS) surveys (4 in total) were performed across the study site from May 2015 through September 2016 using a Riegl V1000 multiple return sensor (Table 9) (Figure 23). Survey intervals were chosen based on the timing of foredune disturbance regimes (i.e., invasive vegetation removal, winter storm regimes, and plant phenological changes) (Table 9). Scanning positions throughout the beach, foredune and backdune were chosen to maximize point coverage and density between scans and minimize survey shadow zones around vegetation and complex topography at the site (Bangen et al., 2014). Post-processing of data point clouds included multiple iterations of digital terrain filtering (2.5D Raster Filter) and surface comparison, tools available in Riegl RiSCAN PRO 3D Laser Scanner Processing software package and for the deletion of spurious data points (Table 10). The 2.5D Raster Filter tool creates a rough terrain model raster, increasing in resolution with sequential iterations based on the minimum elevation value in each cell. Ground points are separated from non-ground points using the surface comparison tool, which removes points over specified height thresholds that might represent spurious ground returns from objects such as vegetation and large woody debris (Table 10). Using these tools in seven iterations (Table 10) allowed for the creation of progressively finer resolution terrain models and the removal of unwanted (non-surface) data points with higher precision. The resulting 0.1 m resolution 'bare earth' point clouds were then georeferenced to the 1983 North American Datum (NAD83) and UTM Zone 10 coordinate systems. Bare earth digital elevation models (DEMs) were created subsequently from the point clouds in Surfer^{TM} version 13. Due to the high density of data points in each point cloud, inverse distance weighting was

chosen to interpolate cell values based on the distance-weighted average of sampled elevation pixel values.

3.4.1.3 Kite aerial photogrammetry (KAP) and Structure from Motion (SfM) mapping

Digital orthophotograph mosaics and surface models were produced from KAP imagery for analysis of spatial patterns of vegetation and geomorphic units. High resolution orthophotographs allowed for assessing vegetation cover along with geomorphic interpretation of discrete landforms within the beach-dune complex. 3 KAP surveys were performed on alternating months through the vegetation growth period from April through September 2016 in order to monitor the effects of vegetation establishment on foredune morphology and recovery from erosive storm events (Table 9) (Figure 23). Ten ground control points (GCPs) were placed across the study site and georeferenced using the RTK-DGPS system. A kite with mounted GoPro™ Hero Session digital camera was flown on north-south lines parallel to the water line extending landward to ensure full, overlapping coverage of the study site and GCPs. The camera was generally oriented towards nadir and set to collect continuous video footage from which 1 frame per second was extracted. Photos were then aligned using Agisoft PhotoScan™ software to create orthomosaics and three-dimensional digital surface models (DSMs) of the study site (Table 11). The ground resolution of resulting DSMs (1.99 cm, 8.53 cm, 3.53 cm for April, July and September surveys, respectively) was calculated in the software from camera resolution (2720 x 2040), focal length (2.77 mm), sensor width (4.54 mm) and average flight elevation (32.4 – 71.6 m). Orthomosaics and DSMs were then georeferenced using coordinates of corresponding GCPs for each respective survey interval (April, July, September) (Table 11). Georeferencing error for both orthomosaics

and DSMs were calculated using the residual x and y positional uncertainty values for corresponding GCP coordinates (Table 11). Finally, orthomosaics were brought into ArcGIS and resampled using bilinear interpolation to represent equal pixel resolutions of 0.10 m (Table 11).

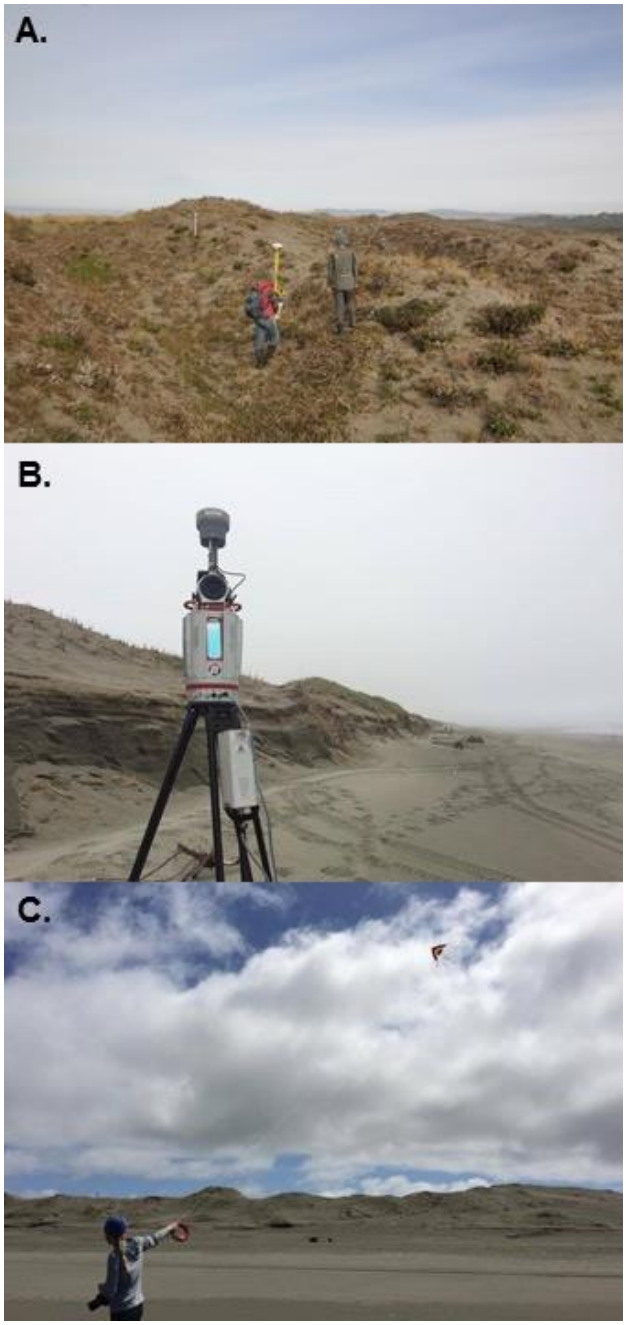

Figure 23. (A) RTK-GPS survey in progress to record elevation data at established cross shore transects (January 2012 – February 2017). (B) Riegl VZ-1000 TLS set up on the backshore of the study site. (C) KAP survey of the study site.

Table 9. Timeline of data acquisition using RTK-DGPS, TLS and KAP surveying methods in relation to vegetation disturbance regimes. RTK-DGPS surveys took place along transects 1 and 2 only, while TLS and KAP surveys collected data across the entire study site.

Date of Acquisition	Survey Method	Disturbance Regime
January 2012 – January 2015 (Seasonal)	RTK-GPS	Pre-vegetation removal
May, 2015	TLS	Pre-vegetation removal
July, 2015	RTK-GPS	Pre-vegetation removal
November, 2015	TLS	Post-vegetation removal Pre-winter storm season
January, 2016	RTK-GPS	Post-vegetation removal Mid-winter storm season
April, 2016	TLS KAP	Post-winter storm season Pre-dominant vegetation growth season
July, 2016	KAP RTK-GPS	Mid-vegetation growth season
September, 2016	TLS KAP	Post-vegetation growth season Pre-native vegetation Planting
February, 2017	RTK-GPS	Post-native planting

Table 10. 2.5D Filter and Surface Comparison tool (RiSCAN PRO Software, see section 3.1.3) iterations used to define raster resolution and exclude spurious data points from vegetation during bare earth model processing.

Iteration #	2.5D Filter – Raster Resolution (m)	Surface Comparison-Max/Min. (m) Distance from Surface
1	5.00	3.00
2	2.50	1.25
3	1.75	1.15
4	0.75	0.50
5	0.30	0.25
6	0.25	0.15
7	0.10	0.05

Table 11. Georeferencing, digitization and total error values for orthomosaics and surface models derived from KAP surveys

KAP Orthomosaic and Surface Model Error Delineation			
KAP Survey Time	Georeferencing Error (m)	Digitization Error (m)	Total Error (m)
April 2016	0.059	1.240	1.299
July 2016	0.052	1.238	1.290
September 2016	0.179	1.087	1.266

3.4.2 Bare earth DEM analyses and morphometric unit identification

Bare earth DEMs from each TLS survey from May 2015 – September 2016 were imported into ArcGIS version 10 and clipped to represent identical extents of the study site. Slope, aspect and elevation surfaces were generated and draped over a hillshade of each DEM to facilitate the identification and digitization of seven dominant morphometric units: lower, mid and upper stoss slope, foredune stoss toe, foredune crest line, foredune lee slope and foredune lee slope toe (Figure 24). First, using a combination of slope and aspect surfaces generated by their respective spatial analyst tools in ArcGIS, the foredune stoss toe, crest and foredune lee slope toe were digitized from each interval's bare earth DEM. For DEMs from May 2015, November 2015 and September 2016, the foredune stoss toe was defined by the seaward most point of vegetation, following existing definitions of the foredune (Hesp 1988; Hesp, 2002) and informed by both KAP orthomosaics and the classification of the foredune from cross-shore transect data (Figure 24). Due to the absence of a visible vegetation line in the backshore following extensive winter wave erosion, the stoss toe from the April 2016 DEM was digitized as the base of the scarp at the top of the backshore. Foredune crest and lee slope toe lines were digitized in ArcGIS for each survey interval from their respective DEM aspect surfaces, where a shift in aspect from NW to SE indicated the foredune crest and

vice versa for the lee slope and lee slope toe (Figure 24). Finally, DEMs for each study interval were geometrically classified into three elevation classes for the stoss slope. The three resulting elevation groups were used to denote the lower, mid, and upper stoss slope zones for each survey period (Figure 24). Area of each stoss slope zone was calculated in ArcGIS and normalized by dividing the zone specific areas by the respective total stoss slope area in each DEM.

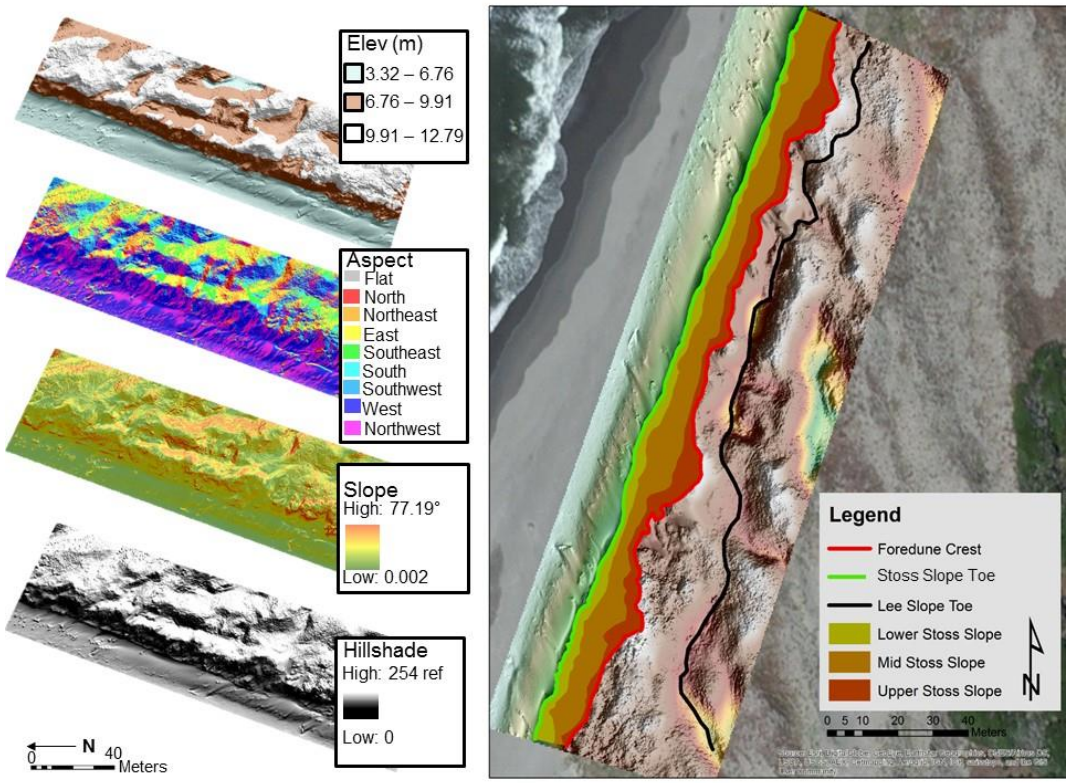

Figure 24. Example of key attributes and landform units derived from each seasonal TLS derived digital elevation model (DEM) including: foredune crest, foredune toe, lee slope toe, lower stoss slope, mid stoss slope and upper stoss slope. The hillshade raster map displays a shaded relief surface in reference to an illumination source from an azimuth of 315°. These particular figures were produced from the April 2016 TLS bare earth DEM for reference.

3.4.2.1 Spatial-temporal change detection

Patterns of erosion and deposition were examined using the Wheaton et al., (2010) Geomorphic Change Detection (GCD) plugin for ArcGIS. GCD performs cell by cell differencing in rasters to create a DEM of difference (DoD) based on statistical significance whereby resultant values indicate positive elevation (deposition), negative elevation (erosion) change. GCD was performed to assess both long-term (May 2015 - September 2016) and seasonal (Table 9) elevation changes and associated sediment volumes.

Three geomorphic units (beach, foredune stoss slope and foredune lee slope) were defined for each scan interval using the corresponding foredune toe, foredune crest and lee slope toe lines from the first TLS survey of each interval (Figure 23). Geomorphic change in the lee slope zone was not examined in the May 2015 DEM, collected prior to vegetation removal, because of very dense coverage of *Ammophila arenaria* that inhibited measurement of the underlying sand surface using the TLS. Therefore, GCD was used to analyze sediment deposition and erosion patterns within and between the beach and foredune stoss slope zones for 2 intervals (May 2015 – September 2016, May - November 2015), while geomorphic change between all three zones (beach, foredune stoss slope, foredune lee slope) was analyzed for the 2 intervals following vegetation removal in August 2015 (November 2015 – April 2016, and April 2016 – September 2016).

Characterization of DoD uncertainty was performed following the methods outlined by Wheaton et al., (2010). First, a minimum level of detection (vertical error threshold) of 0.011 m was assumed based on the largest reported error from established GPS

surveyed control benchmarks. Second, the defined error was propagated across the entire DoD surface using probabilistic thresholding per Lane et al. (2003). For probabilistic thresholding, a two-tailed 95% confidence limit was chosen in which DoD pixels with insignificant elevation change values (under t distribution, $t < 1.96$) were excluded from the resulting surface.

3.4.3 Geomorphic unit identification from kite aerial photogrammetry (KAP) surveys

Orthophotographs produced from 3 (April 2016 – September 2016) KAP flights were used to interpret the development of geomorphic units at the study site following vegetation establishment. This time interval was chosen to isolate potential foredune recovery following extreme storms during the winter of 2016 and during subsequent vegetation regrowth and foredune recovery the following summer. Orthophotos were imported into ArcGIS for visualization and digitization of geomorphic unit polygons. Erosional landforms (e.g., blowouts, concave depressions) and depositional units (e.g., convex knolls, incipient foredunes) were identified predominantly through orthophotograph interpretation and, as necessary, slope and elevation analysis. The area of each geomorphic unit was calculated to examine the change in area throughout each survey period. Finally, the area of each specific geomorphic unit (i.e., incipient foredune, depressions, knolls, blowouts) was divided by the area of all geomorphic units for each time period to produce normalized proportional areas.

Digitization error for the foredune toe was calculated following methods outlined in Thieler et al. (1994) (Table 11). First the seaward extent of the foredune, as defined by the seaward most line of vegetation, was digitized by the same user three separate times for each orthophotograph. Second, digitization error was generated for each orthophoto

using the shoreline change envelope (SCE) statistic calculated by the Digital Shoreline Analysis System (DSAS) developed by the United States Geological Survey (USGS) (Thieler et al., 2009). The SCE statistic indicates the total distance between specified digitized shapefiles that are closest to, and farthest from, a user defined baseline, which is used as a proxy for total digitization error. Next, a total error value was calculated for each orthophoto by adding the digitization error to the corresponding georeferencing error (Table 11).

The percent of open sand surface was calculated from each orthophotograph to examine the link between the presence and/or establishment of vegetation and observed patterns and changes in geomorphic units. A standard supervised classification of vegetation and bare sand cover types was performed in ArcGIS. Areas of vegetation and bare sand were visually identified from the color orthophotographs to create 35 training samples of each classified cover type. Percent open sand surface and vegetation cover were calculated and compared with areal changes in erosional and depositional geomorphic units.

3.5 Results

3.5.1 Changes in foredune extent and morphology

Figure 25 displays the normalized area of the lower, mid and upper foredune stoss slope segments for all TLS survey intervals from May 2015 through September 2016. From May to November 2015 the normalized area of the mid stoss slope decreased by +0.11 while the normalized area of the upper stoss slope increased by +0.20, resulting in very similar normalized areas of upper (0.39) and lower (0.40) stoss slopes. Areal changes in stoss slope zones during this period correspond to the timing of an increase in

open sand surface available for aeolian sand transport following the initial stages of vegetation removal. From November 2015 to April 2016, normalized area for the lower and upper stoss slope decreased (normalized areal decrease by -0.20 in both), while the mid stoss slope normalized area increased (+0.40). A distinct shift occurred during this period, with the mid stoss slope showing the largest normalized areal extent in April 2016 (0.61). During the following April to September 2016 period, an increase in vegetation density occurred across the foredune alongside a decrease in upper and mid stoss slope normalized area (-0.02 and -0.07, respectively) and a +0.08 increase in normalized lower stoss slope area.

Topographic measurements from two, longer-term (January 2012 - February 2017) oblique cross-shore transects are plotted in Figure 25. From July 2015 – February 2017 (following vegetation removal in August 2015) the foredune lee and stoss slopes at transect 1 became less sleep, while the foredune zone increased in average elevation (+ 0.20 m). During the same time period, sediment accumulation occurred on the foredune stoss slope at transect 2, alongside the slope becoming more gradual and less morphologically complex. Elevation in the beach zone decreased following wave scarp from winter storms, indicating net erosion seaward of the foredune toe in the winter months.

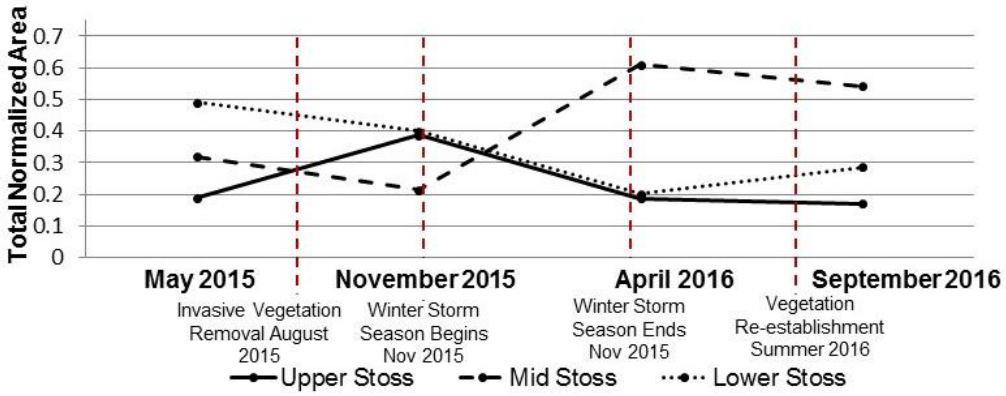

Figure 25. Proportional area of the lower, mid and upper stoss slopes, as defined by changes in elevation. Vertical dashed lines indicate the occurrence of three dominant disturbance events

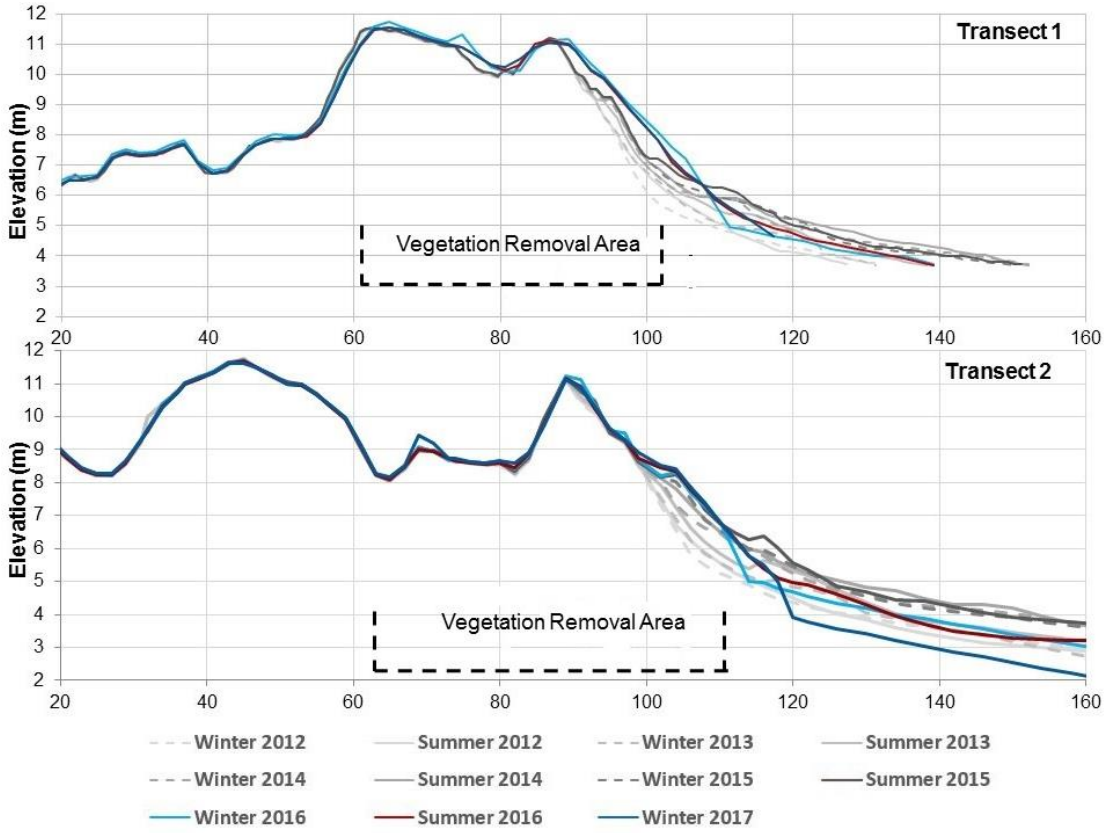

Figure 26. Topographic measurements (January 2012 – February 2017) from cross shore transects #1 and #2 at the study site. Grey lines indicate profiles collected prior to vegetation removal (pre-restoration state), while colored lines indicate morphological responses following vegetation removal in August 2015 and high water level and wave disturbance in winter 2016. The extent of vegetation removal is indicated for each transect.

3.5.2 Seasonal changes in erosional and depositional units and vegetation cover

Figure 27 shows areal observations of erosional units, (blowouts, concave depressions) and depositional units, (incipient foredunes and convex knolls) from April to September 2016, a period of vegetation re-establishment following initial removal in the summer of 2015. Digitized geomorphic units are displayed in Figure 28. From April to July 2016 an areal increase occurred in incipient foredunes (43.6%), convex knolls (2.2%) and blowouts (85.3%). During the same time period, the area of concave depressions decreased by 12.9 %. From July to September 2016 the incipient foredune increased fourfold (+63.4 m^2, 467.8%), while both erosional depressions, blowouts and the area of depositional knolls decreased. Ground cover classification maps identifying vegetation are shown in Figure 29 while Figure 30 shows photographs from April and September 2016, taken pointing north over the study site to exemplify an increase in vegetation. A net 8.1% increase in vegetation cover is observed across the study site from April to September. The majority of the vegetation cover increase occurred from July to September (+8.4%), corresponding to an increase in normalized incipient foredune area (0.06) (Figure 27, Figure 29). Most of the incipient foredune vegetation consisted of colonizing sea rocket (*Cakile* spp.), a species primarily found on the backshore. The majority of vegetation increase on the foredune was the result of resprouting *Ammophila arenaria*, although native dune species formed a greater component of the vegetation after July.

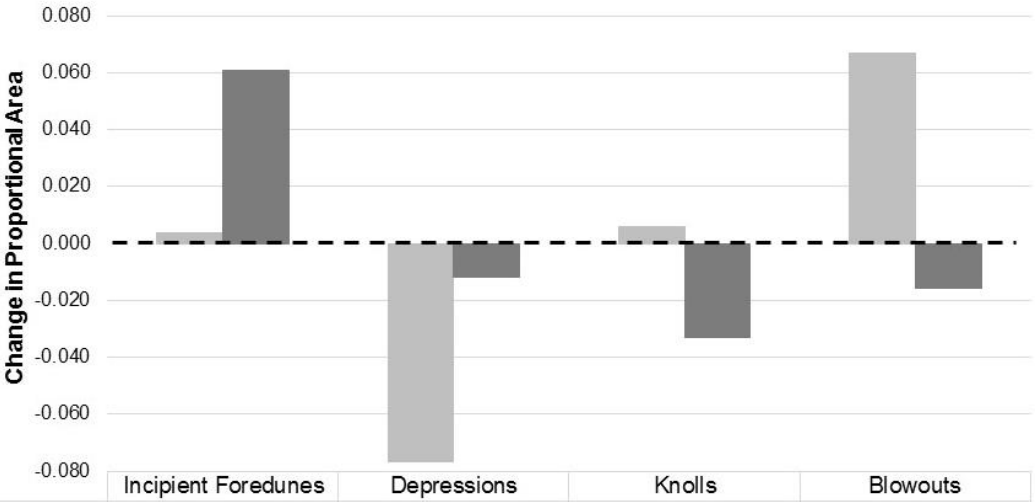

	Incipient Foredunes	Depressions	Knolls	Blowouts
April - July	0.004	-0.077	0.006	0.067
July - September	0.061	-0.012	-0.033	-0.016

Figure 27. Proportional areal change of identified geomorphic units from April – July 2016 and July – September 2016, respectively.

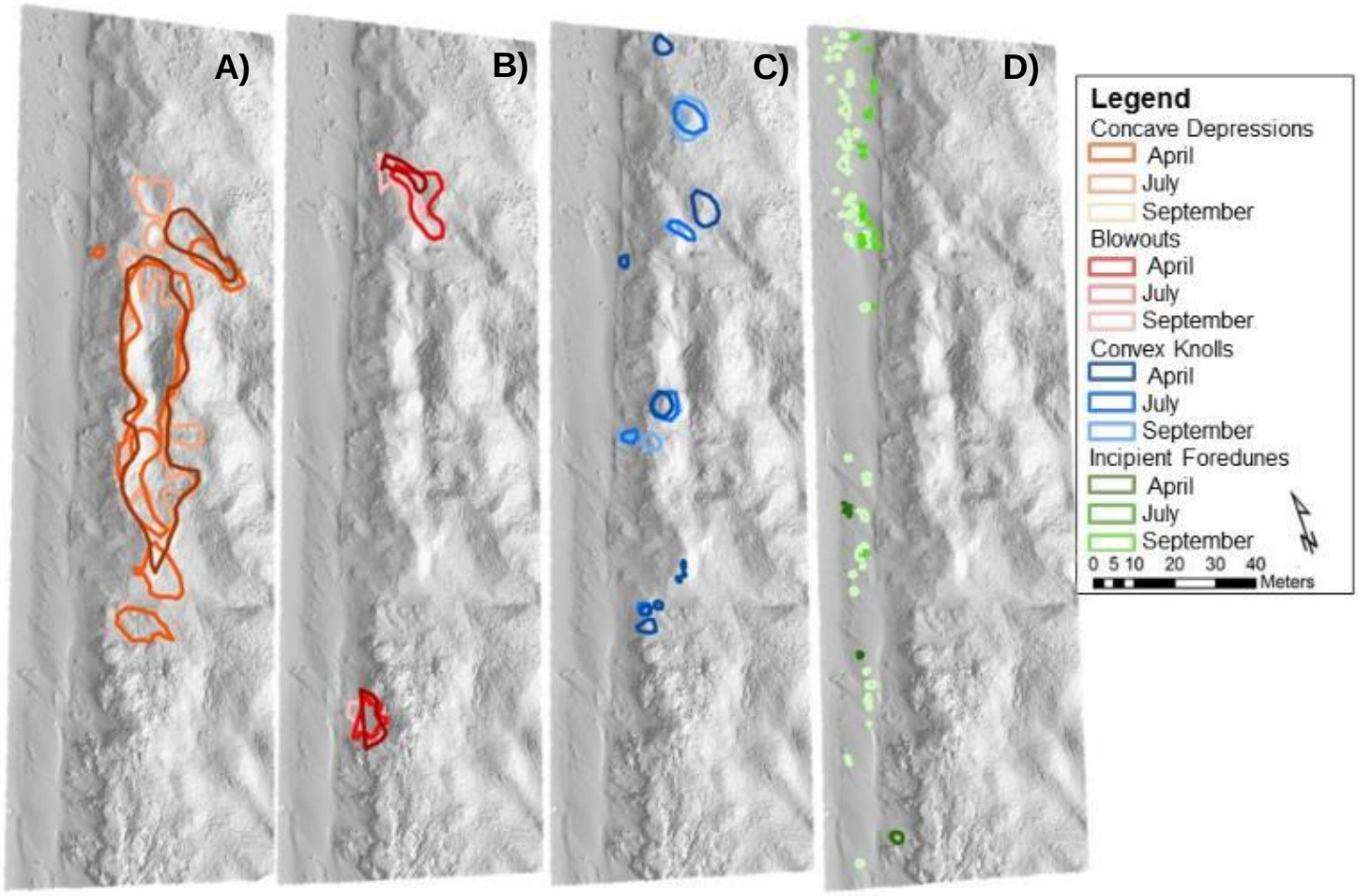

Figure 28. Digitized geomorphic units in 2016: Concave depressions (A), blowouts (B), convex knolls (C) and incipient foredunes (D). The units were digitized from examination of KAP derived orthophotographs and 3D visualizations of surface models as necessary. Geomorphic unit shapefiles are draped over September 2016 TLS bare earth DEM for visualization purposes.

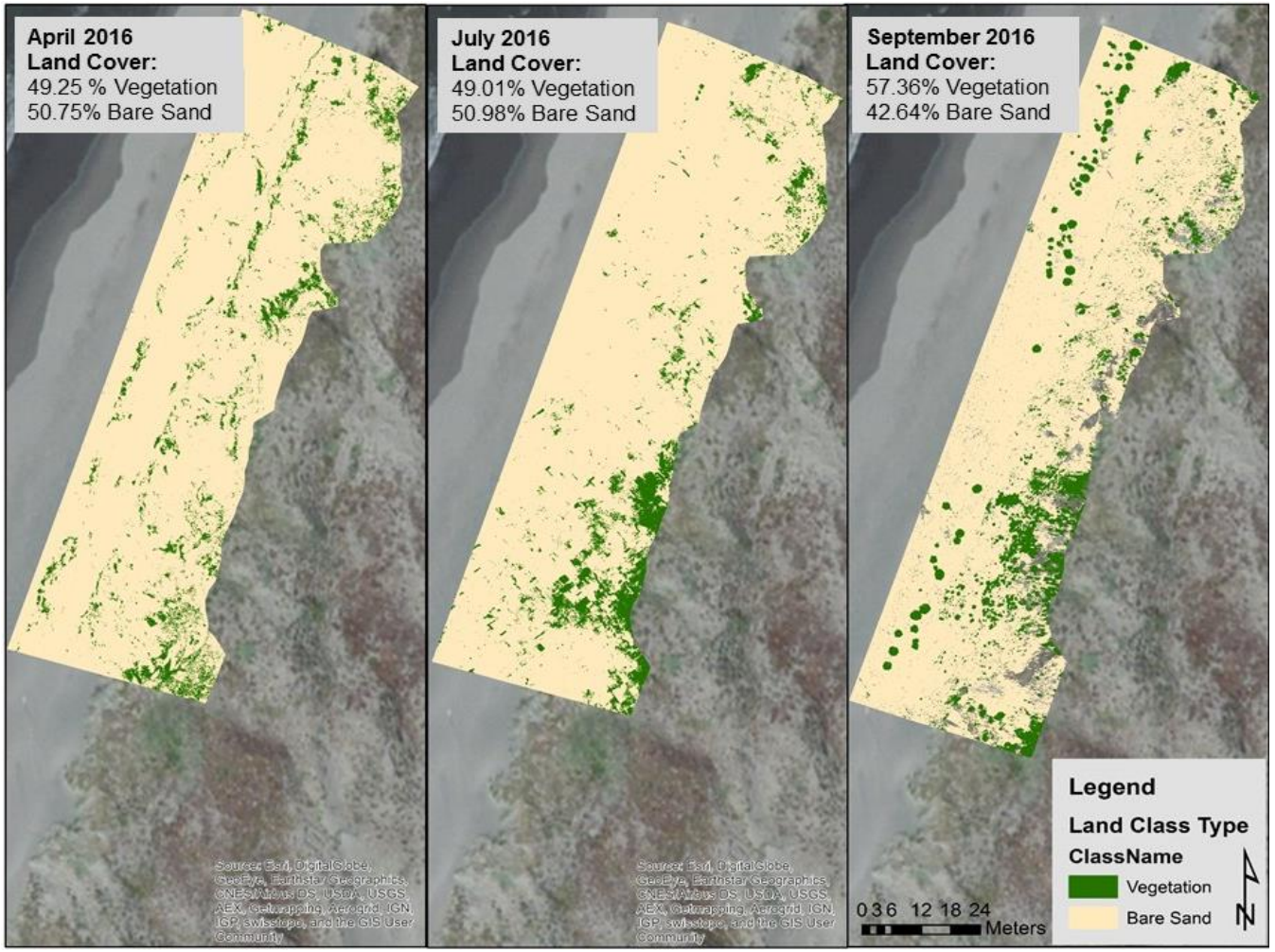

Figure 29. Vegetation cover classification maps for April, July and September 2016 derived from KAP survey data.

Figure 30. Photographs taken in April 2016 and September 2016 from looking north over the study site from the foredune crest (A, B) and the backshore (C, D). Significant vegetation growth can be seen throughout the stoss slope and on the incipient foredune between April to September, 2016.

3.5.3 Detection of significant volumetric changes

Long term (May 2015 – September 2016) GCD results (Figure 31) display elevation loss (erosion up to -1.3 m) on the beach zone, resulting in net area normalized volume change of -0.38 m^3 m^{-2}. During the same interval, elevation gain (deposition up to +1.2 m) on the stoss slope resulted in net area normalized volume change of +0.54 m^3 m^{-2} on the foredune. Figure 32 displays maps of seasonal volumetric change during sub-intervals of the study period. From May through November 2015, the beach and foredune stoss slope zone were characterized by net positive area normalized volume change (+0.23 and +0.47 m^3 m^{-2}, respectively) and appreciable deposition across the entire site

(up to +1.4 m) (Figure 32). Net erosion occurred from November 2015 through April 2016 (elevation loss up to -1.1 m) with the largest measured erosion on the beach north of transect 1. Concurrently, large erosive areas evolved near the April 2016 crest line south of transect 2. During this time period the beach, foredune stoss and lee slopes showed area normalized volume loss (-0.65, -0.44, -0.04 $m^3 m^{-2}$, respectively). From April to September 2016 the beach, foredune stoss and foredune lee slopes exhibited positive net area normalized volume change (+0.12, +0.09, +0.09 $m^3 m^{-2}$, respectively). Accretion on the upper beach and the foredune toe occurred between April and September 2016, with the largest recorded deposition north of transect 1 (+0.4 m). Erosive areas persisted along the crestline on the southern section of foredune, with low levels of erosion on both foredune stoss and lee slopes. The largest amounts of erosion occurred during the November 2015 – April 2016 interval for all three geomorphic zones (Figure 33). In general, there was a higher area of positive elevation change in the summer study intervals (May 2015 – November 2015, April 2016 – September 2016) than the winter (November 2015 – April 2016) (Figure 33).

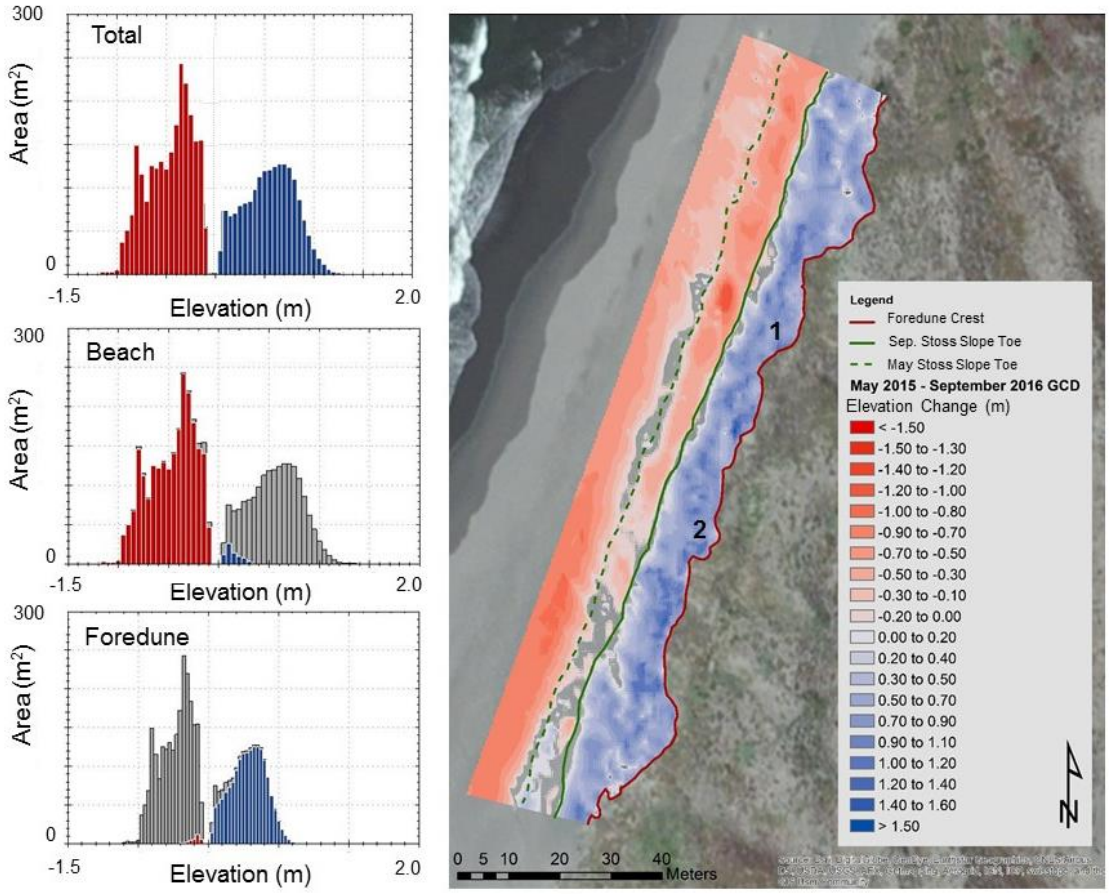

Figure 31. Map of long term (May 2015 – September 2016) GCD results, displaying the difference in elevation values from May 2015 through September 2016. The lines indicating the stoss toe of the foredune from both May 2015 and September 2016 and the September 2016 crest line are shown for reference. Histograms display the frequency (area) of pixels for each zone with positive elevation change (deposition) in blue while area of negative elevation change (erosion) is shown in red. Grey bars represent the total area of erosion and deposition for both geomorphic zones combined.

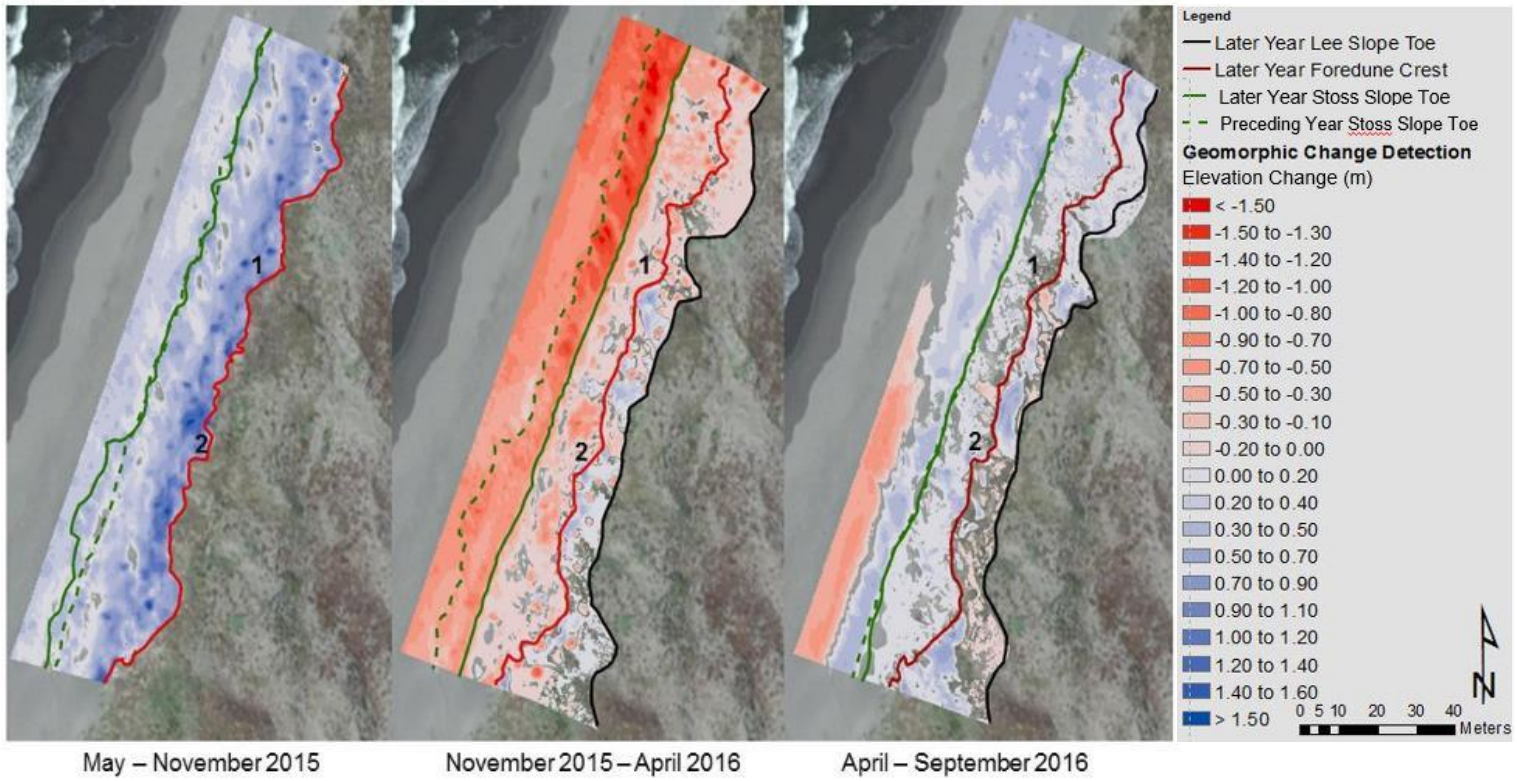

Figure 32. Maps of seasonal elevation changes from May 2015 – November 2015, November 2015 – April 2016, April 2016 – September 2016, respectively. Background photo from each interval is from 2016. Positions of the foredune toe for both the start of each interval (preceding) (dotted green) and the end (later) of each interval (solid green) are shown as well as the position of the foredune crest (red line) and lee slope toe (black line) at the end of the intervals. Volumetric change results in the lee of the foredune crest were not calculated for the May – Nov 2015 interval (prior to vegetation removal July 2016) due to the dense vegetation cover and limited LiDAR ground return points during these surveys.

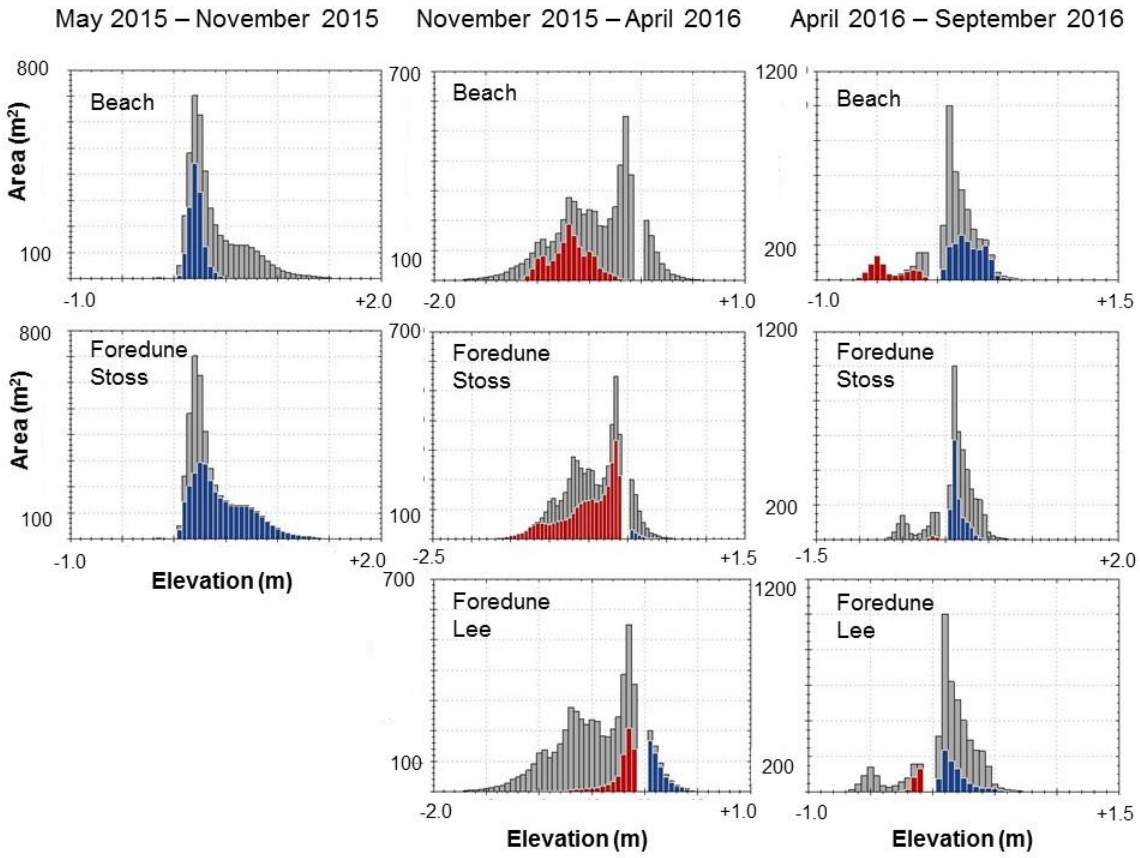

Figure 33. Histograms produced from each survey interval showing the total area of significant elevation change (m) in each geomorphic zone (beach, foredune stoss slope and foredune lee slope). The frequency (area) of pixels with positive elevation change (deposition) is displayed in blue while area of negative elevation change (erosion) is shown in red. Grey bars represent the total area of erosion and deposition for all geomorphic zones combined for each interval

3.6 Discussion

3.6.1 Seasonal to interannual sediment budget responses to foredune disturbance

In August-October 2015, the foredune experienced a widespread disturbance due to the removal of invasive *Ammophila arenaria.* In the following January of 2016, high water and wave action further disturbed the foredune system resulting in extensive scarping and beach lowering. Over the course of the study (May 2015 – September

2016), approximately 92% of the study site area experienced significant erosion or deposition, with net deposition occurring on the foredune stoss slope, and net erosion on the beach (Figure 31). A seasonal sediment budget examination indicates that from November 2015 – April 2016 the observed net erosional trend on the beach is largely attributed to a period of winter from January 2016 – March 2016, in which observed mean water level (5.79 m above NAVD88) and significant wave height (3.36 m) were elevated above long-term (1980 – 2016) values (5.53 m above NAVD88, 2.96 m, respectively). Increased water level and significant wave heights during this time resulted in extensive beach lowering and the landward retreat of the foredune by as much as 11.8 m (Figure 26 and 32). During summer to early fall monitoring intervals (i.e., May – November 2015, April – September, 2016), deposition occurred widely throughout the beach, predominantly in broad alongshore bands in the backshore (Figure 32). The annual sediment budget of the beach appears to be controlled by seasonal variations in wave and high water level conditions, indicated through widespread sediment loss during winter storm events and net positive sediment budgets during the summer, characterized by lower average wave energies, water levels and precipitation. Large-scale deposition during the drier summer months, through a combination of aeolian and offshore sediment delivery results in the replenishment of sediment throughout the beach and may contribute to the long-term trend of accretion in the backshore (Figure 26). Differences in seasonal wind and wave regimes, as recorded at the study site (Figure 19 and 20), have been documented elsewhere to influence beach volumetric changes and resultant supply of sediment from the beach to the foredune (e.g., Davidson-Arnott and Law, 1996; Christiansen 2003; Kuriyama et al., 2005).

Although annual sediment budget patterns of the beach and foredune exhibit opposing trends, previous studies (e.g., Short and Hesp, 1982; Sherman and Bauer, 1993; Hesp, 2012; Eamer et al., 2013; Walker et al., 2013; Darke et al., 2016) conclude that there are often strong seasonal relationships and coupling of sediment exchanges between the two zones. In this study, coincident with increased sediment delivery onto the beach, appreciable deposition occurred on the foredune during both summer monitoring intervals (Figure 32). Dominant winds from the NNW (Figure 20) and lower rates of precipitation in the summer provide the highest opportunity for aeolian sediment delivery from the beach onto the foredune. Sediment deposition on the foredune stoss slope was highest from May – November 2015, corresponding to the increase aeolian sand transport potential on the foredune following vegetation removal (Figure 33). However, sediment accumulation and an increase in foredune volume was seen, despite temporal variation in plant cover following both initial vegetation removal in August 2015 and plant nodal re-establishment in the summer of 2016. Following initial vegetation removal, flow over the newly denuded foredune from May – November 2015 likely resulted in greater site-wide sediment delivery and/or deposition in subsequent intervals, particularly in the lower and upper stoss zones as seen in Figures 25 and 32.

Previous studies on coastal dune restoration in British Columbia, Canada and in New Zealand note that high sediment inputs to the beach and increased aeolian activity on the foredune following vegetation removal may result in the re-coupling of foredune and backdune sediment budgets (Hilton et al., 2006; 2009; Konlechner, 2008; Eamer et al., 2013; Walker et al., 2013; Darke et al., 2016). At the study site, sediment accumulation on the foredune stoss slope, widening of the foredune crest and recorded

deposition on the lee slope (Figure 26 and 32) suggest the re-activation of sediment following vegetation removal, as sediment previously anchored by dense vegetation canopies can be mobilized by competent winds and transported widely throughout the foredune. Localized accretion in the lee slope could also be attributed to secondary flow patterns behind the foredune as some combination of deflected and/or separated flow. In conjunction with suspended sand raining down onto the lee slope, slumping and avalanching from the foredune crest further contributes to sediment deposition in the lee slope sediment deposition, as seen just north of transect 2 (Figure 32 and 34). The presence of lee slope ripples confirms the influence of topographic steering of deflected alongshore flow steered over a variable crest morphology and influence by a stable relict dune ridge behind the established foredune (Figure 22 and 26). Complex flow patterns introduced along the lee slope in the absence of vegetation drive sediment transport pathways from the foredune stoss slope into the lee and north to south between the primary and relic dune ridges (Figure 34).

Sediment accumulation on the foredune results from sediment transport from the beach up the stoss slope where deposits are stored within re-establishing vegetation. Simultaneously, rhizome networks work to stabilize sediment, reducing avalanche potential from the crest and resulting sediment transport onto the lee slope. This is observed at the study site through corresponding localized areas of increased stoss slope vegetation cover (Figure 29) and little to no elevation change in the lee slope (Figure 32). While the quantity of sediment transported onto a foredune may largely be controlled by available sediment on the beach (e.g., Psuty, 1988a; Nickling and Davidson-Arnott, 1990), foredune accretion and localized deposition patterns are furthermore controlled by

vegetation type, density and zonation (Hesp 1988; Sarre, 1989; Arens, 1995; 1996; Hesp et al., 2005). As such, stoss and lee slope sediment budget patterns at the study site may be primarily controlled by wind and wave patterns that drive onshore sediment delivery to the beach, while presence/absence of vegetation secondarily controls localized distribution of sediment within and between foredune zones.

Figure 34. A) Photograph oriented to the north just landward of the foredune crest at transect 2. Solid black lines indicate ripple formation and related transport pathway directions on the lee slope. Black dashed lines indicate landward migration of ripples on the foredune crest and subsequent separation and avalanching in the lee slope. B) Photograph looking seaward at southern boundary of restoration site shows avalanching of sediment into the lee slope. C) Photograph oriented south, landward of the foredune crest indicates avalanching of sediment onto the foredune lee slope.

3.6.2 Foredune geomorphic response to wave erosion and rebuilding

In early January 2016, the Lanphere Dunes experienced large-scale erosion during the 2016 La Niña winter storm season (Figure 32 and 35) due to higher than long-term average seasonal wave heights and water levels. The result was site-wide undercutting of the foredune toe and beach lowering (Figure 32 and 35) with a higher scarp wall in the northern portion of the study site (Figure 26). As discussed above, abrupt changes to seasonal sediment budgets, resulting from extensive beach erosion, have obvious implications for aeolian sediment transport to the foredune and resulting variation in localized deposition in the lower, mid and upper stoss slope zones.

In a study of airflow patterns around topographic obstacles, Qian et al., (2011) note that echo dunes often form upwind of an escarpment following an abrupt decrease in velocity and downward shift in flow near the toe of an obstacle with a steep stoss toe angle (> 60°). Accordingly, the effect of a vertically scarped foredune at the study site on seasonal onshore transporting winds and lower precipitation might have resulted in flow stagnation and scouring at the base of the scarp to produce similar forms (Figure 35). (Qian et al., 2011; Christiansen and Davidson-Arnot 2004). Hesp (1988) shows that the development of echo dunes is often an early stage in foredune scarp rebuilding as aeolian transport and avalanching over the echo dune eventually leads to the development of low sand ramps that attach to the scarp face and may eventually rejoin the existing foredune stoss slope. An increase in lower stoss slope area (April – September 2016) and more gradual summer foredune profiles at both transects 1 and 2 following winter scarping indicate that a scarp fill ramp developed through echo dune formation and attachment to the foredune stoss slope (Figure 26). However, alongshore gradients in scarp height

resulted in similar north to south variation in scarp fill, with ramp attachment occurring by April 2016 in the south and late June 2016 in the north where taller scarps were present (Figure 35).

The formation of scarp fill sand ramps alter aeolian transport pathways by introducing more uniform slope and flow dynamics both upwind and downwind of foredunes (e.g., Bowen and Lindley, 1977; Christiansen and Davidson-Arnott, 2004; Qian et al., 2011). Arens (1996) describes that steep slope gradients in aeolian transport rates often result in thick and spatially limited sediment deposits (i.e., predominance of mid-stoss slope sedimentation) and vice versa for gentle sediment transport gradients. Although this model applies predominantly to vegetated foredunes, a similar trend is observed for the denuded foredune at the study site through an increase in mid-stoss slope area from November 2015 – April 2016, corresponding to the steepening of the stoss slope from erosive waves and early stages of ramp development (Figure 25). As the sand ramp continues to develop on the scarp face, flow is accelerated up the stoss slope with an increase in flow velocity and shear surface stress toward the foredune crest line.

Numerous studies (e.g., Sherman and Bauer, 1993; Arens, 1996; Christiansen, 2003; Christiansen and Davidson-Arnott, 2004; Hesp et al., 2005) have indicated that scarp fill and ramp building from aeolian sediment deposition assists in supplying sediment to the upper stoss slope and crest, nourishing these regions following storm erosion. As such, a north to south gradient in scarp fill may have resulted in a similar variation in sediment transport to the foredune at the study site. For example, greater sediment accretion along the upper beach and foredune toe at transect 2 in the south (Figure 26) could be a result of earlier ramp attachment to a smaller scarp face. In areas

with earlier ramp attachment there is a greater opportunity for flow acceleration up a developed ramp and subsequent deposition on the foredune. Site-wide ramp attachment was seen by July 2016 (Figure 35), furthermore facilitating deposition on the foredune stoss and lee slopes. As such, the presence of a scarp ramp and more gradual foredune stoss slope may be directly linked to sediment deposition in the foredune. Net positive annual sediment budgets on the foredune stoss slope alongside recorded seasonal sediment deposition along backdune following both vegetation removal and winter storm erosion, indicate that ramp development at the study site plays a key role in foredune accretion and overall beach-foredune sediment budgets.

Figure 35. Scarp fill and sand ramp development in months following initial high water event in early January, 2017, resulting in site-wide undercutting of the foredune toe (A). A) is taken oriented south from the foredune stoss slope, while photos B – E are taken from the backshore at the southern boundary of the restoration site, oriented to the north.

3.6.3 Impacts of vegetation re-establishment

Pioneer plant colonization on the backshore often occurs in prograding systems (Hesp, 2013), such as the Lanphere Dunes, which are characterized by a net positive sediment budget following seasonal variations in sediment deposition patterns. An 8.35%

increase in vegetation cover from July – September 2016 was largely a product of widespread establishment of *Cakile spp.* along the backshore (Figure 29 and 30). Higher densities of vegetation and plant height result in increased drag force on near surface winds and higher rates of localized sediment deposition (Hesp, 1988; 1989; Arens, 1996; 2001; Ruggiero et al., 2011). Furthermore, Davidson-Arnott and Law (1996) describe that vegetation on the backshore interrupts aeolian transport, causing the deposition of sediment seaward of the foredune toe and resultant formation of incipient foredunes. At the study site, the establishment of *Cakile spp.* in the backshore and appreciable onshore sediment supply during the summer resulted in multiple nebkah dunes forming a broad accretionary band in the backshore from April to September, 2016, indicating early stages of incipient foredune development (Figure 28 and 32).

As onshore winds contact newly developed incipient foredunes, wind velocities decrease, resulting in sediment deposition on the incipient dune (Hesp, 1988; 1989; Levin et al., 2008; Hesp, 2002; Bochev-van der Burgh et al., 2011). Aeolian transport of sediment onto the foredune stoss slope may vary alongshore with differences in plant distribution and resultant sediment accumulation in the backshore. At the same time, variation in the vegetation growth along the foredune stoss slope, such as re-sprouting *Ammophila arenaria* and localized establishment of native vegetation further alters sediment transport and deposition throughout the foredune. Multiple studies (e.g., Hesp, 1983; 1989; Sarre, 1989; Arens, 1996; 2001; Hesp et al., 2005) describe that vegetation controls sedimentation on the foredune, particularly on the lee slope, where sediment delivery and deposition depends predominantly on wind flow over the crest for sediment deposition. In some transport systems, sediment within vegetation may be distributed

throughout the foredune stoss slope by near surface wind flow, however the opportunity for sediment suspension above the vegetation and deposition in the backdune is limited as vegetation densities increase (Arens, 1996; Hesp et al., 2005). Due to later development of scarp fill ramps at the northern portion of the study site (Figure 35), sediment accumulation on the lee slope north of transect 1 may be largely attributed to sediment transport by deflected, alongshore or oblique surface flows between low density re-sprouts of *Ammophila* arenaria from the stoss slope and crest from April to July, 2016 (Figure 32). Alternatively, neutral lee slope sedimentation trends south of transect 2 may have been caused by corresponding areas of increased vegetation density on the stoss slope, effectively trapping stoss slope sediment deposits and complex alongshore flow patterns in the lee slope (Figure 29 and 32). As such, re-establishment of vegetation at the study site from April – September 2016 resulted in the stabilization of some areas of sediment from the transport system as sediment is stored under vegetation canopies. The effect of limited sediment transport through the increase in vegetation cover further supports the idea that, alongside sediment supply in the beach zone, the presence/absence of vegetation plays a large role in seasonal sediment budget patterns. Future research at the study site following the replanting of native vegetation species may provide more information on the impacts of vegetation density on foredune sedimentation and resulting beach-foredune sediment budget patterns at the Lanphere Dunes.

3.7 Conclusions

Observations in a year encompassing preliminary stages of a dynamic restoration project (May 2015 – September 2016) were used to document the effect of human (vegetation management) and environmentally (storm erosion) induced disturbances on

foredune sediment budgets, morphodynamics and rebuilding processes at the HBNWR. Key findings include:

1. Seasonal trends in elevation change from May 2016 through September 2016 indicate appreciable sediment deposition within the beach and foredune stoss slope zones during the summer months and large-scale sediment erosion from November 2015 – April 2016. Summer sediment inputs to the beach zone contribute to increases in elevation and sediment replenishment across the stoss slope of the established foredune, resulting in a net positive sediment budget and site-wide seaward progradation.
2. Seasonal wave run-up and high water events during the winter of 2016 eroded the beach and lower foredune stoss slope, which in turn effects the development of the upper stoss and lee slope regions, as observed in other studies. Following, scarp fill ramp development plays a key role in foredune sediment budgets, assisting in foredune nourishment following storm events and facilitating the localized deposition of sediment throughout the foredune and backdune regions.
3. The re-establishment of vegetation throughout the foredune (April – September 2016) promotes sediment deposition in the backshore and foredune stoss, contributing to variation in localized sediment deposition and stabilization across the foredune. As such, the presence/absence of vegetation secondarily controls sediment distribution within and beach-dune system.
4. Sediment accumulation on the foredune in the year following vegetation removal is seen at the study site, despite the presence/absence of vegetation and greater than average wave height and water levels. Ramp formation following erosion of

the foredune toe alongside complex sediment transport pathways at the foredune crest and lee slope facilitated sediment deposition on the foredune stoss slope. Sediment accumulation on foredunes at the study site in the year following vegetation removal supports the longer-term pattern of foredune progradation seen at the Lanphere Dunes.

4. Summary and conclusions

4.1 Summary

This thesis provides a comprehensive analysis of foredune morphodynamics at the Humboldt Bay National Wildlife Refuge (HBNWR) in northern California, USA, from long-term (75-year) established foredune position and (monthly to seasonal) sediment volumetric changes and resulting geomorphic response. Results were used to document seasonal foredune morphodynamics following disturbance intervals (i.e., invasive vegetation removal, seasonal storm energy, vegetation establishment), and implications for long-term foredune sediment budgets and development. Thesis structure is based on two results sections (chapters 2 and 3) that document findings along the Lanphere and Ma-le'l sand dune units within the HBNWR, Northern California.

The purpose of chapter 2 was to quantify historical foredune position and sediment supply conditions at the HBNWR. Long-term (1939 – 2014) established foredune position was determined from a 75 year aerial photograph record. Recent (2012 – 2015) seasonal sediment volume trends were analyzed from cross shore profile measurements. Combined with regional meteorological and oceanographic observations (wind and wave directions, water level, Hs, climate variability indices), sediment volumes were used to explore how seasonal deviations in foredune morphodynamics impact the long-term trend in foredune position and development. The foredune system demonstrates a long-term alongshore gradient in rate of foredune position change, with foredune progradation in the north (up to +0.51 m a^{-1}) and foredune retreat in the south (up to -0.49 m a^{-1}). Additionally, there is a statistically significant difference in foredune elevation ($p = < 2 \times 10^{-16}$) and volume ($p = 5.95 \times 10^{-9}$) between the north, central and

south alongshore zones, in which north and central foredunes were taller and greater in foredune volume then those in the south. Statistically significant larger area of southern erosive features are observed over those in the north and central zones ($p = 4.87 \times 10^{-7}$). Foredune position change and morphodynamics suggest a north to south gradient in foredune evolution, with prograding and densely vegetated stage 1 foredunes in the north, transitioning to less densely vegetated and lower volume stage 3 foredunes in the south, according to the Hesp (1988; 2002) model on established foredune evolution. Foredune developmental stages are partially driven by seasonal to interannual wind and wave patterns that fuel bidirectional littoral drift in the Eureka Littoral Cell and related variations in offshore sediment transport to the beach and the subsequent storage of beach sediments underneath stabilizing agents such as vegetation. Therefore, beaches in the south are disproportionately affected by erosive wave energies and experience longer recovery intervals due to lower vegetation densities, sediment input and storage.

The purpose of chapter 3 was to document and describe local erosion response and recovery of at a restoration site along the Lanphere foredune system in the year following invasive vegetation removal and during the winter storm season and vegetation re-establishment. This chapter quantified geomorphic change in the beach and foredune from LiDAR derived bare earth models and using Geomorphic Change Detection software (GCD). Further linkages of sedimentation, geomorphic feature evolution and vegetation growth are made using longer-term (January 2012 – February 2017) elevation data from cross shore profiles and short term (April – September 2016) SfM derived orthomosaics. Spatio-temporal patterns of volume change indicate that in a year encompassing the initial removal of invasive vegetation the foredune system experienced

a net positive sediment budget (+0.54 m^3 m^{-2}) while net erosion occurred on the beach (-0.38 m^3 m^{-2}). Examination of sediment budget patterns at shorter seasonal scales indicates site-wide erosion during winter periods and site-wide sediment accretion during spring-summer intervals. Seasonal sediment exchanges indicate that ramp building from scarp fill following winter storm events plays a significant role in foredune recovery and development, despite the presence/absence of vegetation. However, sediment transport pathways between the beach and foredune lee slope were established following vegetation removal, as lower vegetation densities facilitated the re-activation of sediment previously stored underneath dense plant canopies. These results combined with evidence of extensive vegetation growth from April 2016 – September 2016 indicate that beach-foredune sediment budgets are primarily controlled by sediment availability in the beach zone, while the presence/absence of vegetation secondarily controls localized transport of sediment onto the foredune.

4.2 Research contributions and future directions

The principal contribution of this research is an extensive look into beach-dune morphodynamics and resulting foredune evolution at the HBNWR at a variety of temporal resolutions. The completed study provides an in depth understanding of monthly to interannual foredune sediment budget response and the resultant long-term patterns of established foredune position. By analyzing long-term historical rate of foredune position change from aerial photograph analysis, local patterns of foredune position were derived and qualitatively discussed in terms of foredune development, providing insight into local morphological variability. The exploration of historical and

recent patterns in foredune morphodynamics at this site provides a framework for the classification of foredune resilience and vulnerability to erosive wind and wave energies.

Overall, the compilation of both two dimensional data sets (i.e., aerial photographs, cross shore transect measurements) and high resolution three dimensional topographic data (i.e. LiDAR derived bare earth models) at a variety of spatial and temporal scales allows for comprehensive monitoring of rapid onset forces (wind, wave, human induced) that drive morphological variation within a foredune system. Although this study used a variety of data collection and survey methods, future monitoring at the study site may be limited by available time and resources. For example, the performance of regular high-resolution TLS surveys has high upfront costs and the quality of resulting bare earth models decreases in densely vegetated environments, such as portions of the foredune system at the HBNWR. As such, continued monitoring of previously established cross-shore profiles with RTK-DGPS in combination with periodic KAP surveys would provide the most cost-effective and efficient way to collect comprehensive geospatial data at this HBNWR, particularly during the next stages of restoration which include the replanting of native vegetation.

The Lanphere and Ma-le'l sand dune units provide a unique opportunity for monitoring the relationship between the presence of vegetation and foredune geomorphology due to the implication of a vegetation restoration project beginning in August 2015. Future research at this site should include continued monitoring of the foredune system using both cross-shore profile monitoring and SfM techniques, through at least the next vegetation growth period, in order to obtain high resolution topographic datasets that span the restoration project from pre- vegetation removal to post native

vegetation planting. Continued monitoring creates opportunities to examine the impact of different stages of vegetation removal, re-establishment and re-planting alongside simultaneous periods of winter storm erosion and summer sediment transport regimes on foredune morphology from seasonal to multi-year scales. In addition to monitoring the restoration site, future studies would benefit from the analysis of an unrestored control site, in order to compare how beach-dune sediment budget patterns and resulting foredune development may differ between restored and unrestored areas. Furthermore, a micro scale examination of aeolian flow over the foredune following the planting of native vegetation may provide critical information regarding the impact of lower density vegetation on aeolian transport over the foredune.

5.0 References

Abeysirigunawardena, D.S., Walker, I.J. (2008). Sea level responses to climate variability and change in northern British Columbia. *Atmosphere-ocean, 46*(3): 277 – 296.

Abeysirigunawardena, D.S., Gilleland, E., Bronaugh, D., Wong, P. (2009). Extreme wind regime responses to climate variability and change in the inner south coast of British Columbia, Canada. *Atmosphere-ocean, 47*(1): 1480 – 9214.

Abhar, K.C., Walker, I.J., Hesp, P.A., Gares, P. (2015). Spatial-Temporal evolution of aeolian blowout dunes at Cape Cod. *Geomorphology, 236:*148 – 162.

Allan, J.C., Komar, P.D. (2002). Extreme storms on the Pacific Northwest coast during the 1997 – 98 El Niño and 1998 – 99 La Niña. *Journal of coastal research, 18*(1): 175 – 193.

Allan, J.C., Komar, P.D., Priest, G.R. (2003). Shoreline variability on the high-energy Oregon Coast and its usefulness in erosion-hazard assessments. *Journal of coastal research, 38*: 183 – 105.

Anthony, E.J., Vanhee, S., Ruz, M. (2006). Short-term beach-dune sand budgets on the North Sea coast of France: Sand supply from shoreface to dunes, and the role of wind and fetch. *Geomorphology, 81*(3-4): 316 – 329.

Arens, S.M., Wiersma, J. (1994). The Dutch foredunes: Inventory and classification. *Journal of coastal research, 10*(1): 189 – 202.

Arens, S.M., van Kaam-Peters, H.M.E., van Boxel, J.H. (1995). Air flow over foredunes and implications for sand transport. *Earth surface processes and landforms, 20*: 315 – 332.

Arens, S.M. (1996). Patterns of sand transport on vegetated foredunes. *Geomorphology, 17*: 339 – 350.

Arens, S.M., Jungenus, P.D., van Der Meulen, F. (2001). Coastal dunes. In: Warren, A., French, J.R. (Eds.). *Habitat Conservation: Managing the physical environment,* John Wiley & Sons Ltd.: 229 – 272.

Arens, S.M., Baas, A.C.W., van Boxel, J.H., Kalkman, C. (2001). Influence of reed stem density on foredune development. *Earth surface processes and landforms, 26:* 1161 – 1176.

Arens, S.M., Geelen, L.H.W.T. (2006). Dune landscape rejuvenation by intended destabilization in the Amsterdam water supply dunes. *Journal of coastal research, 22*(5): 1094 – 1107.

Arens S., Slings, Q., Geelen, L. (2013). Restoration of dune mobility in the Netherlands. In: *Restoration of coastal dunes,* Martinez, M.L., Delgado-Fernandez, J.B., Hesp, P.A. (eds.), Springer Series on Environmental Management. Springer-Verlag: Berlin; 107 – 124.

Bangen, S. G., Wheaton, J.M., Bouwes, N., Bouwes, B., Jordan C. (2014). A methodological intercomparison of topographic survey techniques for characterizing wadeable streams and rivers. *Geomorphology, 206:* 343 – 361.

Barbour, M.G., DeJong, T.M. (1977). Response of west coast beach taxa to salt spray, seawater inundation, and soil salinity; *Bulletin of the Torrey Botanical Club, 104*(1): 29 – 34.

Barbour, M.G., De Jong, T.M., Pavlik, B.M., (1985). Marine beach and dune plant communities. In: Chabot, B.F., Mooney, H.A., (eds.) *Physiological ecology of North American plant communities.* Springer: Dordrecht: 296 – 322.

Barnard, P., Short, A., Harley, M., Splinter, K., Vitousek, S., Turner, I., Allan, J., Banno, M., Bryan, K., Doria, A., Hansen, J., Kato, S., Kuriyama, Y., Randall-Goodwin, E., Ruggiero, P., Walker, I.J., Heathfield, D. (2015). Coastal vulnerability across the Pacific dominated by El Niño/Southern Oscillation. *Nature geoscience, 8*: 801 – 807.

Bauer, B. O., Davidson-Arnott, R. G. D. (2002). A general framework for modelling sediment supply to coastal dunes including wind angle, beach geometry, and fetch effects. *Geomorphology, 49:* 89–108.

Bishop, M.P., James, L.A., Shroder Jr., J.F., Walsh, S.J. (2012). Geospatial technologies and digital geomorphological mapping: Concepts, issues and research. *Geomorphology, 137*(1): 5 – 26.

Blott, S.J., Pye, K. (2001). GRADISTAT: a grain size distribution and statistics package for the analysis of unconsolidated sediments. *Earth surface processes and landforms, 26*: 1237 – 1248.

Bochev-van der Burgh, L.M., Wijnberg, K.M., Hulscher, S.J.M.H. (2011). Decadal-scale morphologic variability of managed coastal dunes. *Coastal engineering, 58*(9): 927 – 936.

Bowen, A.J., Lindley, D. (1977). A wind-tunnel investigation of the wind speed and turbulence characteristics close to the ground over various escarpment shapes. *Boundary-layer meteorology, 12*: 259 – 271.

Buckley, E.C.B., Hilton, M.J., Konlechner, T.M., Lord, J.M. (2016). Downwind sedimentation and habitat development following Ammophila arenaria removal and dune erosion, Mason Bay, New Zealand. *Journal of coastal research, 75*: 268 – 272.

Christiansen, M.B. (2003). Effects of dune ramps on sediment supply to coastal foredunes: Skallingen, SW Denmark. *Proceedings of the international conference on coastal sediments 2003.* CD-ROM Published by World Scientific Publishing Corp. and East Meets West Productions, Corpus Christi, Texas, USA.

Christiansen, M.B., Davidson-Arnott, R. (2004). Rates of landward sand transport over the foredune at Skallingen, Denmark and the role of dune ramps. *Danish journal of geography, 104*(1): 31 – 43.

Darke, I.B., Eamer, J.B.R., Beaugrand, H.E.R., Walker, I.J. (2013). Monitoring considerations for a dynamic dune restoration project: Pacific Rim National Park Reserve, British Columbia, Canada. *Earth surface processes and landforms, 38*(9): 983 – 993.

Darke, I.B., Walker, I.J., Hesp, P.A. (2016). Beach-dune sediment budgets and dune morphodynamics following coastal dune restoration, Wickanninish Dunes, Canada. *Earth surface processes and landforms, 41*(10): 1370 – 1385.

Davidson-Arnott, R.G.D., Law, M.N. (1996). Measurement and prediction of long-term sediment supply to coastal foredunes. *Journal of coastal research, 12*(3): 654 – 663.

Davidson-Arnott, R.G.D., Macquarrie, K., Aagaard, T. (2005). The effect of wind gusts, moisture content and fetch length on sand transport on a beach. *Geomorphology, 68:* 115 – 129.

Delgado-Fernandez, I., Davidson-Arnott, R. (2009). Sediment input to foredunes: Description and frequency of transport events at Greenwich Dunes, PEI, Canada. *Journal of Coastal Research, SI56:* 302–306.

Delgado-Fernandez, I., Davidson-Arnott, R. (2011). Meso-scale aeolian sediment input to coastal dunes: The nature of aeolian transport events. *Geomorphology, 126*(1–2): 217–232.

De Vries, S., Southgate, H.N., Kanning, W., Ranasinghe, R. (2012). Dune behaviour and aeolian transport on decadal timescales. *Coastal engineering*, *67*: 41 – 53.

Dingler, J.R., Clifton, H.E. (1994). Barrier systems of California, Oregon, and Washington. In Davis, R.A. (Ed.), *Geology of Holocene Barrier Island Systems* (115 – 166). New York, NY: Springer-Verlag.

Dugan, J.E., Hubbard, D.M. (2010). Loss of coastal strand habitat in southern California: The role of beach grooming. *Estuaries and Coasts 33*:67–77.

Eamer, J.B.R., Walker, I.J. (2010). Quantifying sand storage capacity of large woody debris on beaches using LiDAR. *Geomorphology*, *118*: 33 – 47.

Esler, A. E. (1970). Manawatu sand dune vegetation. *Proceedings of the New Zealand Ecological Society*, *17*: 41–46.

Fisher, R.A. (1935). *The design of experiments.* London: Oliver & Boyd.

Fryberger, S.G., Dean, G. (1979). Dune forms and wind regime. In: McKee, (ed.), *A study of global sand seas,* Geol. Survey prof. paper 1052, US Govt. Printing Office, Washington (1979), pp. 137 – 170.

Gares, P.A., Nordstrom, K.F. (1995). A cyclic model of foredune blowout evolution for a leeward coast: Island Beach, New Jersey. *Annals of the association of American geographers, 85*(1): 1 – 20.

Godfrey, P.J. (1977). Climate, plant response, and development of dunes on barrier beaches along the US east coast. *International Journal of Biometeorology 21*: 203–215.

Goldsmith, V. (1989). Coastal sand dunes as geomorphological systems. *Proceedings of the royal society of Edinburgh, 96B*: 3 – 15.

Grootjans, A.P., Geelen, H.W.T., Jansen, A.J.M., Lammerts, E.J. (2002). Restoration of coastal dune slacks in the Netherlands. *Hydrobiologia, 478*: 181 – 203.

Hapke, C.J., Reid, D., Richmond, B.M., Ruggiero, P., List, J. (2006). National assessment of shoreline change part 3: Historical shoreline change and associated coastal land loss along sandy shorelines of the California coast. Open- File report 2006: 1219.

Hapke, C.J., Reid, D., Richmond, B. (2009). Rates and trends of coastal change in California and the regional behaviour of the beach and cliff system. *Journal of coastal research, 25*(3): 603 – 615.

Harris, C.K., Traykovski, P.A., Geyer, W.R. (2005). Flood dispersion and deposition by near-bed gravitational sediment flows and oceanographic transport: A numerical modeling study of the Eel River shelf, northern California. *Journal of geophysical research, 110*(C9): DOI: 10.1029/2004JC002727

Heathfield, D.K., Walker, I.J. (2011). Analysis of coastal dune dynamics, shoreline position, and large woody debris at Wickaninnish Bay, Pacific Rim National Park, British Columbia. *Canadian journal of earth sciences, 48*(7): 1185 – 1198.

Heathfield, D.K., Walker, I.J., Atkinson, D.E. (2013). Erosive water level regime and climatic variability forcing of beach-dune systems on south-western Vancouver Island, British Columbia, Canada. *Earth surface processes and landforms, 38*(7): 751 – 762.

Hemming, M. A., Nieuwenhuize, J. (1990). Seagrass wrack-induced dune formation on a tropical coast (Banc d'Arguin, Mauritania). *Estuarine, Coastal and Shelf Science, 31*: 499–502

Hesp, P.A., 1984; Foredune formation in Southeast Australia; In: B.G. Thom (Ed.) *Coastal Geomorphology in Australia*: 69-97. Academic Press.

Hesp, P. (1988). Morphology, dynamics and internal stratification of some established foredunes in Southeast Australia. *Sedimentary geology, 55*(1-2): 17 – 41.

Hesp, P. A. (1989). A review of biological and geomorphological processes involved in the initiation and development of incipient foredunes. *Proceedings of the Royal Society of Edinburgh 98B*:181–201.

Hesp, P.A. (1991). Ecological processes and plant adaptations on coastal dunes. J. Arid Environments 21: 165-191.

Hesp, P.A. (1999). The Beach Backshore and Beyond. In: A.D. Short (Ed.), *Handbook of Beach and Shoreface Morphodynamics*: 145-170. John Wiley.

Hesp, P. (2002). Foredunes and blowouts: Initiation, geomorphology and dynamics. *Geomorphology*, *48*(1-3): 245 – 268.

Hesp, P. A. and Martinez, M. (2007). Disturbance in coastal dune ecosystems. In: E.A. Johnson, K. Miyanishi (Eds.), *Plant Disturbance Ecology: The Process and Response.* Academic Press: 215-247.

Hesp, P.A., Davidson- Arnott, R., Walker, I.J., Ollerhead, J. (2005). Flow dynamics over a foredune at Prince Edward Island, Canada. *Geomorphology, 65*(1 – 2): 71 – 84.

Hesp, P. (2013). A 34 year record of foredune evolution, Dark Point, NSW, Australia. *Journal of coastal research, 65*(sp2): 1295 – 1300.

Hesp, P.A. and Smyth, T.A.G., 2016. Surfzone-beach-dune interactions: Review and the role of the intertidal beach, *Journal of Coastal Research S.I. 75*: 8-12.

Hilton, M., Duncan, M., & Jul, A. (2005). Processes of Ammophila arenaria (marram grass) invasion and indigenous species displacement, Stewart Island, New Zealand. *Journal of Coastal Research*, 175-185.

Hilton, M.J. (2006). The loss of New Zealand's active dunes and the spread of marram grass (*Ammophila arenaria). New Zealand geographer, 62*(2): 105 – 120.

Hilton, M., Harvey, N., Hart, A., James, K., Arbuckle, C. (2006). The impact of exotic dune grass species on foredune development in Australia and New Zealand: A cast study of *Ammophila arenaria* and *Thinopyrum junceiforme. Australian geographer*, *37*(3): 313 – 334.

Hilton, M., Woodley, D., Sweeney, C., Konlechner, T. (2009). The development of a prograded foredune barrier following Ammophila arenaria eradication, Doughboy Bay, Stewart Island. *Journal of coastal research, 56*(1): 317 – 321.

Houser, C., & Ellis, J. (2013). *Beach and Dune Interaction*. *Treatise on Geomorphology* (Vol. 10). Elsevier Ltd. http://doi.org/10.1016/B978-0-12-374739-6.00283-9http://doi.org/10.1016/B978-0-12-374739-6.00283-9

Konlechner, T.M. (2008). The management challenge posed by marine dispersal of terrestrial plants in coastal dune systems. *New Zealand geographer, 64*: 154 – 156.

Kuriyama, Y., Mockizuki, N., Nakashima, T. (2005). Influence on vegetation on aeolian sand transport from a backshore to a foredune in Hasaki, Japan. *Sedimentology, 52*: 1123 – 1132.

Levin, N., Kidron, G.J., Ben-Dor, E. (2008). A field quantification of coastal dune perennial plants as indicators of surface stability, erosion or deposition. *Sedimentology, 55*: 751 – 772.

Lim, N., Petley, D.N., Rosser, N.J., Allison, R.J., Long, A.J., Pybus, D. (2005). Combined digital photogrammetry and time-of-flight laser scanning for monitoring cliff evolution. *Photogrammetric record, 20*(110): 109 – 129.

Lindenbergh., R.C., Soudarissanane, S.S., de Vries, S., Gorte, B.G.H., de Schipper, M.A. (2011). Aeolian beach sand transport monitored by terrestrial laser scanning. *The photogrammetric record, 136*(26): 384 – 399.

Luna, M.C.M., Parteli, E.J.R., Duran, O., Herrmann, H.J. (2011). Model for the genesis of coastal dune fields with vegetation. *Geomorphology, 129:* 215 – 224.

McLean, R.F., Thom, B.G. (1979). Beach changes at Moruya, 1972 – 74. In: *Second Australian conference on coastal and ocean engineering, 1975: The engineer, the coast and the ocean,* (12 – 17). Sydney: Institution of Engineers.

Mantel, N. (1967). The detection of disease clustering and a generalized regression approach. *Cancer research, 27*(2): 209 – 220.

Martinez, M. L., & Psuty, N. P. (Eds.). (2004). *Dunes: Ecology and Conservation. Ecological Studies, Vol. 171*. New York, NY: Springer.

Martinez, M.L., Gallego-Fernandez, J.B., Hesp, P.A. (Eds.). (2013). *Restoration of coastal dunes*. New York, NY: Springer.

McLean, R.F., Thom, B.G. (1975). Beach changes at Moruya, 1974 – 74. In: *Second Australian conference on coastal and ocean engineering, 1975: The engineer, the coast and the ocean.* Sydney: Institution of Engineers, Australia: 12 – 17.

Miot da Silva, G., Hesp, P. (2010). Coastline orientation, Aeolian sediment transport and foredune and dunefield dynamics of Mocambique Beach, Southern Brazil. *Geomorphology, 120*(3): 258 – 278.

Nickling, W.G., Davidson-Arnott, R.G.D. (1990). Aeolian sediment transport on beaches and coastal dunes. *Proceedings Canadian symposium on coastal sand dunes 1990.* 1 – 35.

Nordstrom, K. F., Lampe, R., Vandemark, L. M. (2000). Reestablishing naturally functioning dunes on developed coasts. *Environmental Management, 25*(1), 37–51.

Nordstrom, K., F., Jackson, N., L., Korotky, K.H. (2011a). Aeolian sediment transport across beach wrack. *Journal of Coastal Research, SI59*:211–217.

Nordstrom, K., F., Jackson, N., L., Korotky, K., H., Puleo, J., A. (2011b). Aeolian transport rates across raked and unraked beaches on a developed coast. *Earth Surface Processes and Landforms, 36*: 779–789

Nordstrom, K.F., Jackson, N.L., Kraus, N.C., Kana, T.W., Bearce, R., Bocamazo, L.M., Young, D.R., de Butts, H.A. (2011). Enhancing geomorphic and biologic functions and values on backshores and dunes of developed shores: A review of opportunities and constraints. *Environmental conservation, 38*(3): 288 – 302.

Ollerhead, J., Davidson-Arnott, R., Walker, I.J., Mathew, S. (2013). Annual to decadal morphodynamics of the foredune system at Greenwich Dunes, Prince Edward Island, Canada. *Earth surface processes and landforms, 38*(3): 284 – 298.

Pickart, A.J. (2013). Dune restoration over two decades at the Lanphere and Ma-le'l Dunes in Northern California. In Martinez, M.L., Gallego-Fernandez, J.B., Hesp, P.A. (Eds.), *Restoration of coastal dunes* (159 – 171). New York, NY: Springer.

Pickart, A. (2014). *Predicting and measuring climate change impacts at a coastal dune site: A progress report.* (USFWS Pub). Arcata, CA.

Pickart, A.J., Barbour, M.G. (2007). Beach and dune. In: Barbour, M.G., Keeler-Wolf, T., Schoenherr, A.A. (Eds.), *Terrestrial vegetation of California*, Berkeley, CA: University of California Press: 155 – 179.

Pickart, A.J., Sawyer, J.O. (1998). *Ecology and restoration of Northern California coastal dunes.* California Native Plant Society: Sacramento, CA.

Pike, R.J. (2000). Geomorphometry: Diversity in quantitative surface analysis. *Progress in physical geography, 24*(1): 1 – 20.

Psuty, N.P. (1988). Sediment budget and dune/beach interaction. *Journal of Coastal Research, Special Issue 3*: 1 – 4.

Qian, G., Dong, Z., Luo, W., Lu, J. (2011). Mean airflow patterns upwind of topographic obstacles and their implications for the formation of echo dunes: A wind tunnel simulation of the effects of windward slope. *Journal of geophysical research, 116* (F04026).

Riksen, M., Spaan, W., Stroosnijder, L. (2008). How to use wind erosion to restore and maintain the inland drift-sand ecotype in the Netherlands? *Journal for nature conservation, 16*(1): 26 – 43.

Ruggiero, P., Komar, P.D., McDougal, W.G., Marra, J.J., Beach, R.A. (2001). Wave run up, extreme water levels and the erosion of properties backing beaches. *Journal of coastal research, 17*(2): 407 – 419.

Ruggiero, P., Buijsman, M., Kaminsky, G.M., Gelfendbaum, G. (2010). Modeling the effects of wave climate and sediment supply variability on large-scale shoreline change. *Marine geology, 273* (1 – 4): 127 – 140.

Ruggiero, P., Mull, J., Zarnetske, P., Hacker, S., Seabloom, E. (2011). Interannual to decadal foredune evolution. *Proceedings of coastal sediments 2011, 3*: 698 – 711.

Runyan, K., Griggs, G.B. (2003). The effects of armouring seacliffs on the natural sand supply to the beaches of California. *Journal of coastal research, 19*(2): 336 – 347.

Sawyer, J.O., Keeler-Wolf, T., Evens, J.M. (2009*). A manual of California vegetation*. California Native Plant Society: Scramento, CA.

Schwing, F.B., Murphree, T., Green, P.M. (2002). The northern oscillation index (NOI): A new climate index from the northeast Pacific. *Progress in oceanography, 53*(2 – 4): 115 – 139.

Scott, D., Mathew, S., Davidson-Arnott, G.D., Ollerhead, J. (2010). Evolution of a beach-dune system following a catastrophic storm overwash event: Greenwich Dunes,

Prince Edward Island, 1936 – 2005. *Canadian journal of earth sciences, 47*(3): 273 – 290.
Seabloom, E.W., Wiedemann, A.M. (1994). Distribution and effects of *Ammophila breviligulata* Fern. (American Beachgrass) on the foredunes of the Washington coast. *Journal of coastal research, 10*(1): 178 – 188.
Shepard, E.P. (1950). Beach cycles in southern California. *U.S. Army Corps of Engineers, beach erosion board technical memorandum, 20*: Washington, D.C.
Sherman, D.J., Bauer, B.O. (1993). Dynamics of beach-dune systems. *Progress in Physical Geography, 17*(4): 413-447.
Short, A.D., Hesp, P.A. (1982). Wave, beach and dune interactions in southeastern Australia. *Marine geology, 48*(3 – 4): 259 – 284.
Smith, M.J., Chandler, J., Rose, J. (2009). High spatial resolution data acquisition for the geosciences: Kite aerial photography. *Earth surfaces processes and landforms, 34*: 155 – 161.
Storlazzi, C.D., Willis, C.M., Griggs, G.B. (2000). Comparative impacts of the 1982 – 83 and 1997 – 98 El Niño winters on the central California coast. *Journal of coastal research, 16*(4): 1022 – 1036.
Storlazzi, C.D., Wingfield, D.K. (2005). Spatial and temporal variations in oceanographic and meteorologic forcing along the central California coast, 1980 – 2002. Open file report, 2005: 5085.
Subbotina, M.M., Thomson, R.E., Rabinovich, A.B. (2001). Spectral characteristics of sea level variability along the west coast of North America during the 1982 – 83 and 1997 – 98 El Niño events. *Progress in oceanography, 49*(1 – 4): 353 – 372.
Thom, B.G., Hall, W. (1991). Behaviour of beach profiles during accretion and erosion dominated periods. *Earth surface processes and landforms, 16*: 113 – 127.
Thieler, E.R., Danforth, W.W. (1994). Historical shoreline mapping (II): Application of the Digital Shoreline Mapping and Analysis Systems (DSMS/DSAS) to shoreline change mapping in Puerto Rico. *Journal of coastal research, 10*(3): 600 – 620.
Thieler, E.R., Himmelstoss, E.A., Zichichi, J.L., and Ergul, Ayhan, 2009, Digital Shoreline Analysis System (DSAS) version 4.0— An ArcGIS extension for calculating shoreline change: U.S. Geological Survey Open-File Report 2008-1278.
Van Der Hagen, H.G.J.M., Geelen, L.H.W.T., de Vries, C.N. (2008). Dune slack restoration in Dutch mainland coastal dunes. *Journal for nature conservation, 16*(1): 1 – 11.
Walker, I.J. (1999). Secondary airflow and sediment transport in the lee of a reversing dune. *Earth surface processes and landforms, 24:* 437 – 448.
Walker, I.J., Eamer, J.B.R., Darke, I.B. (2013). Assessing significant geomorphic changes and effectiveness of dynamic restoration in a coastal dune ecosystem. *Geomorphology, 199:* 192 – 204.
Warrick, J.A. (2014). Eel River margin source-to-sink sediment budgets: Revisited. *Marine geology, 351*: 25 – 37.
Wheatcroft, R.A., Sommerfield, C.K. (2005). River sediment flux and shelf accumulation rates on the Pacific Northwest margin. *Continental shelf research, 25*: 311 – 332.

Wheaton, J.M., Brasington, J., Darby, S.E., Sear, S.A. (2010). Accounting for uncertainty in DEMs from repeat topographic surveys: Improved sediment budgets. *Earth surface processes and landforms, 35*: 136 – 156.

Wiedemann, A.M., Pickart, A. (1996). The Ammophila problem of the Northwest coast of North America. *Landscape and urban planning, 34:* 287 – 299.

Wolter, K., Timlin, M.S. (1998). Measuring the strength of ENSO events: How does 1997/98 rank? *Weather*, *53*(9): 315 – 324.

Zarnetske, P.L., Hacker, S.D., Seabloom, E.W., Ruggiero, P., Killian, J.R., Maddux, T.B., Cox, D. (2012). Biophysical feedback mediates effects of invasive grasses on coastal dune shape. *Ecology, 93*(6): 1439 – 1450.

Zarnetske, P.L., Ruggiero, P., Seabloom, E.W., Hacker, S.D. (2015). Coastal foredune evolution: the relative influence of vegetation and sand supply in the US Pacific Northwest. *Journal of the royal society interface, 12:* 20150017.